

**ADSORPTION-ELECTROCOAGULATION PROCESS
FOR REMOVAL REACTIVE BLACK 5 DYE FROM
AQUEOUS SOLUTION**

MOOK WEI TZE

**FACULTY OF ENGINEERING
UNIVERSITY OF MALAYA
KUALA LUMPUR**

2018

**ADSORPTION-ELECTROCOAGULATION PROCESS
FOR REMOVAL REACTIVE BLACK 5 DYE FROM
AQUEOUS SOLUTION**

MOOK WEI TZE

**THESIS SUBMITTED IN FULFILMENT OF THE
REQUIREMENTS FOR THE DEGREE OF DOCTOR OF
PHILOSOPHY**

**FACULTY OF ENGINEERING
UNIVERSITY OF MALAYA
KUALA LUMPUR**

2018

UNIVERSITY OF MALAYA

ORIGINAL LITERARY WORK DECLARATION

Name of Candidate: MOOK WEITZE

Registration/Matric No: KHA 130135

Name of Degree: DOCTOR OF PHILOSOPHY

Title of Project Paper/Research Report/Dissertation/Thesis (“this Work”):
ADSORPTION-ELECTROCOAGULATION PROCESS FOR REMOVAL REACTIVE
BLACK 5 DYE FROM AQUEOUS SOLUTION

Field of Study: SEPARATION AND PURIFICATION PROCESS

I do solemnly and sincerely declare that:

- (1) I am the sole author/writer of this Work;
- (2) This Work is original;
- (3) Any use of any work in which copyright exists was done by way of fair dealing and for permitted purposes and any excerpt or extract from, or reference to or reproduction of any copyright work has been disclosed expressly and sufficiently and the title of the Work and its authorship have been acknowledged in this Work;
- (4) I do not have any actual knowledge nor do I ought reasonably to know that the making of this work constitutes an infringement of any copyright work;
- (5) I hereby assign all and every rights in the copyright to this Work to the University of Malaya (“UM”), who henceforth shall be owner of the copyright in this Work and that any reproduction or use in any form or by any means whatsoever is prohibited without the written consent of UM having been first had and obtained;
- (6) I am fully aware that if in the course of making this Work I have infringed any copyright whether intentionally or otherwise, I may be subject to legal action or any other action as may be determined by UM.

Candidate’s Signature

Date:

Subscribed and solemnly declared before,

Witness’s Signature

Date:

Name:

Designation:

ADSORPTION-ELECTROCOAGULATION PROCESS FOR REMOVAL REACTIVE BLACK 5 DYE FROM AQUEOUS SOLUTION

ABSTRACT

In recent years, a significant amount of residual dye can be found in textile industry wastewater produced from the dyeing rinsing process. The excessive amount of reactive dye discharged into receiving bodies is dangerous and it can threaten the aquatic environment and human health. In this work, combined process of adsorption and electrocoagulation was developed to treat Reactive Black 5 dye (RB5) from aqueous solution. The activated carbon derived from biomass waste, namely commercialise palm shell was evaluated as a potential adsorbent for the removal of RB5. The equilibrium isotherms and the kinetics of the adsorption process were investigated. Adsorption tests were conducted to determine the effects of various parameters, such as contact time, RB5 concentration, temperature, initial solution pH, adsorbent dose and the presence of coexisting anion, on the treatment performance. The Langmuir model provided the best fit for the obtained equilibrium isotherm data, while the adsorption kinetics was best represented by the pseudo-first-order model. The adsorption capacity of the adsorbent used in the study was higher in acidic medium. The activation energy of RB5 adsorption was 12.619 kJ/mol. The maximum adsorption capacity of the adsorbent was 25.12 mg/g at pH 2. Commercial palm shell activated carbon is shown to have great potential in the adsorption of RB5 from aqueous solution. In the second part of the study, a novel anode configuration consisting of a double layer iron mesh is proposed for the electrocoagulation treatment of wastewater. At a constant anode surface area and identical process operating parameters, the double layer iron mesh electrode showed better performance compared with the single layer iron mesh in terms of RB5 and COD removal efficiency, the kinetic rate constant, diffusion coefficient and electrical energy consumption. Besides that, the effect of various parameters such as pH of the solution,

current density, supporting electrolyte and electrocoagulation time was investigated. A new approach of combined adsorption and electrocoagulation processes (A-EC) in a single setup was introduced. The effects of initial pH, current density, adsorbent dose and initial RB5 concentration in the combined process were investigated. The A-EC showed great potential to treat higher dye concentration as compared with the individual adsorption and electrocoagulation. Response Surface Methodology (RSM) was used as a computing tool for analysing the data and predict the optimum conditions that maximize the RB5 removal. The application of optimum conditions of combined process, i.e. initial pH of 6.17, an adsorbent dose of 15.04 g/L, a current density of 2.03 mA/cm² and a process time of 57.18 min, resulted in RB5 and COD removal efficiency of 97.2% and 86.8%, respectively. The A-EC gave the best performance in the subject of RB5 and COD removal efficiency, the kinetic rate constant, sludge volume, electrical energy consumption, and operating costs. The GC-MS results show that no aromatic compounds found in the final effluent after A-EC treatment. The RB5 compound was completely decomposed and transformed into a heterocyclic compound with smaller molecular size. Additionally, the XRD patterns indicated that the iron complexes were found in the sludge.

Keywords: Adsorption; Electrocoagulation; Combined; RSM

PROSES PENJERAPAN-ELECTROPENGGUMPALAN UNTUK MERAWAT PEWARNA REAKTIF BLACK 5 DARIPADA LARUTAN AKUEUS

ABSTRAK

Dalam tahun kebelakangan ini, jumlah besar pewarna telah didapatkan dalam air sisa dari industri tekstil yang dihasilkan dalam proses pembilasan semasa pencelupan bahan. Berlebihan pewarna reaktif yang dilepaskan adalah berbahaya, mengancam persekitaran akuatik dan kesihatan manusia. Dalam karya ini, pergabungan proses penjerapan dan elektro-penggumpalan dikaji untuk merawat pewarna Reaktif Black 5 (RB5) daripada larutan akueus. Aktif karbon dihasilkan daripada sisa biojisim, iaitu komersial tempurung sawit dinilai sebagai penjerap yang berpotensi untuk merawat RB5. Keseimbangan isoterma dan proses kinetik penjerapan telah dikaji. Ujikaji penjerapan dijalankan untuk menyiasat kesan pelbagai jenis parameter terhadap prestasi rawatan seperti masa, kepekatan RB5, suhu, awalan pH, dos penjerap dan kewujudan anion. Model Langmuir adalah terbaik untuk mewakili data keseimbangan isoterma, manakala kinetik penjerapan terbaik diwakili oleh model pseudo-pertama. Penjerapan RB5 dalam kajian ini adalah lebih tinggi dalam medium berasid dan banyak dos penjerap. RB5 penjerapan adalah endotermik proses dengan tenaga pengaktifan 12.619 kJ/mol. Maksimum kapasiti penjerapan adalah 25.12 mg/g pada pH 2. Komersial aktif karbon daripada tempurung sawit telah dibuktikan mempunyai potensi yang tinggi dalam penjerapan RB5 daripada larutan akueus. Dalam bahagian kajian kedua, pendekatan baru konfigurasi anod terdiri daripada besi petak dua lapisan dicadangkan dalam proses elektro-penggumpalan untuk merawat air sisa. Pada kesamaan permukaan anod dan parameter operasi, besi petak dua lapisan elektrod menunjukkan prestasi yang lebih baik berbanding dengan petak satu lapisan daripada aspek kecekapan penyingkiran RB5 dan COD, pemalar kinetik, pekali peresapan dan penggunaan tenaga elektrik. Selain itu, pelbagai pengaruh parameter seperti pH larutan, ketumpatan arus, elektrolit penyokong dan masa elektro-

penggumpalan telah disiasatkan. Satu pendekatan baru penggabungan proses penjerapan dan elektro-penggumpalan (A-EC) dalam tunggal system diperkenalkan. Kesan awalan pH, ketumpatan arus, penjerap dos dan kepekatan RB5 dalam penggabungan proses telah disiasat. A-EC menunjukkan potensi yang besar untuk merawat kepekatan pewarna yang lebih tinggi berbanding dengan tunggal penjerapan dan elektro-penggumpalan proses. Response Surface Methodology (RSM) telah digunakan sebagai perisian pengkomputeran untuk menganalisis data untuk meramalkan keadaan optimum yang memaksimumkan penyingkiran RB5. Penggunaan keadaan optimum rawatan A-EC, iaitu awalan pH 6.17, penjerap dos 15.04 g/L, ketumpatan arus 2.03 mA/cm² dan masa proses 57.18 min, mengakibatkan penyikiran RB5 dan COD sebanyak 97.2% dan 86.8% masing-masing. Hasil kajian menunjukkan bahawa A-EC memberikan keputusan yang terbaik dalam subjek penyikiran RB5 dan COD, pemalar kinetik, jumlah mendapan, penggunaan tenaga elektrik dan kos operasi. Hasil GC-MS menunjukkan bahawa tiada sebatian aromatik yang berbahaya ditemui dalam efluen akhir selepas rawatan A-EC. RB5 telah diuraikan dan berubah menjadi sebatian heterocyclic dengan saiz molekul yang lebih kecil. Secara tambahan, corak XRD menunjukkan bahawa kompleks besi ditemui dalam mendapan.

Keywords: Penjerapan; Elektropenggumpalan; Pergabungan; RSM

ACKNOWLEDGEMENTS

First and foremost, I would like to convey my heartfelt gratitude to my supervisor Prof. Dr. Mohamed Kheireddine Bin Taieb Aroua for his valuable advice during our fruitful discussions to fulfil this work. I appreciate his continuous guidance, patience, and support throughout the period of my study. In fact, I feel grateful to work under his supervision.

I would also like to thank my co-supervisor from Wrocław University of Science and Technology, Asst. Prof. Małgorzata Szlachta. She has given me helpful advice and encouragement to surpass all obstacles I encountered.

I am grateful to the High Impact Research Grant (HIR Grant No: HIR/MOHE/ENG/43) which support this work financially.

My sincere thanks to Mr. Mohammed Ajeel for his helpful suggestions and ideas which greatly inspired me. He always shares his knowledge and working experience, which guided me to think out of the box and move forward.

I express my special thanks to all the supporting staff from Chemical Engineering Department, University of Malaya, especially Mr. Kamarudin and Mr. Azaruddin for their help in constructing the electrodes and reactor. I would also like to thank Ms. Faziza and Mrs. Norhayah, laboratory assistants, for their help in analysis work.

Many thanks to all my friends and the members of the Thermodynamic Lab, Chemical Engineering Department, University of Malaya. I am thankful to everyone who has, directly and indirectly, helped to the success of this research.

My deep profound appreciation goes to my beloved parents and family for their tolerance, support, and encouragement I received from them all these years. Without them, I would not have been able to complete the work in the present form. Thank you so much.

TABLE OF CONTENT

ABSTRACT.....	III
ABSTRAK.....	V
ACKNOWLEDGEMENTS.....	VII
TABLE OF CONTENT.....	VIII
LIST OF FIGURES.....	XII
LIST OF TABLES.....	XV
LIST SYMBOLS AND ABBREVIATIONS.....	XVII
CHAPTER 1: INTRODUCTION.....	1
1.1 Introduction.....	1
1.2 Problem statement.....	5
1.3 Research objectives.....	6
1.4 Scope of research.....	6
1.5 Outline of research.....	7
CHAPTER 2: LITERATURE REVIEW.....	9
2.1 Textile industry.....	9
2.2 Reactive dye.....	10
2.3 RB5 removal methods.....	11
2.3.1 Physical methods.....	11
2.3.2 Chemical methods.....	12
2.3.3 Biological methods.....	13
2.3.4 Advanced oxidation process.....	14
2.3.5 Electrochemical technology.....	16

2.3.6	Adsorption.....	18
2.3.6.1	Adsorption mechanism.....	19
2.3.6.2	Adsorbent	21
2.3.6.3	Solution pH	23
2.3.6.4	Temperature	24
2.3.6.5	Initial dye concentration.....	25
2.3.6.6	Adsorbent dose.....	25
2.3.7	Electrocoagulation technology.....	26
2.3.7.1	Interface of colloidal particles.....	27
2.3.7.2	Anodic material and shape	29
2.3.7.3	Solution pH	31
2.3.7.4	Electric current	32
2.3.8	Combined processes.....	33
2.4	Summary.....	34
CHAPTER 3: RESEARCH METHODOLOGY		35
3.1	Experimental flow-chart.....	35
3.2	Adsorption process	36
3.2.1	Activated carbon preparation	36
3.2.2	Characterization of activated carbon.....	36
3.2.3	Adsorption equilibrium isotherm experiments.....	37
3.2.4	Adsorption kinetics studies	38
3.2.5	Effect of variables on adsorption	38
3.2.6	Parameters of optimization	39
3.2.7	Fixed-bed column experiment.....	40
3.2.8	Analytical methods.....	41
3.3	Electrocoagulation process	41
3.3.1	Electrodes preparation.....	41
3.3.2	Comparison of anode configurations	41
3.3.3	Parameters optimization.....	43
3.3.4	Analytical methods.....	44

3.4	Combined process of adsorption and electrocoagulation	44
3.4.1	Experimental setup	44
3.4.2	Evaluation and optimization parameters	45
3.4.3	Analytical methods.....	46
 CHAPTER 4: RESULTS AND DISCUSSION		47
4.1	Adsorption RB5 on commercialized palm shell activated carbon.....	47
4.1.1	Characteristics of palm shell activated carbon.....	47
4.1.2	Equilibrium isotherms.....	48
4.1.3	Adsorption kinetics	50
4.1.3.1	Effect of initial dye concentration.....	50
4.1.3.2	Effect of temperature.....	54
4.1.3.3	Effect of pH.....	57
4.1.3.4	Effect of adsorbent dose.....	58
4.1.3.5	Effect of coexisting anion	59
4.1.4	Response Surface Methodology (RSM)	60
4.1.4.1	Development of regression equation and statistical analysis	60
4.1.4.2	Interaction effect of parameters.....	63
4.1.4.3	Optimization operating conditions.....	64
4.1.5	Column experiments	64
4.2	Electrocoagulation of RB5 by iron mesh.....	66
4.2.1	Anode configurations	66
4.2.2	Response Surface Methodology (RSM)	71
4.2.2.1	Development of regression equation and statistical analysis	71
4.2.2.2	Interaction effect of parameters.....	75
4.2.2.3	Optimization operating conditions.....	81
4.2.2.4	Zeta potential.....	83
4.3	Combined adsorption and electrocoagulation process to treat RB5.....	84
4.3.1	Effect of process parameters	84
4.3.1.1	Effect of pH.....	84
4.3.1.2	Effect of current density.....	86

4.3.1.3	Effect of adsorbent dose.....	87
4.3.1.4	Effect of initial RB5 concentration	88
4.3.2	Response Surface Methodology (RSM)	90
4.3.2.1	Development of regression equation and statistical analysis	90
4.3.2.2	Effect of the parameters on RB5 removal.....	94
4.3.2.3	Optimization operating conditions.....	96
4.3.3	Sludge analysis.....	100
4.3.4	Effluent analysis.....	103
4.3.5	Comparison studies	106
 CHAPTER 5: CONCLUSIONS AND RECOMMENDATIONS.....		108
5.1	Conclusions	108
5.2	Recommendations.....	110
REFERENCES.....		112
LIST OF PUBLICATIONS AND PAPERS PRESENTED		124
APPENDIX.....		126

LIST OF FIGURES

Figure 2.1: Reactive Black 5 dye (RB5)	11
Figure 2.2: Mechanism of adsorption	19
Figure 2.3: Possible interaction contributing to the mechanism of methylene green 5 adsorption on activated charcoal	20
Figure 2.4: A general method to prepare activated carbon from agricultural waste	23
Figure 2.5: Schematic of electrocoagulation process	27
Figure 2.6: Structure of EDL	29
Figure 2.7: Mole fraction of hydrolysed Fe(III) species versus different pH	32
Figure 3.1: Experimental flow-chart of the adsorption, electrocoagulation, and combined adsorption/electrocoagulation experiments	35
Figure 3.2: Schematic diagram of (i) single layer electrode and (ii) double layer electrode	42
Figure 3.3: Experimental setup of combined process	45
Figure 4.1: SEM image of palm shell activated carbon	47
Figure 4.2: Langmuir and Freundlich adsorption isotherms of RB5 dye on activated carbon at pH 2, 6, and 10	49
Figure 4.3: Kinetics for adsorption of RB5 by palm shell activated carbon at various dye concentrations and a constant temperature of 28 °C	51
Figure 4.4: Weber and Morris intra-particle diffusion plot 28 °C	54
Figure 4.5: Kinetics for RB5 adsorption at various temperatures	56
Figure 4.6: Plot of $\ln k_1$ versus $1/T$	56
Figure 4.7: Effect of pH on RB5 removal by palm shell activated carbon	58
Figure 4.8: Effect of adsorbent dose on RB5 removal by palm shell activated carbon ..	59
Figure 4.9: Effect of competitive adsorption on RB5 removal by palm shell activated carbon	60

Figure 4.10: Predicted RB5 removal efficiency from the response surface model against experimental adsorption data	63
Figure 4.11: Interaction between initial pH solution and adsorbent dose on RB5 adsorption.....	64
Figure 4.12: Breakthrough curve at different RB5 concentration.....	65
Figure 4.13: Comparison of anode configuration on RB5 removal.....	67
Figure 4.14: Kinetic analysis for single and double layer electrode	67
Figure 4.15: Chronoamperometry of iron mesh single and double layer electrodes in blank (0.2 g/L NaCl) and RB5 solution (0.2 g/l NaCl + 40 mg/L RB5 dye).....	69
Figure 4.16: Predicted RB5 removal efficiency from the response surface model against experimental electrocoagulation data.....	73
Figure 4.17: Response surface plot of RB5 removal efficiency (a) interaction between pH and electrocoagulation time, (b) interaction between pH and electrolyte dose, (c) interaction between electrolyte dose and current density, (d) interaction between current density and electrocoagulation time.....	76
Figure 4.18: Predominance-zone diagrams for Fe(III) chemical species in aqueous solution (Şengil & Özacar, 2009)	79
Figure 4.19: UV-Vis spectra of RB5 before and after treatment	82
Figure 4.20: Changes in zeta potential with time at optimum conditions of the EC process	84
Figure 4.21: Effect of pH on RB5 removal by combined process ($C_0 = 40$ mg/L, current density = 2.33 mA/cm ² , adsorbent dose = 15 g/L, agitation = 160 rpm).....	86
Figure 4.22: Effect of current density on RB5 removal by combined process ($C_0 = 40$ mg/L, pH = 6 , adsorbent dose = 15 g/L, agitation = 160 rpm)	87
Figure 4.23: Effect of adsorbent dose on RB5 removal by combined process ($C_0 = 40$ mg/L, pH = 6 , current density = 2.33 mA/cm ² , agitation = 160 rpm)	88
Figure 4.24: Effect of initial RB5 concentration on RB5 removal by combined process ($C_0 = 40$ mg/L, pH = 6 , current density = 2.33 mA/cm ² , agitation = 160 rpm).....	89
Figure 4.25: Comparison of combined process with individual adsorption and electrocoagulation (pH = 6 , current density = 2.33 mA/cm ² , adsorbent dose = 15 g/L)	90

Figure 4.26: Predicted RB5 removal efficiency from the response surface model against experimental combined process data	91
Figure 4.27: Response surface plot of combined process (a) interaction between pH and current density	95
Figure 4.28: Comparison of RB5 removal efficiency of optimum combined and individual adsorption and electrocoagulation process.....	97
Figure 4.29: FESEM image of sludge in A-EC process	100
Figure 4.30: Total ion chromatogram of the final treated solution from GC-MS analysis	104
Figure 4.31: GC-MS spectrum of Caprolactam (at retention time = 13.5 min).....	104
Figure 4.32: Proposed reaction pathway for the degradation of RB5 dye	105

University of Malaya

LIST OF TABLES

Table 2.1: Advantages and disadvantages of the existing methods for RB5 removal	18
Table 2.2: Comparison between physisorption and chemisorption	21
Table 2.3: Comparison of Adsorption Capacity of RB5 Adsorption by Various Agricultural Waste-based Activated Carbons	26
Table 2.4: Summary electrocoagulation of RB5 using iron as anode material of RB5 ..	33
Table 3.1: Parameters of adsorption and their corresponding levels	40
Table 3.2: Parameters of electrocoagulation and their corresponding levels.....	44
Table 3.3: Parameters of combined process and their corresponding levels	46
Table 4.1: Properties of palm shell activated carbon	47
Table 4.2: Langmuir and Freundlich Isotherm Model parameters and correlation coefficients for RB5 adsorption	49
Table 4.3: Comparison of adsorption capacity of RB5 adsorption by various agricultural waste-based activated carbons	50
Table 4.4: Kinetic model parameters for various initial dye concentrations at 28°C	52
Table 4.5: Parameters of Intra-Particle Diffusion Model.....	54
Table 4.6: Kinetic model parameters for different temperatures with a RB5 concentration of 40 mg/L.....	56
Table 4.7: Central composite design for experimental and predicted RB5 removal	61
Table 4.8: ANOVA results for the fitted model.....	62
Table 4.9: Column parameters for RB5 adsorption onto palm shell-based activated carbon	65
Table 4.10: Performance summary for the single and double layer electrode.....	70
Table 4.11: Comparison between different anode configurations for electrocoagulation of RB5	70
Table 4.12: Central composite design for experimental and predicted RB5 removal	72
Table 4.13: ANOVA results for the fitted model.....	74

Table 4.14: Central composite design for experimental and predicted RB5 removal	92
Table 4.15: ANOVA results for the fitted model.....	93
Table 4.16: Performance summary for the single adsorption, electrocoagulation and combined process under optimum conditions.....	100
Table 4.17: XRD data of the sludge collected after the combined process	101
Table 4.18: Comparison between different combined approaches for the removal of RB5 dye solution	106

University of Malaya

LIST SYMBOLS AND ABBREVIATIONS

q_e	:	Calculated adsorption capacity (mg/g)
q_m	:	Maximum monolayer adsorption capacity (mg/g)
q_{exp}	:	Experiment adsorption capacity (mg/g)
q_b	:	Breakthrough adsorption capacity (mg/g)
q_s	:	Saturation adsorption capacity (mg/g)
b	:	Langmuir constant (L/mg)
C_e	:	Equilibrium concentration of the adsorbate (mg/L)
m	:	Mass of dry adsorbent used (g)
K	:	Freundlich constant (mg/g)(L/mg)
k_1	:	Rate constant of pseudo-first-order adsorption (min^{-1})
k_2	:	Rate constant of pseudo-second-order adsorption (g/mg min)
k_{ind}	:	Intra-particle diffusion rate constant ($\text{mg/g min}^{-0.5}$)
I	:	Boundary layer thickness (mg/g)
X	:	Amount of the adsorbent packed in the column (g)
n	:	Number of electrons
A	:	Surface area of electrode (cm^2)
D	:	Diffusion coefficient (cm^2/sec)
I	:	Current (A)
RB5	:	Reactive Black 5
A-EC	:	Combined process of adsorption-electrocoagulation
DLVO	:	Derjaguin-Landau-Verwey-Overbeek
RSM	:	Response Surface Methodology
CCD	:	Central Composite Design
ANOVA	:	Analysis of variance

SVI	:	Sludge volume index
EEC	:	Electrical energy consumption (EEC, kWh/kg dye removed)
XRD	:	X-ray diffraction
FESEM	:	Field Emission Scanning Electron Microscope
GC:MS	:	Gas Chromatography Mass Spectroscopy
BJH	:	Barrett-Joyner-Halenda method
SS	:	Sum of squares
MS	:	Mean of square
AP	:	Adequate precision
SD	:	Standard division

University of Malaya

CHAPTER 1: INTRODUCTION

1.1 Introduction

Water is vital in a human's daily life. It is used widely in agricultural, industrial, household, recreational and environmental activities. However, toxic effluent in industrial wastewater is a major contributor to water pollution. There are rising concerns among the public on the health consequences particularly caused by the wastewater discharge from the textile industry. The textile industry is the highest water consuming industry and produces a large amount of wastewater containing a variety of pollutants (Ghaly, Ananthashankar, Alhattab, & Ramakrishnan, 2014). Some of these pollutants are non-biodegradable and carcinogenic.

Reactive dye is widely used in textile industry and comprises about 20 to 30% of the total dye market which mainly due to its vivid colours and attach easily to a fibre polymer. The global usage of reactive dye is increasing dramatically to be more than 200% over the last 16 years (Ghaly et al., 2014). Reactive Black 5 dye (RB5) is commonly used in textile industry for dyeing of cotton, woollen and nylon fabrics. It contributes up to 50% of the total world demand for reactive dye (Schumacher, 2012).

However, due to the relatively low fixation of reactive dye on fibre during the dyeing process, high amounts of dye are released into the dye bath effluent. Excessive amounts of reactive dye discharged into receiving bodies are dangerous and threatening the aquatic environments and human health (El-Zawahry, Abdelghaffar, Abdelghaffar, & Hassabo, 2016). Thus, introducing the step to eliminate the RB5 from textile wastewater is essential before discharging the effluent into the aquatic environment.

Several treatment processes have been successfully used in the past to remove RB5 from wastewater which includes membrane filtration, ion exchange, adsorption, coagulation, flocculation, biological treatment, advanced oxidation process (AOP) and

electrochemical treatment where each method has its own advantages and disadvantages. For example, despite their respective advantages, the use of membrane filtration is affected by the fouling problem; while chemical coagulation method requires the coagulants to be added externally. The lack of successful biological treatment probably due to the fact that the reactive dye is recalcitrant compounds which are difficult to be degraded by the microorganism. While the AOP's require a higher cost to implement the process (Gowri, Vijayaraghavan, & Meenambigai, 2014). Thus, there is a need to develop methods with low cost, easy to operate, high effectiveness and applicability on large scales to treat the RB5 solution.

Among the techniques mentioned, adsorption and electrocoagulation are the more efficient methods for RB5 removal from aqueous solution. Adsorption is widely used for textile wastewater treatment due to its high removal efficiency and no sludge produced at the end of the process. The typical adsorbent material is activated carbon, which has a large specific surface area ranging from 600 to 2000 m²/g (Grassi, Kaykioglu, Belgiorno, & Lofrano, 2012). Thus, it could adsorb different types of dyes and organic compounds. However, the cost of activated carbon is relatively high, which may limit its application for industrial purposes.

At present, the conversion of agricultural wastes into activated carbon for wastewater treatment has been intensively investigated because the amount of biomass that converted to a new adsorbent is leading to new ways of handling agricultural waste and treat wastewater. The development of activated carbon from biomass is considered as environmentally friendly alternatives and allows the reduction of the cost of waste disposal (Ani, 2004; Hoseinzadeh Hesas, Arami-Niya, Wan Daud, & Sahu, 2013). In Malaysia, palm trees are planted on a large scale and approximately 77% of the agricultural land is used for palm oil plantations (Palm oil, 2014). The waste, such as palm shell from palm fruit processing is burned in the open air or used as boiler fuel to produce

steam in the mill (Issabayeva, Aroua, & Sulaiman, 2006). This contributes to the air pollution and raises public concerns. Hence, the usage of palm shell for the production of activated carbon could reduce the abundant waste and be beneficial for treatment costs.

Electrocoagulation is an alternative method for treatment textile dyeing wastewater (Nandi & Patel, 2013). The electrocoagulation process has distinct advantages over conventional chemical coagulation. It is simple, requires low-cost equipment and efficient since the coagulant is produced in situ through electro-oxidation of a sacrificial anode (Garg & Prasad, 2016). Furthermore, electrocoagulation is characterized by low sludge generation and with no secondary pollution, as the process is completed without an addition of any chemical coagulants (Mollah, et al., 2004). The electrocoagulation process typically involves three mechanisms: (i) production of coagulants by electro-oxidation of the sacrificial anode; (ii) destabilization of the contaminants, particle suspension and breaking emulsions; and (iii) aggregation of the destabilized phases to form flocs (Gomes et al., 2007).

There are many factors that affect the performance electrocoagulation of RB5 from aqueous solution. The main factors are current density, electrode material, electrolyte specifications (electrolyte concentration, pH, and temperature) and cell design. However, one of the crucial factors influencing the electrocoagulation process is the configuration of the anode. Several studies have been conducted for dye removal with the use of different anode shapes such as a plane and mesh (Del Río, Benimeli, Molina, Bonastre, & Cases, 2012; Méndez-Martínez et al., 2012; Mohan, Balasubramanian, & Basha, 2007; Nandi & Patel, 2013; Pajootan, Arami, & Mahmoodi, 2012). A mesh type electrode produces a higher discharge current than a plane type due to a higher electric field intensity at the edge of the mesh holes (Kuroda et al., 2003). Moreover, the mesh produces a larger specific surface area than a flat sheet which could boost the formation of iron hydroxides.

Electric current applied to the system is one of the important parameters in the electrocoagulation process. According to the Faraday's law, the formation of coagulant from the cation of dissolved iron is directly proportional to the electric current. Nevertheless, the operating costs related to the price of the electric current may limit its application. Hence, the optimum electric current needs to be investigated as it is one of the important factors that affect the lifespan of the electrodes and electricity cost.

The optimum operating parameters could be investigated by response surface methodology (RSM). RSM is a useful tool to investigate the interaction of all parameters and optimize the performance of the process. In addition, RSM will produce a regression model equation which can be used for design purpose. Suitable ranges of the operating parameters should be determined prior to the RSM study.

The sequential of two processes is getting popular to overcome the drawbacks of individual unit operation and improve overall treatment performance. Few researchers have proved that sequential process is efficient in term of removal efficiency and cost. Raghu and Basha (2007) using the electrocoagulation followed by an ion-exchange process for the removal of textile dye. Their results showed that the sequential process was very effective and the effluent fulfilled the reuse standard requirement of the textile industry in India (Raghu & Ahmed Basha, 2007). Furthermore, most of the sequential processes were coupled with coagulation and adsorption for the removal of reactive dye, with a high decolourization and chemical oxygen demand removal efficiency (Lee, Choi, Thiruvengkatachari, Shim, & Moon, 2006; Papić, Koprivanac, Lončarić Božić, & Meteš, 2004). There is limited research available in the literature on the sequential treatment process of adsorption and electrocoagulation on RB5 removal, which only investigated by Chang et al. (2010). They tested the electrocoagulation followed by adsorption process. The results found that the sequential process was more efficient to remove

recalcitrant dye from aqueous solution than the electrocoagulation carried out as a single process (Chang et al., 2010).

1.2 Problem statement

Wastewater discharge from dye manufacturing and textile industries has become a global concern and is one of the major causes of environmental pollution. To provide clean and safe water resources in the future, treatment of textile wastewater has become a necessity. In previous studies, membrane filtration, coagulation, flocculation and biological treatments were used to treat RB5. However, each technique has its own drawbacks. For instance, the working principle of coagulation process is adding an external coagulant such as alum and ferric to destabilize colloidal contaminants and then aggregate the particles. However, the coagulant is relatively expensive and generate a large amount of sludge (Ashtekar et al., 2014). In this regard, a low cost, easy to operate and green technology is introduced in the present study. The combined process of adsorption and electrocoagulation (A-EC) provides better alternatives to treat recalcitrant dye wastewater. The typical adsorbent material is activated carbon, which has successfully adsorbed variety types of dyes and organic compounds. At present, the conversion of agricultural wastes into activated carbons for wastewater treatment purpose has been intensively investigated because the amount of biomass for the production of a new adsorbent is leading to new ways of handling waste and treat wastewater. To the best of my knowledge, usage of commercially available palm shell activated carbon in the removal of RB5 has not yet reported in the open literature. The electrocoagulation process is commonly used to remove colour and high organic compounds. Its treatment cost is low cost as it generates coagulant in-situ through electro-oxidation of the sacrificial anode and no chemical additions. The iron mesh electrode used in this work is a new novel anode and never been tested for the electrocoagulation process. The combined process of adsorption and electrocoagulation in a single reactor is tested for the first time to eliminate

RB5 from aqueous solution. As such, this research is the first of its kind to evaluate the performance of commercialized palm shell activated carbon, iron mesh electrode and combined system to remove RB5 from the aqueous solution.

1.3 Research objectives

The aim of this work is to develop and investigate a combined process to remove recalcitrant dye from aqueous solution. The main objectives of this research are as follows:

1. To investigate the adsorption performance of commercialized palm shell activated carbon in RB5 removal.
2. To evaluate the performance of different configurations of iron mesh electrode in removing RB5 by electrocoagulation.
3. To develop a new process consisting of a combined adsorption and electrocoagulation (A-EC) for the removal of RB5.
4. To optimize and compare the efficiency of adsorption, electrocoagulation and combined process for the RB5 removal.

1.4 Scope of research

This work focuses on the combined treatment process of adsorption and electrocoagulation for Reactive Black 5 dye removal from aqueous solution. RB5 was chosen as the model dye because it is a common reactive dye which is primarily used in textile industry and known as a recalcitrant compound. The commercialized palm shell activated carbon was used as the adsorbent. The properties of the adsorbent such as surface area, pore diameter, pore volume and pH of zero charges were examined. Furthermore, the effect of initial dye concentration, temperature, solution pH, adsorbent dose and the presence of coexisting anion on RB5 adsorption efficiency was investigated. The electrocoagulation was conducted by using a new iron mesh double layer electrode

to investigate the effect of pH, current density, supporting electrolyte and process time on RB5 removal. The parameters of A-EC were analysed and compared with adsorption and electrocoagulation which was performed individually. Response Surface Methodology (RSM) was used to investigate the interaction between the parameters and optimum condition.

1.5 Outline of research

The thesis consists of five chapters describing different aspects relevant to the topic.

Chapter 1: Introduction

This part encompasses the introduction of the research background, objectives and scope of research.

Chapter 2: Literature review

This chapter reviews the traditional treatment methods, advanced oxidation process and electrochemical technology applied for RB5 removal from textile wastewater. A brief assessment of operating parameters in adsorption and electrocoagulation is included as well.

Chapter 3: Methodology

This part demonstrated descriptive information about chemicals, materials and experimental techniques used in the study. The analysis techniques such as UV-Vis spectrophotometer, COD, and GC-MS for determination concentration of RB5 and degradation products are presented in this chapter.

Chapter 4: Results and Discussion

This chapter is divided into three parts. The first part describes the properties of commercialized palm shell activated carbon, equilibrium isotherms, and adsorption kinetics studies. The second part gives results on the comparison of iron mesh double layer with

different iron electrode configurations and optimization results. The last part of this work discusses the performance of combined process and compares with adsorption and electrocoagulation performed as individual processes.

Chapter 5: Conclusions and Recommendations

This chapter concludes all findings in this research and recommends potential suggestions for further investigation.

University of Malaya

CHAPTER 2: LITERATURE REVIEW

2.1 Textile industry

The textile industry is one of the oldest and largest global industries. The importance of the industry can be seen in terms of trade, gross domestic product (GDP) and employment, especially in developing countries (Keane & De Velde, 2008). The top textile exporters worldwide in 2013 were China, India, Italy, Germany, Bangladesh, and Pakistan (Textile, 2016). In 2015, Malaysia was the textile industry tenth largest export earner, contributing 1.7% to Malaysia's total exports of manufactured goods (MIDA, 2017).

Wastewater from the textile industry is considered as one of the major causes of environmental pollution. It is the highest water consuming industry and produces a large amount of wastewater. The water consumption during the dyeing and finishing textile is about 0.08-0.15 m³ to produce 1kg of fabrics (Ghaly et al., 2014). During the dyeing process, there is a portion of dye unfixated to the fabrics and found in the textile effluents. The effluent of these industries consists of various contaminants such as acids, bases, dissolved solids, toxic compounds and colour materials (Kobyas, Demirbas, Can, & Bayramoglu, 2006). Some of these compounds are non-biodegradable and carcinogenic which pose threat to public health and environment.

According to the Malaysian Department of Environment (DOE), approximately 160,000 tons of textile industrial wastewater were discharged within the year 2011 to 2012 and the amount continues to increase annually (DOE, 2012). Thus, the treatment of textile wastewater to a permissible discharge concentration is essential before the release to the aquatic environment.

2.2 Reactive dye

Manufactured fabric can be classified into three main groups, namely cellulose fibres (cotton, rayon, linen, ramie, hemp, and lyocell), protein fibres (wool, angora, mohair, cashmere, and silk) and synthetic fibres (polyester, nylon, spandex, acetate, acrylic, ingeo and polypropylene). The use of dye in the textile industry depends on the fabric material. Reactive dye, direct dye, naphthol and indigo dye are typically used on cellulose fibres. Acid dye and lanaset dye are used to dye protein fibres. Synthetic fibres are dyed using dispersed dyes, basic dye and direct dyes (Ghaly et al., 2014).

Among the aforementioned dyes, reactive dye is extensively used on cellulose fibre especially cotton material. The global usage of reactive dye has recorded positive growth from 60,000 tons to 178,000 tons from 1988 to 2004 (Ghaly et al., 2014; Philips, 1996). In addition, reactive dye is renowned for its vivid colours (Hassan, Awwad, & Aboterika, 2009). It is predicted that the consumption of reactive dye to continue increasing in the future.

However, the relatively low fixation of reactive dye on cellulose fibres during the dyeing process resulted in the high amount of dye (20 to 50%) released into the dye bath effluent (Wallace, 2001). When excessive amounts of reactive dye discharge into receiving waters, it is very dangerous and may pose a serious threat to the aquatic ecosystem. The coloured body of water can limit the penetration of sunlight to disrupt the aquatic plants to perform photosynthesis, by which the released oxygen is important to many aquatic creatures to survive. Moreover, this dye is mutagenic and carcinogenic and thus may cause a severe harm to the human body, especially the liver, digestive and central nervous system (El-Ashtoukhy, Amin, & Abdel-Aziz, 2012). Reactive dye in dyeing wastewater is known as recalcitrant compounds as it has high alkalinity, a high concentration of organic compounds and strong colour compared to other dyes (Barka, Qourzal, Assabbane, Nounah, & Ait-Ichou, 2010).

Reactive Black 5 (RB5) is a diazo acidic reactive dye consist of two sulfonates and two sulfato-ethylsulfon groups (Figure 2.1). It is typically used in textile industries for dyeing cotton fabrics (Elwakeel, El-Kousy, El-Shorbagy, & El-Ghaffar, 2016). In addition, RB5 has a recalcitrant nature and contributes to 50% of the total world demand for reactive dye (Schumacher, 2012).

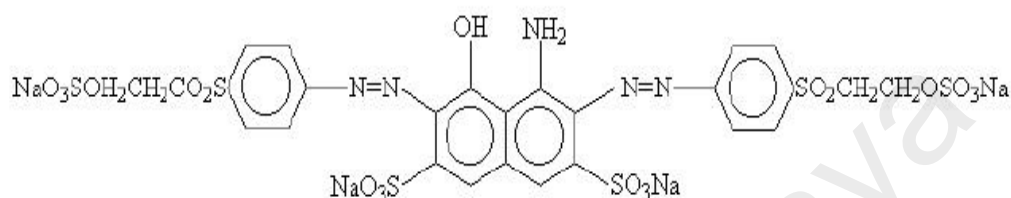


Figure 2.1: Reactive Black 5 dye (RB5)

2.3 RB5 removal methods

Available techniques for removal of RB5 are generally divided into physical, chemical, biological and electrochemical methods as well as advanced oxidation process (AOP). The physical treatment includes membrane filtration, ion exchange, and adsorption, whereas the chemical method is coagulation. All the treatments have their own advantages and disadvantages which are briefly reviewed.

2.3.1 Physical methods

Membrane filtration is one of the methods used for treating wastewater containing dye due to its simplicity and highly selective separation. In addition, it is suitable for removing ions from textile wastewater with high efficiency. For instance, Saffaj et al. (2006) used ultrafiltration membranes consisting of a support layer made of clay, a zirconia interlayer and a $\text{TiO}_2/\text{ZnAl}_2\text{O}_4$ top layer to treat methylene blue solution. They found that the rejection of methylene blue was 85% at pH 2 of the filtered solution. Majouli et al. (2012) prepared microfiltration tubular membrane made of Moroccan Perlite. They proved that the Moroccan Perlite was efficient as material for membrane to treat textile effluent of

jeans washing process. However, the main drawback of membrane process is the clogging of the dye on the membrane after prolong usage, which can be quite costly (Mimi, Ismail, Illias, & Hassan, 2007).

Ion exchange method is carried out by passing the wastewater through the ion exchange resins and then the ions (cations/anions) in the solution will be exchanging with the particular ions within the resin. The resins are insoluble substances containing loosely held ions which can be exchanged with other ions in solutions. The resins are highly ionic, covalently cross-linked and insoluble polyelectrolytes. It can be classified based on the exchangeable cation or anion and the ionic strength of the bound ion (Wawrzekiewicz & Hubicki, 2015). Karcher et al. applied the anion exchange resins for removal of reactive dye from textile wastewater. They found that the anion exchange resins have excellent adsorption capacity and regeneration characteristic (Karcher, Kornmüller, & Jekel, 2002). Nevertheless, ion exchange process is rather difficult to put into practice as wastewater contains calcium, iron, organic matter and chlorine. The performance of ion exchange can be lack due to the clogging the resin beads which affect the ion exchange performance (Alchin, 2008).

Adsorption has greater advantages compared with other methods because of simple design and low investment costs (Rashed, 2013). The application of adsorption process in textile wastewater treatment has become popular due to its practical and economical approach.

2.3.2 Chemical methods

The coagulation process occurs when the coagulant is added to the solution and mixed rapidly to destabilize colloidal contaminants in order to aggregate the particles. The pollutant particles carrying negative surface charges, which repulse each other. The coagulant which carries positive charged are introduced to the solution to destabilize the negative charges on the particles. Then, the particles aggregate and form larger groups,

which are easier to be removed. Following coagulation, the sedimentation is used to remove these aggregated particles from the mixture.

The typical coagulants used for textile wastewater treatment are alum, lime, ferric or ferrous sulphate and polyaluminum chloride. There are two coagulation mechanisms: adsorptive coagulation and precipitation coagulation. In adsorptive coagulation, colloids are adsorbed to the positively charged FeOH^{2+} and FeOH_2^+ . The dosing of coagulant is proportional to the removal of contaminants, and the re-stabilization could occur after overdosing it. It means that the overdose of coagulant stimulates the colloids become positively charged and repulsion of the particles takes place. In precipitation coagulation or sweep coagulation, the colloids are integrated into iron hydroxide flocs. The dose of coagulant required in precipitation coagulation is higher than the adsorptive coagulation in order to form hydroxide flocs (Water treatment, 2017).



Most of the cases coagulation gave a positive result in colour removal efficiency. However, the costs of coagulants and generation of the sludge resulted in the employment of chemical coagulation for decolorizing wastewater is not economically justified (Ashtekar et al., 2014; Mook, Ajeel, Aroua, & Szlachta, 2016).

2.3.3 Biological methods

Biological treatment is more environmentally friendly as there would be no secondary pollution and it is an inexpensive alternative when compared with physical and chemical methods. Bioaccumulation and bio-sorption are the two main technologies utilized for treatment of textile industry effluents. Bioaccumulation mechanism works by using living cells to uptake the pollutants; while in bio-sorption, the toxicants are uptake by non-living or inactive biological materials. The use of bio-sorption is more advisable than

bioaccumulation because living organisms are not suitable for continuous treatment of highly toxic effluents. This issue can easily be solved by utilizing the non-living biomass, which is flexible to environmental conditions and toxicity concentrations (Vijayaraghavan, Basha, & Jegan, 2013).

Referring to oxygen requirement, biological methods can be further categorized into aerobic and anaerobic. In the aerobic process, the microbes carry out the treatment in the presence of oxygen, while the anaerobic method refers to the treatment process in the absence of oxygen (Holkar, Jadhav, Pinjari, Mahamuni, & Pandit, 2016). The sequential anaerobic-aerobic system is typically implemented in practice. The anaerobic decolorize through reduction cleavage of the azo linkages resulting in the formation of colourless and toxicant aromatic amines. Then, these amines could be biotransformed under aerobic conditions (Popli & Patel, 2015).

Since most textile dyes are either low or non-biodegradable, it would be difficult for biological treatment to achieve the desired treatment result. Hence, biological process is often used in combination with another treatment process such as (Khatri, Peerzada, Mohsin, & White, 2015).

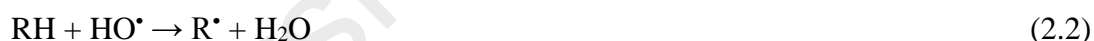
2.3.4 Advanced oxidation process

Advanced oxidation process (AOP) such as ozonation, Fenton process, and photocatalytic process UV/TiO₂ have received attention in textile wastewater treatment. These processes are based on the generation of hydroxyl radicals (HO[•]) which capable of destroying a wide range of organic pollutants (Qiu, Shou, Ren, & Jiang, 2014).

Ozone wastewater treatment is effective in decolorizing textile effluents. An ozone generator required to convert oxygen into ozone by using ultraviolet radiation or electric discharge field. Ozone is a very reactive gas that can oxidize bacteria, molds, organic matter and other pollutants found in water. Moreover, there are no unpleasant odours or residues found after the treatment (Oram, 2014). Few researchers have proved that RB5

could be removed effectively by ozonation process (Colindres, Yee-Madeira, & Reguera, 2010; Zheng, Dai, & Han, 2016). However, ozone treatment might produce by-products which are carcinogenic such as bromate, aldehydes, ketones and carboxylic acids. Hence, the membrane filtration system is usually placed before discharging the final treated effluent to the environment (Oram, 2014).

Among the AOPs, Fenton's process is widely used due to its simplicity, moderate cost, and no special equipment. Fenton's reagent is a homogeneous catalytic oxidation process using hydrogen peroxide (H_2O_2) and ferrous ion (Fe^{2+}). The ferrous ion initiates and catalyses the H_2O_2 to generate hydroxyl radicals, HO^\bullet (Equation 2.1). The radicals are more powerful oxidation agents than ozone and H_2O_2 . They react rapidly with organic pollutants (RH) and then chemically decompose these substances by H-abstraction and addition to C-C unsaturated bonds (Equation 2.2 to 2.4) (Lucas & Peres, 2006). Fenton's reagent could completely destruct contaminants to harmless compound, e.g. CO_2 , water and inorganic salts (Pawar & Gawande, 2015).



The addition of UV light to Fenton's process (photo-Fenton) could accelerate the RB5 degradation process since the UV light has an influence on the direct formation of HO^\bullet radicals (Lucas & Peres, 2006). The generation of HO^\bullet radicals is the pH dependent. At a pH below 2, the H_2O_2 becomes stable and as a result, the reactivity with ferrous ions and hydroxyl radicals reduce. While at a pH above 4, the decolourization decreases because iron starts to precipitate in the form of hydroxide (Modirshahla, Behnajady, & Ghanbary, 2007). Liu et al, (2011) had concluded that the optimum pH for Fenton decolorize RB5 was under acidic condition, pH 2.5 (Liu, Qiu, & Huang, 2011).

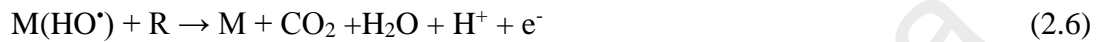
Heterogeneous photocatalysis has been considered as a promising technology for removal of dye containing wastewater. The semiconductor catalysts such as TiO_2 , ZnO , Fe_2O_3 , CdS , GaP and ZnS give a positive conversion of refractory organics into biodegradable compounds, and eventually into carbon dioxide and water. TiO_2 is the most active photocatalyst under the photon energy of 300 nm to 390 nm and remains stable after the catalytic cycles, while CdS and GaP are degraded along to produce toxic products. In addition, TiO_2 is resistance to chemical breakdown and has strong mechanical properties. This promotes TiO_2 has received the greatest attention in photocatalytic wastewater treatment (Chong, Jin, Chow, & Saint, 2010). However, the separation of TiO_2 from the suspension after wastewater treatment is the main drawback and obstacle the process development in industry (Aguedach, Brosillon, Morvan, & Lhadi, 2005).

2.3.5 Electrochemical technology

In the past two decades, the electrochemical method has been introduced and widely used in the water treatment. This method is based on the usage of electric current to induce redox reactions to transform, destruct and complete oxidation organic compounds to CO_2 and H_2O (Vijayaraghavan et al., 2013). The advantages of the electrochemical treatment include high removal efficiency, clean energy conversion, easy operation and compact facilities. Electrochemical methods such as electrooxidation and electrocoagulation are successful in removing dye from containing wastewater, but the rate of degradation pollutants depends mainly on electrode materials, cell design, pH, concentration of pollutants, electric current and supporting electrolyte (Soni & Ruparelia, 2013).

Electrochemical oxidation can be divided into the direct and indirect process. Anodic direct oxidation refers to the pollutant oxidized directly at anode surface through physically adsorbed hydroxyl radicals, $\text{M}(\text{HO}^\bullet)$. The reactions of degradation pollutant are given by Equation 2.5 and 2.6 (Rivera, Pazos, & Sanromán, 2011). The indirect

electro-oxidation is achieved using oxidizing agents such as sodium chloride. Chloride oxidizes form chlorine (Cl₂) and further reacts with water to produce hypochlorous acid (HOCl) and hypochlorite ions (OCl⁻). Then, hypochlorite ions oxidize the pollutant to produce carbon dioxide (Equation 2.7 to 2.10) (Mook, Aroua, & Issabayeva, 2014; Rivera et al., 2011).



Electrocoagulation is a popular technique used for the treatment of textile dyeing wastewater. The removal mechanism is similar to chemical coagulation, but the coagulant is produced in situ by electrolytic oxidation of sacrificial anode (Merzouk, Gourich, Madani, Vial, & Sekki, 2011). The typical anode materials for electrocoagulation process are iron and aluminum.

Each method has its merit and drawback which are summarized in Table 2.1 (Gowri et al., 2014). Membrane filtration, ion exchange, and AOP do not seem to be economically feasible because of their relatively high investment and operational cost (Rashed, 2013). Among these techniques, adsorption and electrocoagulation are the more efficient methods for the removal dye containing wastewater. Both methods are simple in design and require low investment cost, which attracts great attention from the researchers.

Table 2.1: Advantages and disadvantages of the existing methods for RB5 removal

Methods	Advantages	Disadvantages
Membrane filtration	Applied for all types of dye	Expensive, accumulated sludge generation, incapable for large-scale treatment
Ion exchange	Effective with no adsorbent loss	Economic constraints, not effective for all dyes
Adsorption on activated carbon	Effective	High cost of adsorbent
Coagulation and Flocculation	Simple, economically feasible	Large amount sludge production, handling and disposal problems
Biological	Low cost	Longer treatment time
Advanced oxidation process	No sludge production, little consumption of chemicals, efficiency for recalcitrant dyes	Higher cost
Fenton's reagent	Effective for both soluble and insoluble dyes	Fenton's reagent
Ozonation	No sludge generation	Short half-life (20 min)
Photochemical	No sludge generation	Formation of by-products
Electro-oxidation	Efficient process	High energy cost, formation of by-products

2.3.6 Adsorption

Adsorption technique is widely used in textile wastewater treatment as it is high in removal efficiency and produces no sludge. It is a rapid process of separation of adsorbate (dye) from wastewater by the porous material (adsorbent). Adsorption involves three mechanisms: (i) the adsorbate diffuses from the bulk phase to the adsorbent surface; (ii) the adsorbate migrates into the pores of the adsorbent material; (iii) the final step is the

adsorbate molecule binds to the surface of the pore and capillary spaces. Figure 2.2 illustrates the diffusion and adsorption process of a pollutant into the adsorbent (Myoung-Jun & Gyu-Hoon, 2012).

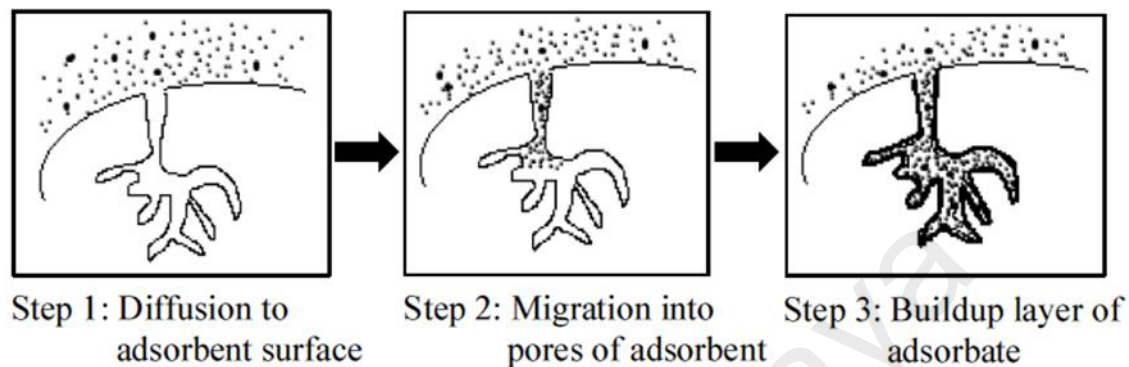


Figure 2.2: Mechanism of adsorption

2.3.6.1 Adsorption mechanism

There are few mechanisms proposed to interpret the dye adsorption on activated carbon, namely: electrostatic attraction, hydrogen bonding formation, $n-\pi$ interaction, pore filling and $\pi-\pi$ interaction. Electrostatic attraction plays a primary role in the adsorption mechanism (Tran, Wang, You & Chao, 2017). It is affected by the solution pH, which determines the surface charge of the adsorbent and ionization of the adsorbate.

Hydrogen bonding interaction could be divided into two types: (1) dipole-dipole H-bonding, which is between hydroxyl groups (H-donor) on the activated carbon surface and H-acceptor atoms (nitrogen and oxygen); (2) Yoshida H-bonding, between hydroxyl groups on the activated carbon surface and the aromatic rings of dye. The presence of dipole-dipole and Yoshida hydrogen bonding interactions could be observed through the shifting of $-\text{OH}$ peak in FTIR spectra after dye adsorption (Tran, Wang, You & Chao, 2017).

In $n-\pi$ interaction, oxygen groups on the activated carbon surface act as electron donors, while the aromatic rings of dye act as electron acceptors. The shifting of intensity C-O group peaks in FTIR analysis shows the presence of $n-\pi$ interaction. The $\pi-\pi$

interaction between the π -electrons in the activated carbon and the π -electrons in the aromatic ring of adsorbate is shown in Figure. 2.3, where methylene green was used as a model dye and commercial activated charcoal as an adsorbent (Tran, Wang, You & Chao, 2017). Huff and Lee (2016) used H_2O_2 to modify the properties of biochar. They found that addition of oxygen functional groups on the surface of biochar, resulted decreasing of adsorption of dye onto biochar surface. This is due to the overall dispersive force of π - π interactions have been turned weakened.

Activated carbon is a highly porous material with a large specific surface area. The decreasing of the specific surface area, total pore volume and pore size of activated carbon upon dye adsorption indicate that pore filling plays a significant role in dye adsorption mechanism (Lee, Liu, Juang, Wang, Lin & Lyu, 2007).

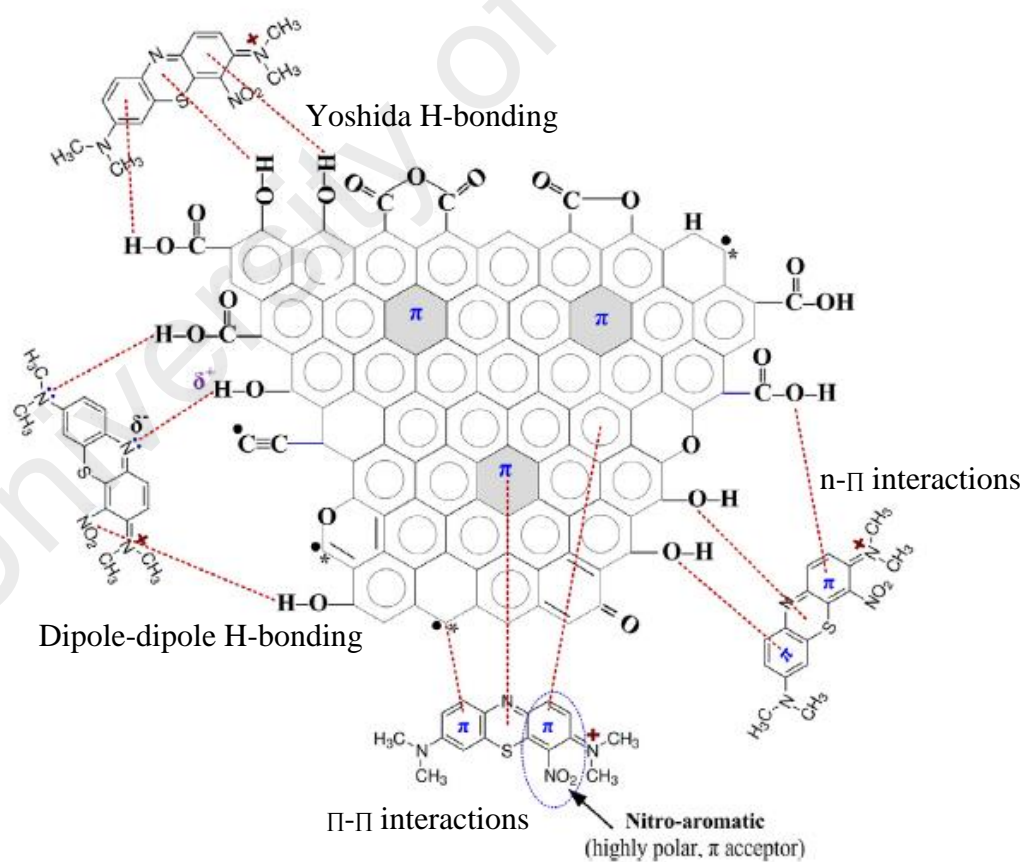


Figure 2.3: Possible interactions contributing to the mechanism of methylene green 5 adsorption on activated charcoal

The interaction of adsorbate and adsorbent is generally classified into physisorption and chemisorption. Physisorption or physical adsorption takes place when an atom or molecule adsorbs on the surface without formation of a chemical bond. This interaction is the result of van der Waals forces between the adsorbate and the adsorbent and small energy requirements (Forrest, 2012).

In chemisorption, atom or molecule is adsorbed onto the surface of adsorbent by forming a chemical bond. The adsorbent is covered by a monolayer of adsorbate (Forrest, 2012). The type of adsorption can be determined from the activation energy, where a low activation energy (less than 4 kJ/mol) suggest physical adsorption, and chemisorption is ranging from 8 to 80 kJ/mol (Ismaiel, Aroua, & Yusoff, 2013). Table 2.2 summarizes the characteristic of physisorption and chemisorption (Jaafar, 2006).

Table 2.2: Comparison between physisorption and chemisorption

Physisorption	Chemisorption
Van der Waals forces interaction	Strong chemical bond interaction
Low activation energy	High activation energy
Adsorption in monolayer or multilayer	Adsorption only in monolayer
Takes place in low temperature	Takes place at high temperature

2.3.6.2 Adsorbent

Activated carbon is the most commonly used adsorbent due to its large surface area, high adsorption capacity, and large pore volume. Activated carbon is prepared through physical and chemical activation methods. The physical activation process involved two stages, namely carbonization of the precursor and activation of the crude char (Baker, 1998). Carbonization stage is the conversion of organic matter to carbon element at a high temperature range from 500 °C to 900 °C. While the activation of crude char is to increase the adsorptive capacity by exposing the char to an oxidizing atmosphere in order to increase the pore volume. The typical activating agents are steam and carbon dioxide

(Yeganeh, Kaghazchi, & Soleimani, 2006). The chemical activation process refers to a condition when the carbonization stage and activation stage occurs simultaneously (Yacob, Majid, Dasril, & Inderan, 2008). It is conducted by using acids (Bhatnagar, Sillanpaa, & Witek-Krowiak, 2015). The activated carbons obtained by physical and chemical activation processes have a high porous structure with a large specific surface area varies in the range from 600 to 2000 m²/g (Grassi et al., 2012). However, the cost of activated carbon is relatively high, which limits its application in the industrial sector.

Researchers have started focusing on using activated carbons developed from waste materials to replace the conventional adsorbent (Hoseinzadeh et al., 2013). The waste materials include fertilizer industrial waste, sewage sludge, and agricultural waste. The conversion of agricultural wastes into adsorbent for wastewater treatment has been intensively investigated due to advantages of being environmentally friendly and would further reduce the cost of waste disposal (Ani, 2004). A variety of agricultural waste has been used as precursors of activated carbon to treat RB5, such as walnut wood, carob, bamboo, palm shell, coconut shell and rice husk (Ahmad & Hameed, 2010; Güzel, Saygılı, Akkaya Saygılı, & Koyuncu, 2015; Heibati et al., 2014; Khan, Chaudhuri, Isa, & Hamid, 2013; Nourouzi, Chuah, & Choong, 2009). The basic components of the agricultural waste include hemicelluloses, lignin, lipids, proteins, simple sugar, water, hydrocarbons, starch and variety of functional groups for the adsorption purpose (Bhatnagar et al., 2015).

The general method of preparation activated carbon from agricultural waste is shown in Figure 2.4. First, the agricultural waste is washed, crushed and sieved. Then, it is impregnated with chemical reagents such as KOH, H₃PO₄, and H₂SO₄ before carbonized at a high temperature in a furnace. Each impregnated sample undergoes activation with either physical (carbon dioxide gas), chemical or physiochemical methods. Lastly, it is dried to further remove water (Thomas & George, 2015).

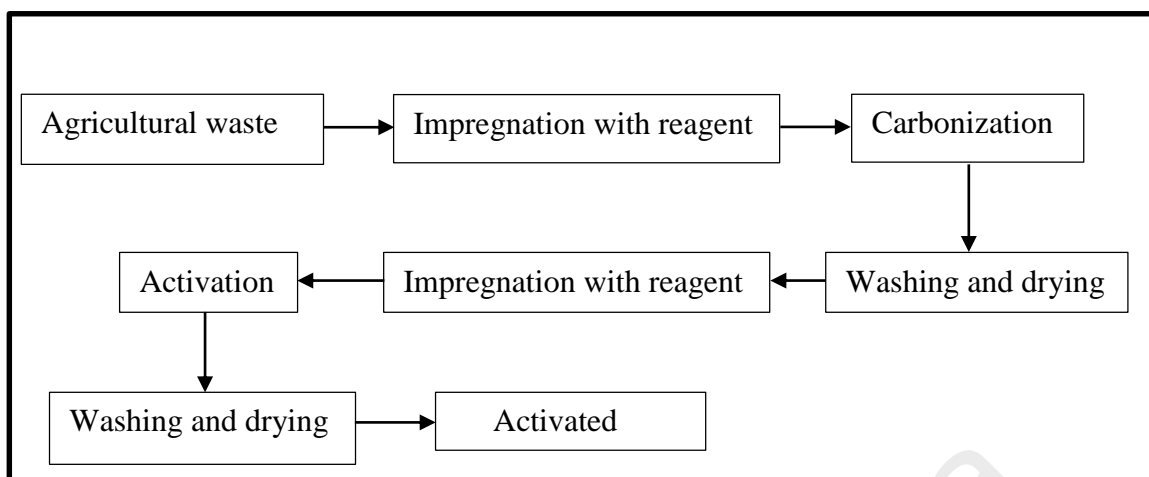


Figure 2.4: A general method to prepare activated carbon from agricultural waste

Palm trees are planted on a large scale in Malaysia and Indonesia, which contributes approximately 85% of the world's palm oil. Other palm oil producer countries include Thailand, Columbia, Nigeria, Papua New Guinea, and Ecuador. Approximately 77% of the agricultural land in Malaysia is used for palm oil plantations (Palm oil, 2014). The waste, palm shell from palm fruit processing is a pressing environmental issue, as it is either burned in the open air or used as boiler fuel to produce steam in the mill (Issabayeva et al., 2006). The usage of palm shells for the production of activated carbon could reduce the waste surplus and can be very beneficial in terms of treatment costs.

To the best of my knowledge, the use of palm shell as an activated carbon to treat RB5 dye solution was presented only by (Nourouzi et al., 2009). Their findings concluded that palm shell based activated carbon has a good adsorption capacity for reactive dye.

There are few main parameters that play important role in RB5 adsorption such as solution pH, temperature, initial dye concentration and adsorbent dose. These parameters are discussed in the subsequent sub-sections.

2.3.6.3 Solution pH

Solution pH leads to the variation surface charge of the adsorbent and degree ionization of the adsorbate. The point of zero charge (pH_{pzc}) is the pH when the surface

charge of adsorbent is zero. The protonated groups of activated carbon are carboxylic group (CO-OH_2^+), phenolic (OH_2^+) and chromenic groups. While, the deprotonated groups of reactive dye are probably sulphonate groups (SO_3^-) (Sun, Zhang, Wang, & Wu, 2013). When the $\text{pH} < \text{pH}_{\text{pzc}}$, the surface of the adsorbent is positively charged. This enhances the deprotonated reactive dye to be adsorbed onto the activated carbon due to the strong electrostatic attraction, resulting in higher removal efficiency of dye (Nekouei, Nekouei, Tyagi, & Gupta, 2015). For the cationic dye, the adsorption is favoured at $\text{pH} > \text{pH}_{\text{pzc}}$ as the adsorbent's surface becomes negatively charged.

For the condition, where the solution pH is lower than $\text{p}K_a$ of the dye, the sulphonate groups of the reactive dye are readily protonated (SO_3H). Consequently, the attraction between the reactive dye and activated carbon decreased resulting in the reduction of dye removal (Sun et al., 2013). However, the $\text{p}K_a$ value of reactive dye is very low and even recorded negative value (e.g. -0.5). This means that the reactive dye is subjected to negative charge even in strongly acidic solution (Sandic et al., 2014).

2.3.6.4 Temperature

The adsorption of dye is related to temperature because the temperature influences the adsorption capacity of the adsorbent. This could be attributed to the pore size of adsorbent which would enlarge at high temperature to increase the penetration of reactive dye inside micropores of the activated carbon. In addition, the higher temperature would create new active sites on the adsorbent surface because of some internal bonds are broken near the edge of active surface sites of adsorbent (Sun et al., 2013).

The adsorption capacity increases with increasing temperature, which categorized as an endothermic process. The uptake of reactive dye on activated carbon typically is an endothermic process, which has been verified by several researchers (Al-Degs, El-Barghouthi, El-Sheikh, & Walker, 2008; Moreira, Soares, José, & Rodrigues, 2001).

Activation energy (E_a) is calculated from the slope of the plot $\ln k$ against $1/T$ (Equation 2.11). The value of E_a is an indicator for two types of adsorption, physical or chemical adsorption. Physical adsorption involves a weak intermolecular force and requires only a small amount of energy (less than 4 kJ/mol). Chemical adsorption, on the other hand, involves much stronger bonding forces and has a greater E_a value, ranging from 80 to 80 kJ/mol (Ismail et al., 2013).

$$\ln k = \ln A - \left(\frac{E_a}{RT} \right) \quad (2.11)$$

where A is the temperature-independent factor (g/mg min); E_a is the activation energy (kJ/mol); R is the gas constant (8.314 J/mol.K), and T is the temperature (K).

2.3.6.5 Initial dye concentration

The effect of initial dye concentration is depending on the interaction between the concentration of the dye and the available sites on an adsorbent surface. Generally, the percentage of dye adsorbed decreases as the initial dye concentration increases. When a higher amount of dye is found in the solution, a longer time is required to reach the equilibrium state.

On the other hand, the increase in adsorption capacity of the adsorbent together with the increasing of initial dye concentration is probably due to the higher driving force for mass transfer (Bulut & Aydın, 2006). The driving force from the higher dye concentration is sufficient to overcome the electrolyte resistance to mass transfer between the solid and liquid phases. Therefore, the higher initial dye concentration will further enhance adsorption process (Banerjee & Chattopadhyaya). At higher initial dye concentration, the adsorption capacity is always higher, while the dye percentage removal is lower.

2.3.6.6 Adsorbent dose

Another crucial parameter influencing the dye removal efficiency is the adsorbent dose. The number of available adsorption sites increases with increasing amount of

adsorbent, therefore, the uptake of dye by adsorbent would likely to be increased as well (Reddy, Kotaiah, & Reddy, 2008).

The adsorption method using agricultural waste-based activated carbon has been applied by many researchers for the removal of RB5 and a summary of the results are presented in Table 2.3.

Table 2.3: Comparison of Adsorption Capacity of RB5 Adsorption by Various Agricultural Waste-based Activated Carbons

Agricultural waste-based activated carbon	Adsorption capacity (mg/g)	References
Walnut wood	19.34	Heibati et al., 2014
Carob	36.90	Güzel et al., 2015
Bamboo	39.02	Ahmad & Hameed, 2010
Palm shell	40	Nourouzi et al., 2009

2.3.7 Electrocoagulation technology

An alternative method to chemical coagulation is electrocoagulation, which is based on the electrochemical technique. During the electrocoagulation process, the coagulant is produced in situ by electrolytic oxidation of sacrificial anode (Merzouk et al., 2011). The potential of electrocoagulation dye removal from wastewater has been proven by other researchers (Nandi & Patel, 2013). The process is characterized by low sludge production, easy flocs separation, low level of total dissolved solids (TDS) and no secondary pollution caused by externally added coagulant (Mollah, Schennach, Parga, & Cocke, 2001).

Electrocoagulation process generates coagulants by an in situ process when an electric current is passed through sacrificial anode which releases metal ions into a solution. The as-synthesized metal ions further react to produce metal hydroxide species (coagulant) which have a strong affinity towards the oppositely charged ions present in the solution to stimulate the coagulation process (Merzouk et al., 2011). The formed flocs have a large surface area which is capable of adsorbing soluble organic compounds and to trap

colloidal particles present in the solution. The accumulated flocs are then removed during sedimentation or flotation process (Aoudj, Khelifa, Drouiche, Hecini, & Hamitouche, 2010). A schematic of the electrocoagulation process is shown in Figure. 2.5 (Figueroa, Valenzuela, Parga, Vazquez, & Valenzuela, 2015).

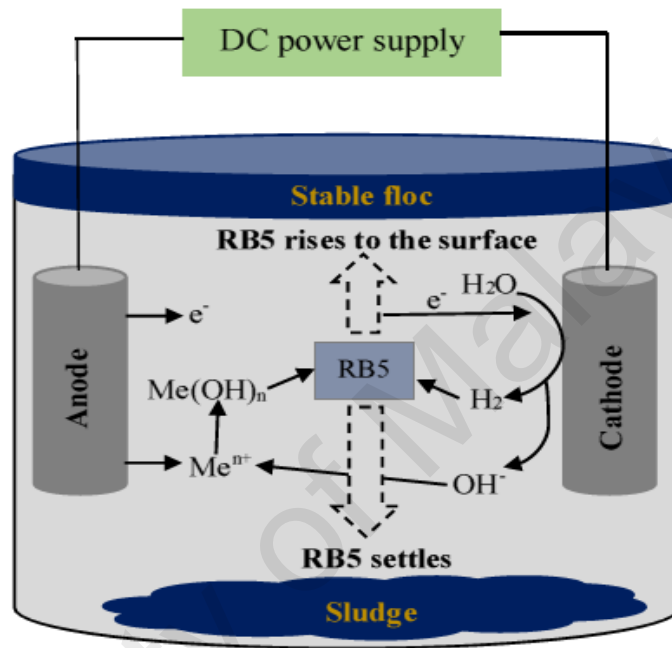


Figure 2.5: Schematic of electrocoagulation process

2.3.7.1 Interface of colloidal particles

Pollutant particles in wastewater are often in a colloidal form. Colloid is stable, and very small in size (1-1000 nm). The surface charge of particles plays an important role in their stability. Surface charge may be formed in many ways, namely ionization of functional surface groups, ion adsorption, dissolution of ionic solids, or isomorphous substitution.

Many surfaces contain ionization functional groups, such as $-\text{OH}$, $-\text{COOH}$ and $-\text{NH}_2$. The surface charge depends on the ionization of these functional groups and consequently on the pH of the solution. Dissolution of ionic solids occurs when the dissolution of anions and cations from the solid is unequal. Isomorphous substitution takes place if the lattice

imperfection occurs at the crystal due to the replacement of some atom in the crystal by another ion that has a different number of electrons resulting in a charged surface (Vepsäläinen, 2012).

A charge formed on the surface influences the ions in the surrounding solution. Stability of colloids is balanced between repulsive electrostatic force and attractive, London-van der Waals force. The theory of Derjaguin-Landau-Verwey-Overbeek (DLVO) is used to estimate these energies of attraction and repulsion.

The ions of the same charge are repelled from the surface. This separation of charges on the particle surface causes the formation of electrical double layer (EDL) as illustrated in Figure 2.6. The EDL plays role in various interfacial electrical phenomena observed in suspension of colloidal particles. The EDL model consists of an inner region called Stern layer or Helmholtz layer and an outer diffusion region called Gouy-Chapman layer. In the inner layer, the particle surface binds ions to itself, whereas in the outer layer, ions may move due to diffusion. When two similar particles approach each other, their diffusion layers come into contact with each other's sphere of influence. As a result, the colloidal particles begin to repel each other. The closer they come to each other, the stronger the repulsive force (Kuokkanen, 2016).

Stable colloids do not affect settling process as their small mass size. They remain in suspension unless they are destabilized chemically, such as coagulant. Coagulation influences the EDL surrounding particles so that the repulsion between the particles decreases and the colloids coincide to microflocs. Destabilization takes place to form flocs through four mechanisms, namely, (i) reduction of surface potential by compression of EDL; (ii) inter-particle bridging of polymers; (iii) surface charge neutralization; (iv) sweep coagulation. Surface charge neutralization and sweep coagulation are the most important mechanisms affected by pH and coagulant dosage (Kuokkanen, 2016).

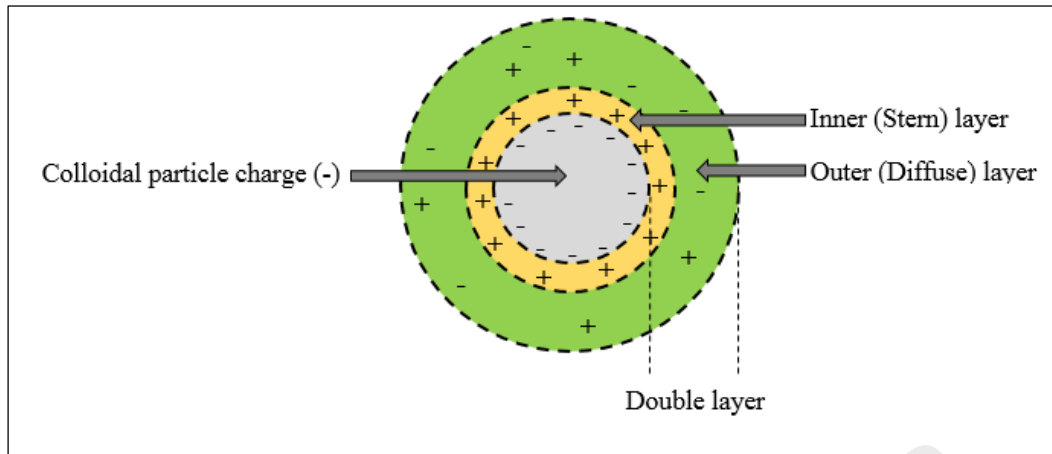


Figure 2.6: Structure of EDL

2.3.7.2 Anodic material and shape

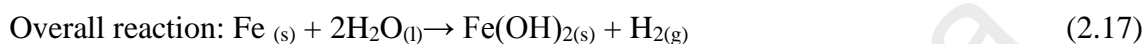
Aluminium and iron are widely used as a sacrificial anode to produce coagulants in electrocoagulation process. The dissolution of anodes is indicated in Equation 2.12 and 2.13. Under certain conditions of electrocoagulation process, iron can be dissolved in divalent Fe(II) and trivalent Fe(III) forms, while aluminium dissolves only in trivalent form Al(III).



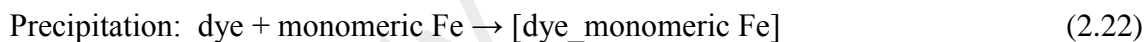
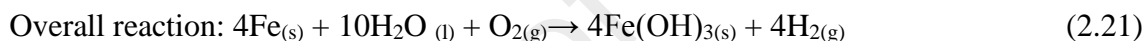
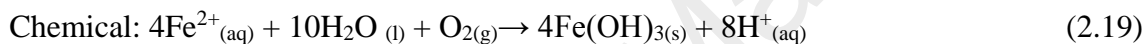
Some researchers have found that the performance of iron as the electrode is better than that of aluminium for reactive dye removal from solution (Amani-Ghadim, Olad, Aber, & Ashassi-Sorkhabi 2012). In addition, the use of iron as sacrificial anode material presents a considerable advantage because of its low energy consumption and the iron complexes is less toxic compared with aluminium complexes (Kobyta, Can, & Bayramoglu, 2003; Mollah et al., 2001). Iron hydroxides can be produced through two mechanisms (Equations 2.14-2.21) and they remove the dye molecules via surface complexation or electrostatic attraction. During surface complexation, the dye will act as

a ligand that binds with hydrous iron through precipitation and adsorption mechanisms (Equations 2.22-2.25) (Körbahti, Artut, Geçgel, & Özer, 2011).

Mechanism I:



Mechanism II:



The configuration of the electrode used in the process is a crucial feature to increase the anodic oxidation and hence, induce higher dye elimination. Several studies have been conducted for dye removal that used different anode shapes such as a plane (Mohan et al., 2007; Nandi & Patel, 2013; Pajootan et al., 2012) and mesh (Del Río et al., 2012; Méndez-Martínez et al., 2012). A mesh type electrode produces a higher discharge current than a plane type due to a higher electric field intensity at the edge of the mesh holes (Kuroda et al., 2003). Moreover, the mesh produces a larger specific surface area than a flat sheet which could boost the formation of iron hydroxides (Ambler & Logan, 2011; Zhang, Merrill, & Logan, 2010).

2.3.7.3 Solution pH

It has been established that pH is an important factor influencing the performance of electrocoagulation process. The formation of coagulant (metal hydroxides) is highly dependent on solution pH. The Fe (II) oxidizes to Fe(III) in the presence of oxygen and pH neutral or alkaline (Equation 2.21). The oxidation rate of Fe(II) to Fe(III) was found negligible at pH 5, moderate occurred at pH 6 and rapidly at pH 7-9 (Sasson, Calmano, & Adin, 2009).

The hydrolysis reactions take place to produce a variety of monomeric iron hydroxide species over a wide pH range. At low pH, soluble $\text{Fe}(\text{OH})_2^+$ and $\text{Fe}(\text{OH})_2^{2+}$ were formed but are not capable of removing the dye. These species are transformed into $\text{Fe}(\text{OH})_3$ in the pH aqueous solution of 6 to 9 (Şengil & Özacar, 2009). $\text{Fe}(\text{OH})_3$ is an insoluble metal hydroxide and it removes the dye molecule through the precipitation and adsorption.

$\text{Fe}(\text{OH})_3$ dissolves to form $\text{Fe}(\text{OH})_4^-$ (Equation 2.26) at pH higher than 9 and migrates to the anode surface to undergo oxidization. Consequently, the formation of coagulant decreased, and thus the dye removal was reduced (Thirugnanasambandham, Sivakumar, & Maran, 2015). Moreover, the formation of $\text{Fe}(\text{OH})_4^-$ which consume OH^- ions cause a slight decrease of the final pH.



Hydrolysed iron cations are dependent on the pH. The mononuclear hydrolysis products of Fe(III) is indicated in Figure 2.6 as a function of pH (Ghernaout et al., 2015).

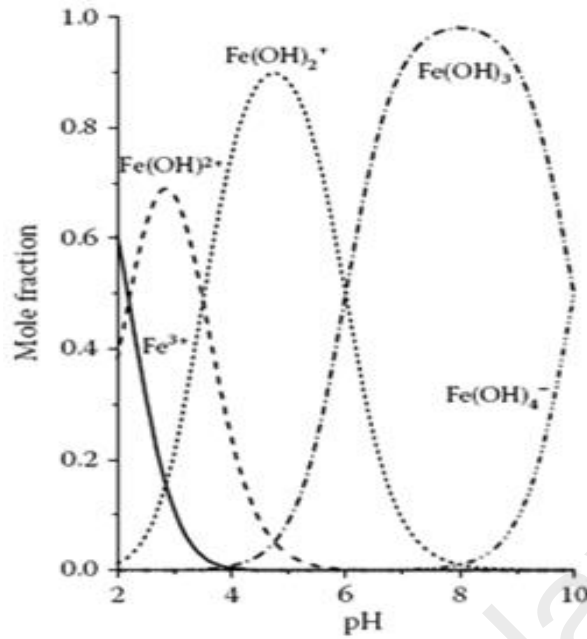


Figure 2.7: Mole fraction of hydrolysed Fe(III) species versus different pH

2.3.7.4 Electric current

Applied current increment has a positive effect on dye removal. The dissolved iron cations could be calculated using Faraday's law. According to the Faraday's law (Equation 2.27), the formation of Fe^{2+} from the anode is directly proportional to the current, which enhances the production of coagulant and in turn higher dye removal efficiency (Mollah et al., 2004). Furthermore, current is a dominant factor to control the gas bubbles generation and their size, and hence controlling the flocs growth (Daneshvar, Khataee, & Djafarzadeh, 2006).

$$m = \frac{ItM_w}{zF} \quad (2.27)$$

where m is the quantity of metal dissolved (g), I is the current (A), t is the operation time (s), M_w is the molecular weight of the iron (g/mol), z is the number of electrons involved in the reaction (iron is +2) and F is the Faraday's constant (96485 C/mol).

However, it is advisable to control the electric current because higher current might cause excessive production of oxygen and hydrogen gas, which disperses current usage for the generation of Fe^{2+} and OH^- (Mollah et al., 2004). Hence, electrical current is one of the crucial parameters for electrocoagulation treatment of wastewater as it leads to increase the electricity consumption and subsequent treatment cost.

The results of RB5 removal using electrocoagulation technique and iron as anode material are summarized in Table 2.4.

Table 2.4: Summary electrocoagulation of RB5 using iron as anode material of RB5

Electrode configuration	Experimental conditions	Results	Reference
A: Iron plate C: Iron plate	pH 5, 4.575 mA/cm ² , 3g/L NaCl	Dye removal: 98.8% EEC: 5.32 kWh/kg _{Fe}	Şengil & Özacar, 2009
A: Iron plate C: SS plate	pH 6.6, 7.5 mA/cm ² , 2 g/L NaCl	Dye removal: 90% EEC: 29 kWh/kg _{dye}	Patel, Ruparelia, & Patel, 2011

2.3.8 Combined processes

The combined processes are getting popular in order to overcome the drawbacks of individual unit operation and improve overall treatment performance. They are typically arranged in sequence arrangement. Raghu and Basha (2007) investigated the efficiency of electrocoagulation treatment followed by the ion-exchanged method to treat textile dye wastewater. The results showed that the sequential process was very effective, and the effluent fulfilled the reuse standard requirement of textile industry India.

The sequential process of coagulation followed by ozonation was found to be superior to the single treatment. The result shows that 99.99% of colour removal and over 90% of COD removal, which fulfilled the standard of Taiwan EPA (Hsu, Yen & Huang, 1998). Similarly, Sarasa *et al.* (1998) noted that when a combination of coagulation and

ozonation was very effective in dye removal (Sarasa, Roche, Ormad, Gimeno, Puig & Ovelleiro, 1998).

Lee and his colleagues (2006) investigated the effects of the sequential process of adsorption and coagulation to remove the dye. They found that the sequences of coagulation followed by the adsorption show higher dye removal efficiency (95.7%) than the adsorption followed by coagulation (79.1%). This proves that the right sequence affects the overall dye removal efficiency and reduce the amount of coagulant and adsorbent used.

There is limited research on the sequence treatment process of electrocoagulation and adsorption on RB5 removal, which was only investigated by Chang et al. (2010). They reported that the sequencing process was more efficient to remove recalcitrant dye from the aqueous solution than the electrocoagulation carried out as a single process. Hence, the combined processes have been classified as efficient in removal efficiency and cost.

2.4 Summary

As described in this chapter, the reactive dye has been widely used in the textile industry. However, it is difficult to be treated by the ordinary methods. Current effective technologies used to treat RB5 are illustrated in the previous section, and the limitations of these methods are discussed. Adsorption and electrocoagulation are highlighted and demonstrated in detail. The existing combined processes used to treat dye effluent are also discussed. By introducing the application of commercialized palm shell activated carbon as an adsorbent, new iron mesh electrode in electrocoagulation and combined adsorption and electrocoagulation (A-EC) will be illustrated in detail in Chapter 4. The RB5 removal efficiency is expected to improve when using A-EC.

CHAPTER 3: RESEARCH METHODOLOGY

3.1 Experimental flow-chart

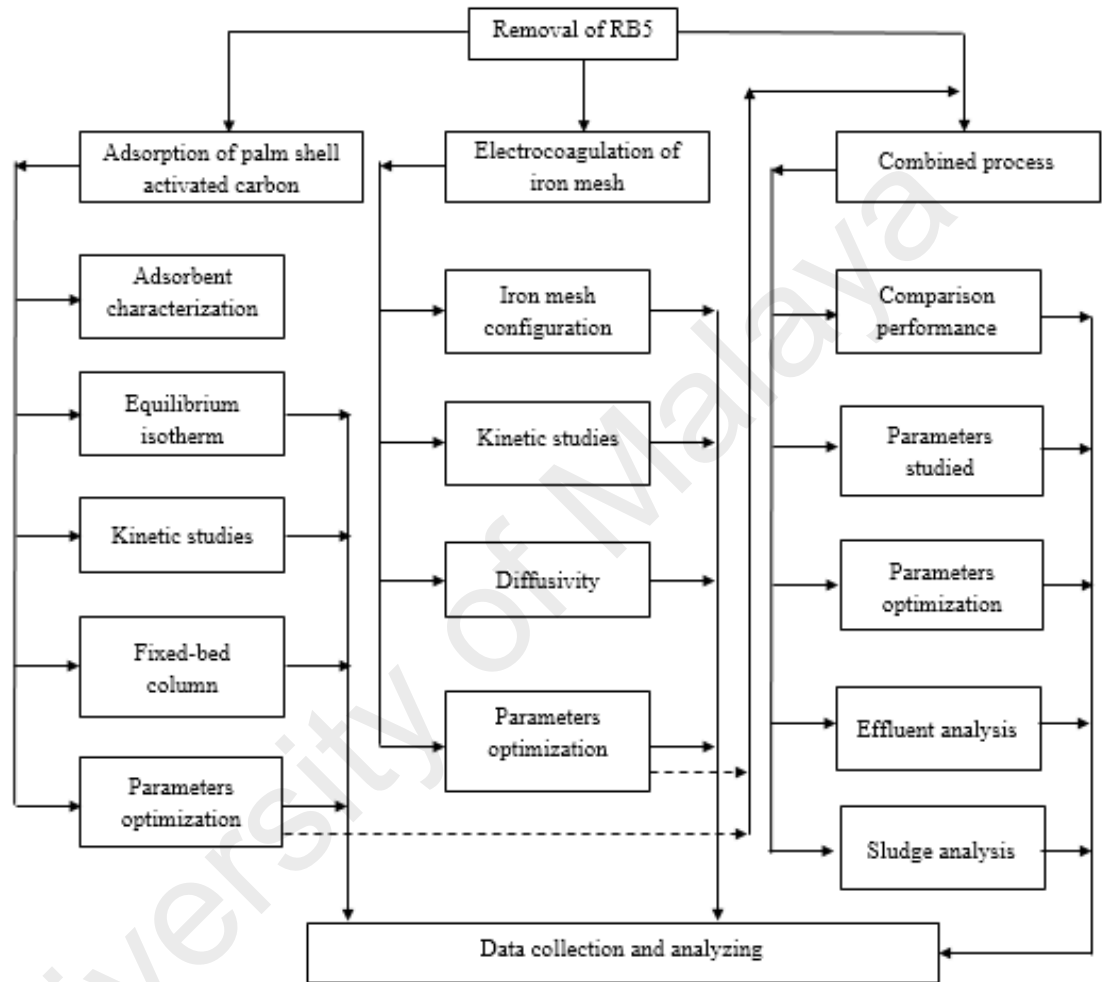


Figure 3.1: Experimental flow-chart of the adsorption, electrocoagulation, and combined adsorption/electrocoagulation experiments

In this research, three methods were investigated to remove RB5 from aqueous solution, the adsorption, electrocoagulation and the combination of adsorption and electrocoagulation (A-EC). The commercial granular palm shell activated carbon was used as a new adsorbent. The equilibrium isotherm results were fitted using Langmuir and Freundlich isotherm. Pseudo-first order, pseudo-second order, and Elovich equation,

were employed to analyse the kinetic data. Then, the adsorption parameters were optimized by RSM. The performance of different configuration of iron mesh electrode in electrocoagulation was evaluated. The selection of configuration iron electrode was subjected according to RB5 and COD removal efficiency, the kinetic rate constant, diffusion coefficient, electrical energy consumption. Then, a combined adsorption and electrocoagulation (A-EC) in a single setup for the removal of RB5 was developed by using optimum conditions of adsorption and electrocoagulation. The effects of initial pH, current density, adsorbent dose and process time on RB5 removal were investigated and optimized. The final effluent and sludge were analysed by GC-MS and XRD, respectively.

3.2 Adsorption process

3.2.1 Activated carbon preparation

Commercial granular palm shell activated carbon was supplied by Bravo Green Sdn Bhd, Sarawak. The adsorbent was crushed and sieved to a size of 350 to 710 μm and washed with distilled water several times to remove dust and suspended solids. The sieved activated carbon was then dried in an oven at 105°C for 24 h to remove the moisture.

3.2.2 Characterization of activated carbon

The adsorbent surface was scanned by ultra-high resolution scanning electron microscopy (SU8000, Hitachi, Japan) at an accelerating voltage of 5000 V. The particle size distribution was determined using a Malvern 2000, United Kingdom.

Adsorption and desorption measurements were carried out by cold nitrogen gas at -196 °C on a Micrometrics ASAP 2020, United States. The average pore diameter was calculated using the Barrett-Joyner-Halenda (BJH) method applied to the desorption isotherm.

3.2.3 Adsorption equilibrium isotherm experiments

Adsorption isotherm tests were carried out using capped vials containing 30 mL of RB5 solution with various initial concentrations in the range of 20 to 140 mg/L and 0.09 g of activated carbon. Prepared samples were agitated in a temperature-controlled orbital shaker at 28 °C for 96 h to reach the equilibrium state. The experiments were performed at a constant pH of 2, 6 (original pH of the dye), or 10.

The Langmuir and Freundlich models were employed to estimate isotherm parameters, as expressed in Equation 3.1 and 3.2. Statistica software (StatSoft, Dell) was used to determine the parameters of the nonlinear isotherm models.

$$q_e = \frac{q_m b C_e}{1 + b C_e} \quad (3.1)$$

$$q_e = K C_e^n \quad (3.2)$$

where q_e is the equilibrium adsorption capacity (mg/g); q_m is the maximum monolayer adsorption capacity (mg/g); b is the Langmuir constant, which is related to the binding energy (L/mg); C_e is the equilibrium concentration of the adsorbate (mg/L); K is the Freundlich constant corresponding to adsorption capacity (mg/g)(L/mg); and n is the measurement of favourable adsorption.

The RB5 removal efficiency and adsorption capacity (q_{exp}) were calculated as follows:

$$\text{Removal efficiency} = \frac{C_0 - C_t}{C_0} \cdot 100\% \quad (3.3)$$

$$q_{exp} = \frac{(C_0 - C_e)V}{m} \quad (3.4)$$

where C_0 and C_t denote the concentration of RB5 at time $t = 0$ and t , respectively; C_e is the equilibrium concentration of adsorbate (mg/L); V is the volume of the solution (L), and m is the mass of dry adsorbent used (g).

3.2.4 Adsorption kinetics studies

Adsorption kinetic tests were carried out at various RB5 concentrations (20, 40, and 60 mg/L) and temperatures (18, 28, and 38 °C) for 5 h. These experiments were conducted at an initial solution pH 6 and an adsorbent dose of 3 g/L, using a magnetic stirrer set at 250 rpm. A temperature-controlled water bath was used to maintain a constant temperature throughout the process. The pseudo-first-order kinetic model (Equation 3.5), the pseudo-second-order kinetic model (Equation 3.6), and the Elovich model (Equation 3.7) were applied to investigate the adsorption kinetics of RB5 onto activated carbon. The diffusion mechanism was identified by the intra-particle diffusion model (Equation 3.8) proposed by Weber and Morris (Bulut & Aydın, 2006; Jiwalak et al., 2010). All the adsorption kinetic parameters were estimated using a non-linear regression by Statsoft Statistica software.

$$q = q_e(1 - e^{-k_1 t}) \quad (3.5)$$

$$q = \frac{k_2 q_e^2 t}{1 + k_2 q_e t} \quad (3.6)$$

$$q = \frac{1}{b} \ln(ab) + \frac{1}{b} \ln(t) \quad (3.7)$$

$$q = k_{ind} t^{0.5} + I \quad (3.8)$$

where q and q_e are the amount of RB5 adsorbed at time t and at equilibrium (mg/g), respectively; t is the contact time (min); k_1 is the rate constant of pseudo-first-order adsorption (min^{-1}); k_2 is the rate constant of pseudo-second-order adsorption (g/mg min); b is the desorption constant (g/mg); a is the initial adsorption rate (mg/g min); k_{ind} is the intra-particle diffusion rate constant ($\text{mg/g min}^{-0.5}$); and I is the constant of boundary layer thickness (mg/g).

3.2.5 Effect of variables on adsorption

To determine the influence of solution pH, adsorbent dose and coexisting anion on adsorption efficiency, a set of tests were conducted using an orbital shaker at 28 °C for

96 h. The effect of pH on RB5 adsorption was investigated at a fixed adsorbent dose of 3 g/L and the dye concentration of 40 mg/L. The pH range was varied from 2 to 11 and kept constant throughout the experiments.

The determination of the influence of adsorbent dose on RB5 adsorption was conducted with various adsorbent doses ranging from 2 to 10 g/L. The concentration of RB5 was 40 mg/L, and the pH solution was set at 6 and maintained throughout the tests.

The effect of the presence of coexisting anion (sulphate) was conducted at a solution pH 6 with a fixed adsorbent dose of 3 g/L. The concentration of anions was 0.0142, 0.1 and 0.142 g/L and the RB5 concentration was 40 mg/L.

3.2.6 Parameters of optimization

To determine the optimum condition of solution pH and adsorbent dose on adsorption of RB5 solution (40 mg/L) containing 0.1 g/L of sodium sulphate, the set of tests was conducted using a magnetic stirrer at 28 °C for 4 h. The Design Expert Software (6.0.10) was used for the statistical design of experiments and data analysis. The Central Composite Design (CCD) in Response Surface Methodology (RSM) was utilized to investigate the interaction between influent pH and adsorbent dose. RSM is a valuable tool for designing experiments. This tool can assist researchers in building models, reducing the number of experiments, exploring the interactions between parameters and obtaining optimum conditions for desirable responses.

The variables' range was divided into five levels (-1, -0.5, 0, +0.5, +1), as shown in Table 3.1. The total set of experiments designed by CCD was 11 runs, including three repeated runs at the central point. Analysis of variance (ANOVA) was used for statistical analysis; it evaluates the significance of the model. The correlation coefficient (R^2) and F-test were utilized to check the quality of the model and the statistical term significance. The significant model terms were examined by *P*-value (probability of error) at a 95%

confidence level. The optimum experimental conditions suggested by RSM were used for subsequent combined process of adsorption and electrocoagulation (section 3.4).

Table 3.1: Parameters of adsorption and their corresponding levels

Parameters	Code	Units	Coded variable level				
			-1	-0.5	0	+0.5	+1
pH	X ₁	-	2	3.5	5	6.5	8
Adsorbent dose	X ₂	g/L	3.00	7.25	11.50	17.75	20.00

3.2.7 Fixed-bed column experiment

A column of 30 cm height and the inner diameter of 3 cm was loaded with the adsorbent (bed height of 5.5 cm) for continuous RB5 adsorption test. Prior performing the experiment, the activated carbon was soaked for 24 hours in deionized water to remove trapped air bubble. The system was operated with an empty bed contact time (EBCT) of 10 min to provide sufficient contact time between the RB5 solution and the adsorbent. The influent solution (40 mg/L of RB5 and 0.1 g/L Na₂SO₄) was pumped downward through the bed at a volumetric flow rate of 6 mL/min using a Masterflex peristaltic pump (Cole-Parmer, USA). The breakthrough capacity of the column (q_b , mg/g) and exhaustion capacity (q_s , mg/g) are calculated by the following expression (Szlachta & Chubar, 2013):

$$q = \frac{\int_{V=0}^{V=V} (C_0 - C) dV}{X} \quad (3.9)$$

where C_0 is the initial RB5 concentration (mg/L); C is the RB5 concentration in the effluent (mg/L); X is the amount of the adsorbent packed in the column (g); V is the volume of solution passed through the column (L). In the q_b case, $V = V_b$ or the volume passing through until the breakthrough moment, and in the q_s case, $V = V_s$ or the volume of total saturation.

3.2.8 Analytical methods

All collected samples for RB5 measurements were filtered through a 0.22 µm filter membrane to remove any suspended solids that could affect the analysis process. The concentration of RB5 was determined using a Lambda 35 UV-Vis spectrophotometer (PerkinElmer, USA) at a wavelength of 597 nm.

3.3 Electrocoagulation process

3.3.1 Electrodes preparation

Iron mesh (woven mesh, hole size 0.5 cm × 0.6 cm) and round iron plate (diameter 9 cm) were supplied by KY Scientific, Malaysia. Each electrode was immersed in 0.01 mol/L H₂SO₄ for 24 h and then rinsed with distilled water. Prior to use, the electrodes were polished by fine grade sandpaper to remove impurities. Then, both electrodes were placed in electrolysis system for 3 hours to further remove impurities.

3.3.2 Comparison of anode configurations

The comparison tests of anode configuration were conducted with the RB5 concentration of 40 mg/L and NaCl of 0.2 g/L in a 1000 mL beaker. The diameter of single layer iron mesh anode is 3.02 cm, while the double layer configuration had a diameter of 1.3 cm and layer distance of 0.2 cm (Figure 3.2). The anode and cathode (iron round plate with diameter 9 cm) were connected to a DC power supply with a current density of 5.02 mA/cm² (7.8-8.5V). The relative kinetic rate constant was calculated using first-order model (Equation 3.12).

$$C_t = C_0 e^{-k_1 t} \quad (3.12)$$

where C_0 (mg/L) and C_t (mg/L) are the amount of RB5 at time $t = 0$ and t (min), respectively; k_1 is the rate constant of first-order kinetic model (min⁻¹).

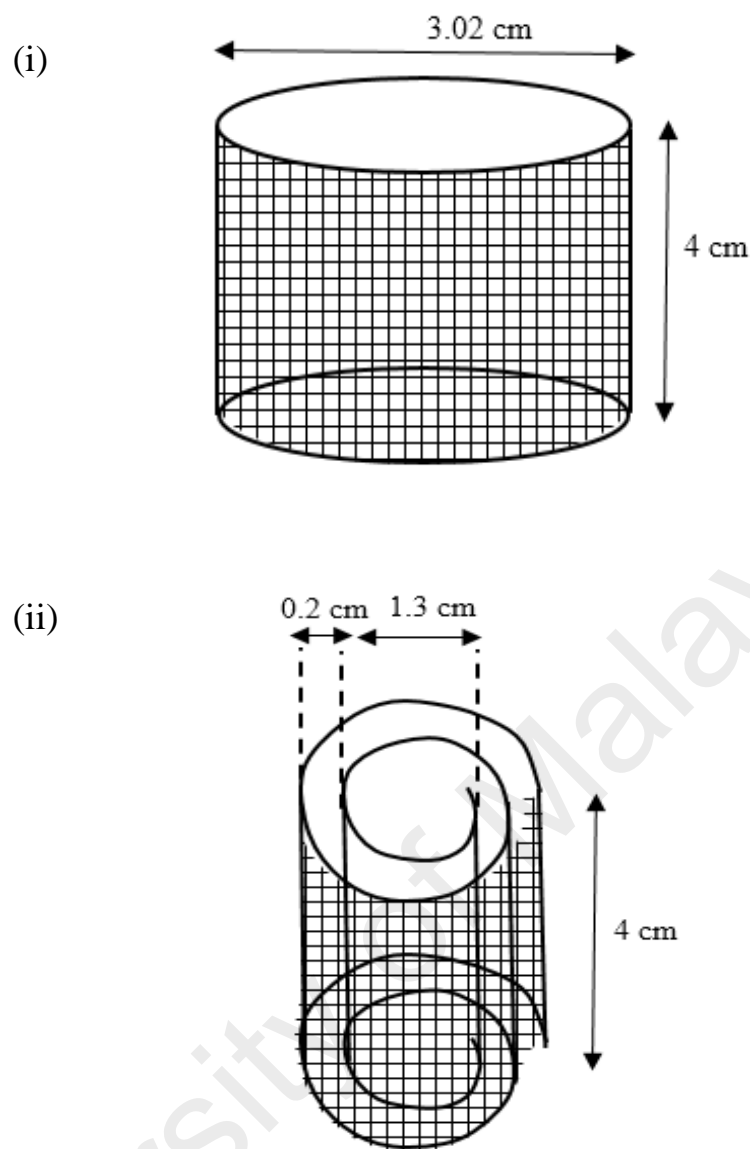


Figure 3.2: Schematic diagram of (i) single layer electrode and (ii) double layer electrode

The chronoamperometry technique was used to investigate the electrochemical diffusivity of RB5 toward the single layer and double layer iron mesh electrodes. The experiments were performed by an EC-lab potentiostat with EC-lab10.40 software. The blank and dye solution of 0.2 g/L NaCl and 40 mg/L RB5 were mixed with 0.2 g/L NaCl, respectively. The following Cottrell equation was used to estimate the diffusivity for both anodes (Bard & Faulkner, 1980).

$$I = \frac{nFAD^{0.5}C_0}{\pi^{0.5}t^{0.5}} \quad (3.13)$$

where n is the number of electrons; A (cm^2) is the surface area of the electrode; D (cm^2/sec) is the diffusion coefficient; C_0 (mol/cm^3) is the initial concentration of RB5 and t is the time (s).

Sludge volume index (SVI, mL/g) was used to determine settling ability of the precipitates. It is defined as the volume (mL) occupied by 1 g of suspension after settling for 30 min. The SVI was calculated according to Equation 3.14. The electrical energy consumption (EEC, $\text{kWh}/\text{kg}_{\text{dye removed}}$) and operating cost ($\text{US}\$/\text{m}^3$) are defined in Equations 3.15-3.16. (El-Ashtouky et al., 2012; Ghosh et al., 2011).

$$SVI = \frac{h_{30}}{h_0SS} \quad (3.14)$$

$$EEC = \frac{UIt \times 1000}{V(C_0 - C_t)} \quad (3.15)$$

$$\text{Operating cost} = (a \times C_{\text{energy}}) + (b_e \times C_{\text{electrode}}) \quad (3.16)$$

where h_0 is the initial sludge height (cm), h_{30} is the settled diluted sludge height after 30 min of settling (cm), SS is the initial sludge concentration after treatment (g/L), C_0 and C_t denote the concentration of RB5 at time $t = 0$ and t , respectively, U represents the voltage (V), I is the current (A), t is the process time (h), V is the volume of dye solution (L), a is the electricity price in Malaysia for the year 2015 ($\text{US}\$ 0.06/\text{kWh}$), b_e is the retail iron mesh price in Malaysia for the year 2015 ($2.73 \text{ US}\$/\text{kg iron mesh}$); C_{energy} is the electrical energy consumption (kWh/m^3) and $C_{\text{electrode}}$ is the iron electrode consumption (kg/m^3).

3.3.3 Parameters optimization

The Design Expert Software (6.0.10) was used for the statistical design of experiments and data analysis. The Central Composite Design (CCD) in Response Surface

Methodology (RSM) was utilized to investigate the interaction between four parameters: pH, current density, electrocoagulation time and Na₂SO₄ dose. These variables' range was divided into five levels (-1, -0.5, 0, +0.5, +1), as shown in Table 3.2. The total set of experiments designed by CCD was 27 runs, including three repeated runs at the central point.

Table 3.2: Parameters of electrocoagulation and their corresponding levels

Parameters	Code	Units	Coded variable level				
			-1	-0.5	0	+0.5	+1
pH	X ₁	-	4	5.5	7	8.5	10
Current density	X ₂	mA/cm ²	1.5	1.97	2.43	2.87	3.33
Electrocoagulation time	X ₃	min	5	18.75	32.5	46.25	60
Na ₂ SO ₄ dose	X ₄	g/L	0.05	0.08	0.1	0.13	0.15

3.3.4 Analytical methods

The concentration of RB5 was determined using a Lambda 35 UV-Vis spectrophotometer (PerkinElmer, USA) at a wavelength of 597 nm. Malvern zeta potential analyser (Malvern Nano ZS 90) was used to measure zeta potential of flocs formed during electrocoagulation process.

3.4 Combined process of adsorption and electrocoagulation

3.4.1 Experimental setup

A reactor with an inner diameter of 10 cm was used for the experiment of combined process of adsorption and electrocoagulation. Both processes occurred simultaneously in the same reactor. The adsorption process took place at the bottom of the reactor, while electrocoagulation was in the upper part of the reactor. A mesh was inserted in the middle of the reactor to keep the activated carbon at the bottom. The batch reactor setup was illustrated in Figure 3.3. In this study, fixed bed column was selected due to the fixed bed adsorption has become popular in the industrial wastewater treatment process.

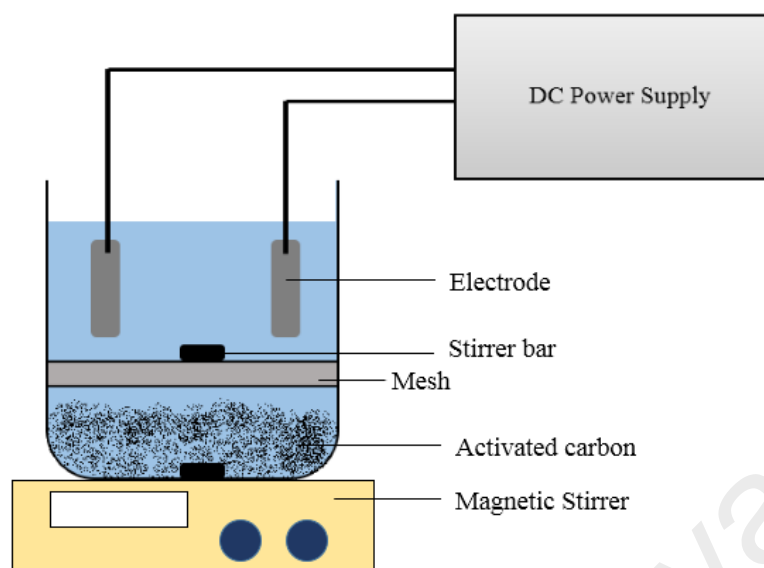


Figure 3.3: Experimental setup of combined process

3.4.2 Evaluation and optimization parameters

The first attempt of combined process was carried out under the optimum condition of individual adsorption and electrocoagulation process. Results obtained for combined process and individual adsorption and electrocoagulation under optimum operating conditions were compared and analyzed. The effect of pH (4-10), current density (1-3 mA/cm²), adsorbent dose (5-20 mg/L) and initial RB5 concentration (20-80 mg/L) were investigated. The suitable parameters ranges were then selected and used for RSM purposes.

The optimum conditions of four parameters were investigated using Central Composite Design (CCD) in Response Surface Methodology (RSM). The four parameters are initial pH, adsorbent dose, current density and process time as shown in Table 3.3. The total set of experiments designed by CCD was 27 runs, including three repeated runs at the central point.

Table 3.3: Parameters of combined process and their corresponding levels

Parameters	Code	Units	Coded variable level				
			-1	-0.5	0	+0.5	+1
pH	X ₁	-	4	5	6	7	8
Adsorbent dose	X ₂	g/L	5	8.75	12.5	16.25	20
Current density	X ₃	mA/cm ²	1.67	2	2.34	2.67	3
Process time	X ₄	min	10	22.5	35	47.5	60

3.4.3 Analytical methods

The sludge produced through the EC process was dried in an oven for 24 h. Then, the nature of the sludge was characterized by Field Emission Scanning Electron Microscope (FESEM) and X-ray diffraction analysis (PANalytical, Malaysia).

The residues remained inside the treated solution were further characterized by a gas chromatography mass spectroscopy (GC-MS) (Agilent, Model 7890) attached with a ZB-Wax column, 30.0 m x 0.25 mm x 0.25 mm (Phenomenex, United States). The initial oven temperature was set at 60 °C and held for 5 min. Later, the temperature ramped at 10 °C/min to the final temperature at 240 °C (held for 5 min). The chemical compounds obtained were compared with the MS library (Agilent ChemStation Software).

CHAPTER 4: RESULTS AND DISCUSSION

4.1 Adsorption RB5 on commercialized palm shell activated carbon

4.1.1 Characteristics of palm shell activated carbon

The activated carbon used in this study is a highly porous material with a specific surface area of 759.78 m²/g. Pores in various sizes in nanometers scale (micropores, mesopores) were identified by the analysis of nitrogen gas adsorption isotherm. The volume of micropores (< 2 nm) was 0.299 cm³/g, which corresponds to 71% of the total volume of pores. The average pore diameter calculated using the BJH method was 4.96 nm. By means of scanning electron microscopy, extrinsic large-size pores on the surface of activated carbon were also recognized. The distinct pores of micrometers in size are readily found on the surface, as shown in Figure 4.1. The properties of palm shell activated carbon are summarized in Table 4.1.

Table 4.1: Properties of palm shell activated carbon

Parameter	Value
Brunauer, Emmett, and Teller (BET) surface area (m ² /g)	759.78
Average pore diameter (nm)	4.96
Micro-pore volume (cm ³ /g)	0.299
Meso-pore volume (cm ³ /g)	0.122
Particle size (μm)	563.68
pH _{pzc}	8.1

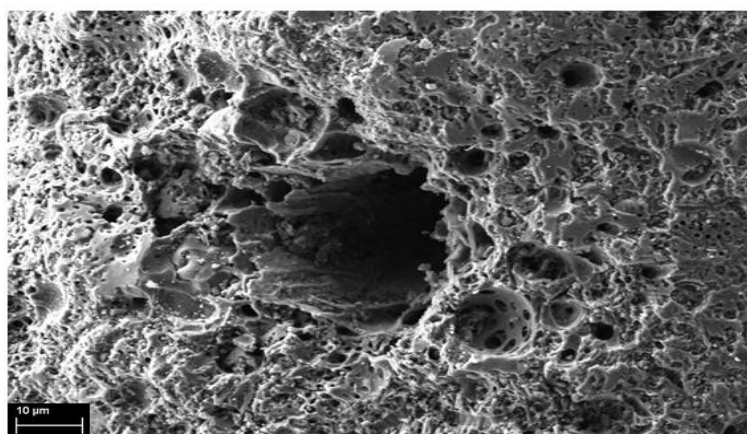


Figure 4.1: SEM image of palm shell activated carbon

4.1.2 Equilibrium isotherms

The adsorption isotherm describes the distribution of dye molecules between the liquid phase and solid phase when the adsorption process reaches an equilibrium state. The Langmuir and Freundlich models were used to evaluate the equilibrium data, as shown in Figure 4.2. The selection of the isotherm model is based on the highest value of the coefficient of determination, R^2 . Isotherm parameters were calculated and presented in Table 4.2.

The typical adsorption capacity ascended progressively to a plateau region at a higher equilibrium adsorbate concentration. The uptake of RB5 was highest at the lowest solution pH because of electrostatic interactions between the adsorbent surface and the dye molecules present in the solution (the RB5 pH-dependency is explained below).

The Langmuir model assumes monolayer adsorption onto an adsorbent surface containing a finite number of adsorption sites, with no transmigration of adsorbate in the plane surface (Desta, 2013). The constant b in the Langmuir isotherm model indicates the adsorption energy and strength of binding sites (Aljeboree, Alshirifi, & Alkaim, 2014). A higher b value is the reason for a steeper isotherm, which indicates higher RB5-activated carbon bond stability. On the other hand, the Freundlich isotherm is an empirical model describing the adsorption characteristics of a heterogeneous surface. The value of the parameter n within the range of 1 to 10 represents a good adsorption. The magnitudes of n were 2.938, 2.807, and 2.542 for solution pH values of 2, 6, and 10, respectively (Table 4.2). These results indicate that the adsorption of RB5 onto palm shell-based activated carbon was favourable.

Moreover, the Langmuir isotherm model resulted in a higher R^2 value, suggesting that the model fits better than the Freundlich model with the adsorption data. This revealed that the accessible surfaces of palm shell-based activated carbon could be modelled as a monolayer occupancy of RB5 molecules in the equivalent sites.

Table 4.2: Langmuir and Freundlich Isotherm Model parameters and correlation coefficients for RB5 adsorption

pH	Langmuir isotherm			Freundlich isotherm		
	q_m (mg/g)	b (L/mg)	R^2	K (mg/g)(L/mg)	n	R^2
2	25.12	0.112	0.951	5.674	2.938	0.996
6	23.61	0.081	0.960	4.602	2.807	0.891
10	24.86	0.089	0.956	4.500	2.542	0.927

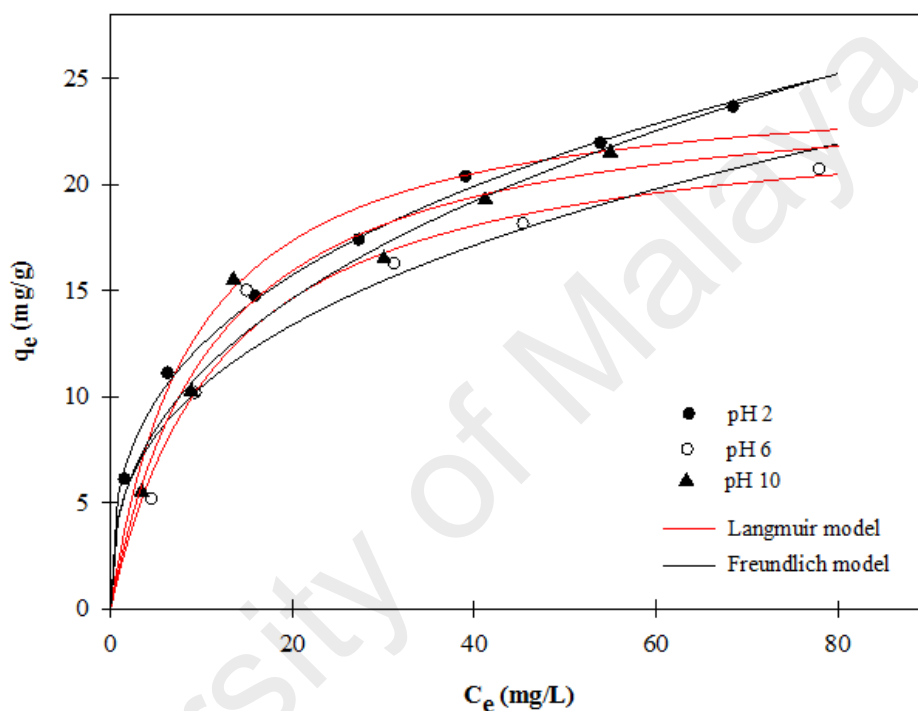


Figure 4.2: Langmuir and Freundlich adsorption isotherms of RB5 dye on activated carbon at pH 2, 6, and 10

The essential features of the Langmuir isotherm parameter can be used to estimate the affinity of adsorbate to adsorbent in terms of dimensionless equilibrium parameters, R_L (Equation 4.1). The R_L value determines if the Langmuir isotherm is either favourable ($0 < R_L < 1$), unfavourable ($R_L > 1$), linear ($R_L = 1$), or irreversible ($R_L = 0$) (Data *et al.* 2012). The R_L for pH 2, 6, and 10 was 0.060, 0.081, and 0.074, respectively, which affirms that the Langmuir isotherm model was favourable for RB5 adsorption onto palm shell activated carbon.

$$R_L = \frac{1}{1+bC_0} \quad (4.1)$$

where b is the Langmuir constant and C_0 is the initial dye concentration (mg/L).

In general, the amount of RB5 adsorbed by the material used in this study was comparable to adsorption capacities of other agricultural waste-based activated carbons, as shown in Table 4.3. Analysing the results obtained for the activated carbons made of the same waste material, it was found that the adsorption capacity of tested adsorbent was lower than the one reported by Nourouzi *et al.* (2009). The lower adsorption of RB5 observed in the study may be related to the difference in pore size distribution of palm shell-based activated carbons and initial solution pH. However, Nourouzi and his colleagues (2009) have used an in-house (laboratory scale) prepared palm shell activated carbon, which could not represent the commercial palm shell activated carbon in a similar manner.

Table 4.3: Comparison of adsorption capacity of RB5 adsorption by various agricultural waste-based activated carbons

Agricultural waste-based activated carbon	Adsorption capacity (mg/g)	References
Walnut wood	19.34	Heibati et al., 2014
Carob	36.90	Güzel et al., 2015
Bamboo	39.02	Ahmad & Hameed, 2010
Palm shell	40	Nourouzi et al., 2009
Palm shell	25.12	This work

4.1.3 Adsorption kinetics

4.1.3.1 Effect of initial dye concentration

Figure 4.3 depicts the experimental and modelled data of RB5 adsorption by palm shell-based activated carbon at various initial dye concentrations, *i.e.*, 20, 40, and 60 mg/L. The adsorption of RB5 increased progressively with contact time. For the lowest

dye concentration (20 mg/L), the adsorption achieved a plateau region within 4 h, which corresponds to a removal efficiency and adsorption capacity of 96.7% and 6.45 mg/g, respectively. In the case of 40 and 60 mg/L of RB5, dye removal was 76.4% and 64.9% after 5 h, respectively. This means that when a higher amount of dye is present in the solution, a longer time is required to reach the equilibrium state. The obtained data are in good agreement with the results presented by (Osma et al., 2007) and (Heibati et al., 2014), where they were using walnut wood and sunflower seed, respectively, for the RB5 removal.

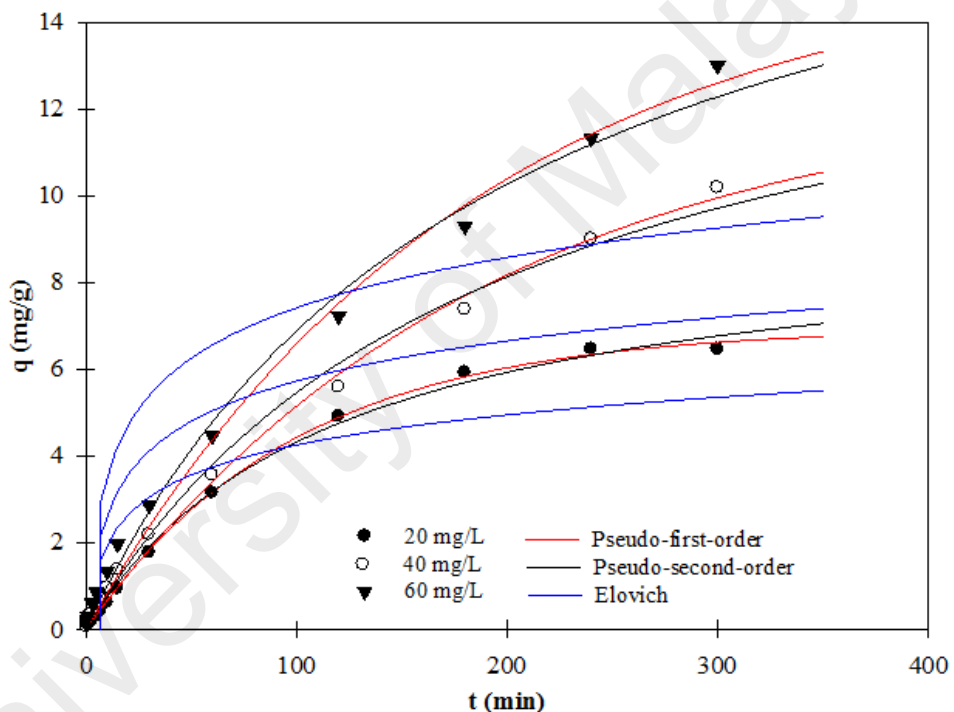


Figure 4.3: Kinetics for adsorption of RB5 by palm shell activated carbon at various dye concentrations and a constant temperature of 28 °C

To evaluate the adsorption rate and reaction mechanisms, the kinetic experimental data were fitted with three models: the pseudo-first-order kinetic model, the pseudo-second-order kinetic model, and the Elovich model. All calculated kinetic parameters are presented in Table 4.4. The pseudo-first-order model showed the best fit to the kinetic data, as the highest R^2 values were obtained for each tested initial dye concentration. Moreover, the calculated (q_e) and experimental equilibrium adsorption capacities (q_{exp})

were in good agreement. This confirms that the pseudo-first-order model is sufficient to interpret the kinetics of RB5 adsorption onto palm shell-based activated carbon. The adsorption rate constant (k_1) was the highest (0.010 min^{-1}) at a low initial concentration (20 mg/L), as the available number of adsorption sites on the activated carbon surface was high enough to remove over 90% of RB5 from the solution.

Table 4.4: Kinetic model parameters for various initial dye concentrations at 28°C

C_0 (mg/L)	RE (%)	q_{exp} (mg/g)	Pseudo-first order		
			k_1 (min^{-1})	q_e (mg/g)	R^2
20	96.7	6.45	0.010	6.95	0.999
40	76.4	10.18	0.005	12.48	0.995
60	64.9	12.99	0.006	15.64	0.992

* RE: Removal efficiency after 5 hours of the process

Table 4.4 continued

C_0 (mg/L)	Pseudo-second order			Elovich equation		
	k_2 (g/mg min)	q_e (mg/g)	R^2	a	b	R^2
20	0.0009	9.43	0.997	0.703	1.001	0.799
40	0.0003	15.91	0.994	0.965	0.748	0.763
60	0.0003	20.19	0.993	1.396	0.597	0.777

A diffusion model proposed by Weber and Morris was applied to determine the rate-limiting step of the adsorption process. Adsorption kinetics are typically controlled by different diffusion mechanisms: (i) film diffusion, in which the mass transfer of the bulk phase to the adsorbent surface is across the boundary layer and is represented by the curve portion; and (ii) intra-particle diffusion (gradual adsorption stage), where diffusion of the adsorbate occurs within the pores of material, binding the pores and capillary spaces. The plateau region (final stage) means that the intra-particle diffusion starts to decrease as low concentrations of adsorbate and fewer available adsorption sites are present (Samiey & Ashoori, 2012). In cases, where a plot of q versus $t^{0.5}$ gives a straight line and passes

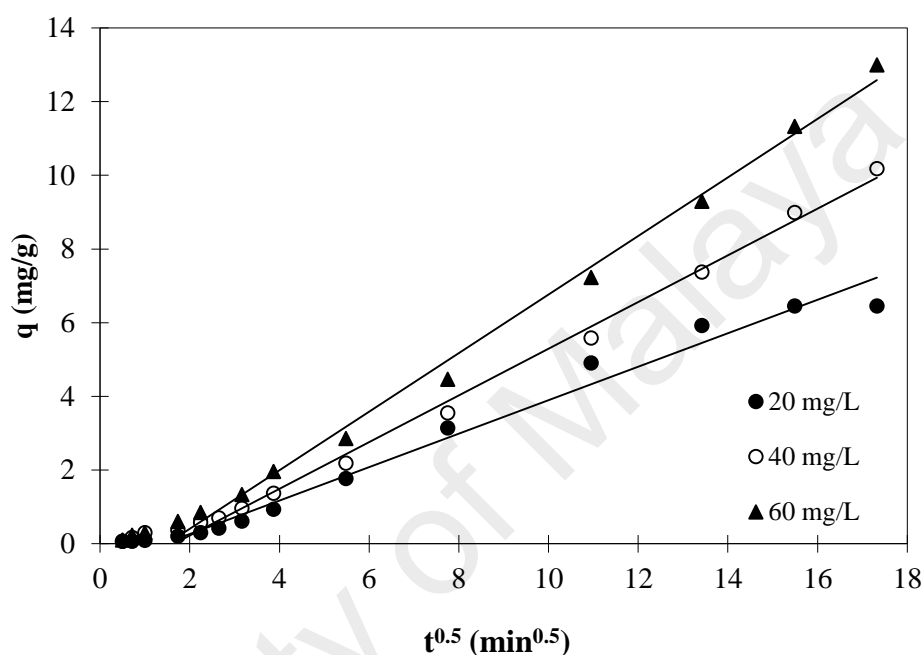
through the origin, this means that intra-particle diffusion is the rate-limiting step. If the plot is linear but does not pass through the origin, the adsorption process involves intra-particle diffusion, but it is not the only limiting step; a multi-linear plot indicates the adsorption process is influenced by two or more processes (Cestari et al, 2005; Szlachta & Chubar, 2013).

Figure 4.4 shows a multi-linear plot that has two different linear regions. The initial region corresponds to the RB5 molecules that diffuse across the boundary layer of palm shell activated carbon. The second region is the region of intra-particle diffusion, where the RB5 molecules gradually diffuse into surface pores and are retained by the micropores of adsorbent. In the case of 20 mg/L dye, a third region of the equilibrium (plateau) was reached, but this did not occur for the 40 and 60 mg/L concentrations of RB5. Thus, this region is not considered to be part of the diffusion mechanism.

The intra-particle diffusion rate constants (k_{ind1} and k_{ind2}) were achieved from the slope of the linear plot q versus $t^{0.5}$, as listed in Table 4.5. The values of k_{ind1} and k_{ind2} increased from 0.063 to 0.390 mg/g min^{-0.5} and 0.454 to 0.795 mg/g min^{-0.5}, respectively, as the initial dye concentration was increased from 20 to 60 mg/L. This could be explained by the high amount of dye molecules that diffuse rapidly to easily available adsorption sites. The intercepts (I_1 and I_2) from the plot provide information about the boundary layer thickness. A larger intercept value represents a greater boundary layer effect. In this study, the negative intercept values suggest that the boundary layer effect was close to a minimum value (Samiey & Ashoori, 2012). The extrapolated lines did not pass through the origin, showing that RB5 adsorption was involved in intra-particle diffusion and was not the only rate-limiting step (Figure 4.4). The results suggested that external film and intra-particle diffusion occurred simultaneously. However, film diffusion played a more dominant role in the beginning of RB5 adsorption and intra-particle diffusion played a major role in the second stage.

Table 4.5: Parameters of Intra-Particle Diffusion Model

C_0 (mg/L)	k_{ind1}	I_1	R^2	k_{ind2}	I_2	R^2
20	0.063	0.024	0.825	0.454	-0.645	0.981
40	0.478	-0.176	0.998	0.633	-1.037	0.996
60	0.390	-0.078	0.932	0.795	-1.182	0.995

**Figure 4.4:** Weber and Morris intra-particle diffusion plot 28 °C

4.1.3.2 Effect of temperature

Figure 4.5 shows the removal of RB5 by the palm shell activated carbon at three different solution temperatures (18, 28, and 38 °C). An increase in solution temperature from 18 to 38 °C yielded an increase in adsorption capacity from 7.29 to 10.61 mg/g, indicating that the adsorption was endothermic in nature (Hsueh, Lu, Hung, Huang, & Chen, 2007). The obtained data are in good agreement with the results presented by Al-Degs *et al.* (2008), as they reported higher reactive dyes adsorption by activated carbon as the temperature increased from about 25 to 55 °C. The higher surface coverage at higher solution temperature was attributed to increased penetration of reactive dyes inside

micropores of the activated carbon or the creation of new active sites on adsorbent surface (Al-Degs et al., 2008).

The pseudo-first-order model and the pseudo-second-order model were used to calculate the adsorption rate constant to evaluate the activation energy. Pseudo-first order model fits well with the experimental data, as the calculated (q_e) and experimental equilibrium adsorption capacities (q_{exp}) were close to each other (Table 4.6). The calculated rate constant (k_1) increased progressively from 0.0062 to 0.0105 min⁻¹ as the temperature increased from 18 to 38 °C. Thus, adsorption of RB5 occurred more rapidly with higher temperature.

These rate constants were then used for the calculation of activation energy (E_a) (Equation 4.2). The E_a value was obtained from the slope of the plot $\ln k_1$ against $1/T$, as presented in Figure 4.6. The value of E_a is an indicator of either physical or chemical adsorption. In physical adsorption, the reaction is easily reversible and equilibrium is achieved rapidly. Hence, it involves a weak intermolecular force and small energy requirements. Chemical adsorption, on the other hand, involves stronger bonding forces and has a greater E_a value, ranging from 8 to 80 kJ/mol (Ismail, Aroua & Yusoff, 2013). In this study, the E_a was 12.619 kJ/mol, indicating that RB5 adsorption onto palm shell activated carbon is a chemical adsorption process.

$$\ln k_1 = \ln A - \left(\frac{E_a}{RT} \right) \quad (4.2)$$

where A is the temperature-independent factor (g/mg min); E_a is the activation energy (kJ/mol); R is the gas constant (8.314 J/mol.K), and T is the temperature (K).

Table 4.6: Kinetic model parameters for different temperatures with a RB5 concentration of 40 mg/L

T (°C)	q_{exp} (mg/g)	Pseudo-first order			Pseudo-second order		
		$k_1 \times 10^{-3}$ (min)	q_e (mg/g)	R^2	$k_2 \times 10^{-4}$ (g/mg min)	q_e (mg/g)	R^2
18	7.29	6.23	12.73	0.991	3.29	17.07	0.992
28	10.01	8.05	15.97	0.996	3.59	20.94	0.998
38	10.61	10.54	15.95	0.994	4.61	20.87	0.998

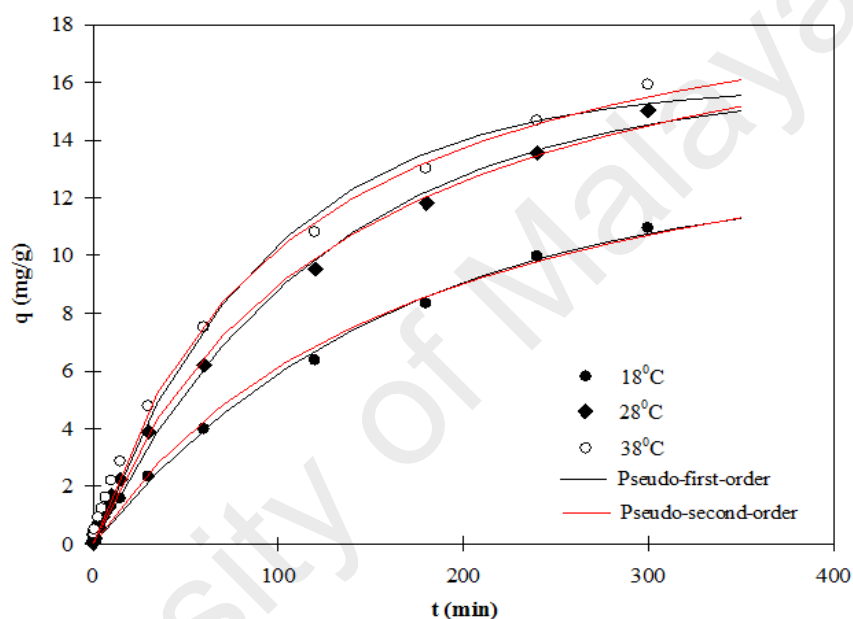


Figure 4.5: Kinetics for RB5 adsorption at various temperatures

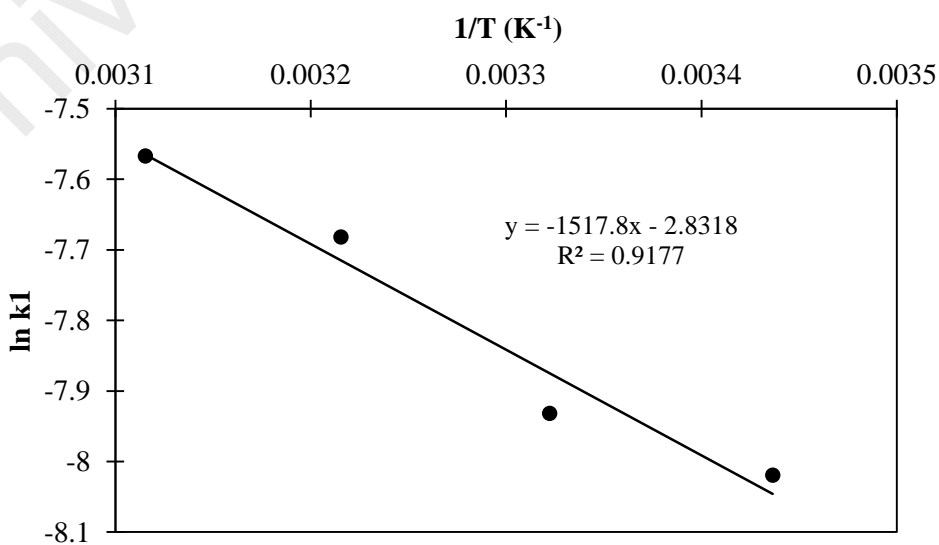


Figure 4.6: Plot of $\ln k_1$ versus $1/T$

4.1.3.3 Effect of pH

Solution pH has been recognized as a crucial factor influencing adsorption performance. Figure 4.7 shows the pH effects on RB5 removal using palm shell activated carbon. The adsorption is highly dependent on the pH, as the removal efficiency decreased with increasing pH. This could be attributed to the electrostatic interaction between RB5 and the adsorbent surface. At low pH, the activated carbon surface is predominantly positively charged and a strong electrostatic attraction between anionic RB5 and the adsorbent surface can be expected to enhance the process. This led to a maximum uptake of RB5 from the solution. As pH increases, OH⁻ ions become more prevalent in the solution and compete with anionic RB5 for active sites on the adsorbent surface. Moreover, repulsion occurred between the adsorbent and RB5 when the solution pH was higher, may contribute to a reduction of removal efficiency (Nekouei et al., 2015).

A slight increase in RB5 removal at pH 4 to 7 was found, indicating that other processes are involved in RB5 removal. There are hydrophobic interactions between hydrophobic parts of the RB5 molecule and the activated carbon surface (Newcombe & Drikas, 1997).

For the tested pH range from 2 to 9, the removal efficiency decreased from 89.6% to 72.7%, respectively. In the alkaline zone, the surface of activated carbon was more negatively charged, and a strengthening force of electrostatic repulsion between RB5 and the adsorbent occurred, reducing the adsorption capacity. The highest RB5 removal was at pH 2, which differs slightly by 8.1% when compared with the original RB5 (pH 6.1-6.5). The original pH was later used for subsequent studies as external addition of acid is not required to adjust the pH.

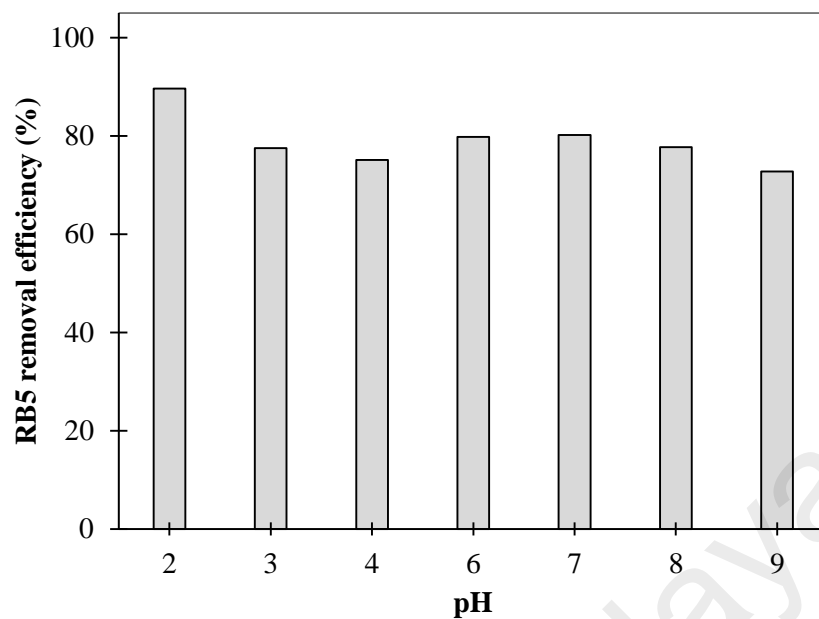


Figure 4.7: Effect of pH on RB5 removal by palm shell activated carbon

4.1.3.4 Effect of adsorbent dose

The adsorption is influenced by the availability of binding sites on the adsorbent surface. Therefore, to determine the effect of the activated carbon dose on RB5 adsorption, a series of tests were conducted and the results obtained are presented in Figure 4.8. As expected, the RB5 removal efficiency increased with an increasing adsorbent dose. A complete depletion was reached for an adsorbent dose greater than 6 g/L. However, the removal only increased slightly, by 5.4%, when the adsorbent dose increased from 4 to 6 g/L. This is attributed to RB5 already being almost completely adsorbed by the 4 g/L adsorbent dose.

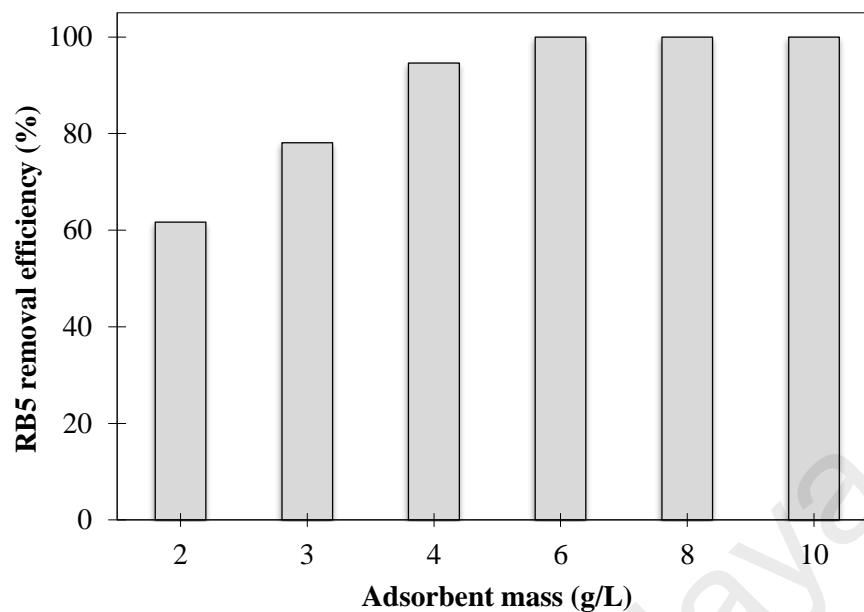


Figure 4.8: Effect of adsorbent dose on RB5 removal by palm shell activated carbon

4.1.3.5 Effect of coexisting anion

Generally, large amounts of salt such as Na_2SO_4 are used in the fabric dyeing process. It is important to investigate the effect of these anions in adsorption process as they will compete with the dye molecules for available adsorption sites. Thus, RB5 removal was evaluated in the absence and presence of sulphate anions at four concentrations as shown in Figure 4.9. RB5 removal depends on the concentration of coexisting anion in solution. The presence of sulphate ion in the solution significantly impacts the RB5 uptake.

The adsorption efficiency decreased in the presence of the Na_2SO_4 . The adsorption efficiency in the absence of electrolyte was 79.8%, while in the presence of 0.0142 g/L SO_2^{4-} anions, the removal efficiency was 52.2%. The reduction in RB5 removal efficiency is probably due to the SO_2^{4-} anions might have competed with anionic dye molecules to bind with the surface sites of the activated carbon. Moreover, the active site was blocked by the added salt thus reducing the possibility of dye molecules adsorbed by the adsorbent (Alexandrica, Silion, Hritcu, & Popa, 2015). There is a decreased in RB5 removal efficiency from 52.2% to 43.7% when the concentration of sulphate changing from 0.0142 g/L to 0.142 g/L. This demonstrates that the sulphate may form a surface

complexes on the adsorbent surface, which reduces the ability of adsorbent potential. Coexisting anions have a great impact on RB5 adsorption onto palm shell based activated carbon, so a higher amount of adsorbent dose is required in order to achieve better performance of RB5 removal.

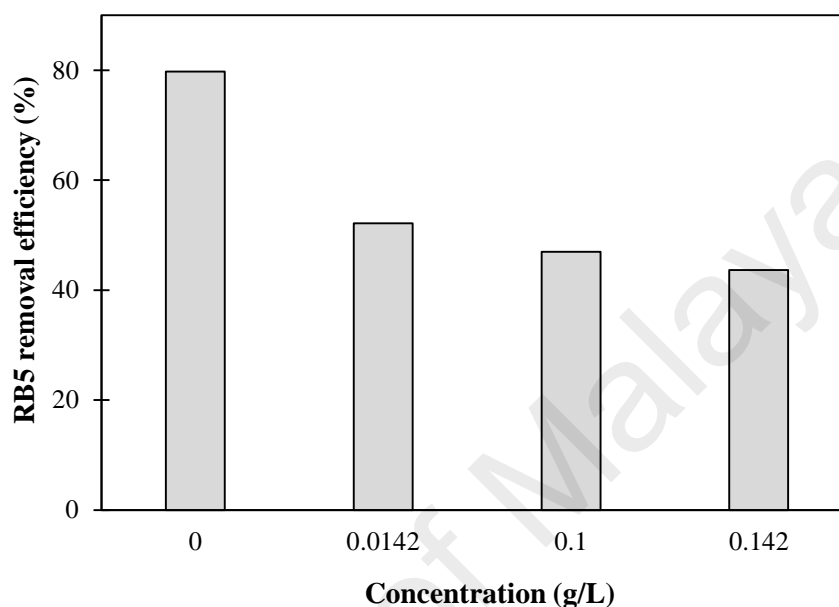


Figure 4.9: Effect of competitive adsorption on RB5 removal by palm shell activated carbon

4.1.4 Response Surface Methodology (RSM)

4.1.4.1 Development of regression equation and statistical analysis

The interaction of pH and dose could be investigated using response surface methodology (RSM), which interpret the obtained results in a statistical form. This analysis technique evaluates the interaction of parameters simultaneously; thus, it gives a good estimation on engineering work. Table 4.7 shows the experimental and predicted values of RB5 removal corresponding to the design matrix of two parameters by Central Composite Design (CCD) in RSM. The analysis suggested quadratic model fitting for the response function. The regression model is presented in Equation 4.3, where Y_{act} represents RB5 removal efficiency and X_1 , and X_2 are pH and adsorbent dose, respectively after excluding insignificant terms.

$$Y_{\text{act}} = 29.70904 - 4.11906X_1 + 10.80392X_2 - 0.36014X_1^2 + 0.10639X_1X_2 \quad (4.3)$$

Table 4.7: Central composite design for experimental and predicted RB5 removal

Run	Independent variables		RB5 removal (%)	
	pH	Adsorbent dose (g/L)	Experimental	Predicted
1	2	3	50.5	51.3
2	8	3	28.1	28.5
3	2	20	98.4	97.8
4	8	20	86.8	85.8
5	3.5	11.5	97.2	96.2
6	6.5	11.5	87.1	87.5
7	5	7.25	74.1	72.4
8	5	15.75	94.4	98.3
9	5	11.5	92.0	91.9
10	5	11.5	90.7	91.9
11	5	11.5	93.8	91.9

The significance and adequacy of the model are determined by analysis of variance (ANOVA). Table 4.8 summarizes the ANOVA results for RB5 adsorption. The statistical significance was evaluated by F-test based on a probability value with 95% confidence level. In other words, by the probability F-value ($Prob.>F$) below 0.05 is considered as a significant term; insignificant model terms are required to be eliminated in order to improve the quality of the regression model. The $Prob.>F$ for the suggested quadratic regression model (Equation 4.3) was less than 0.0001, which implied that the model was highly significant and low probability affected by noise. Table 4.8 shows that X_1 (pH), X_2 (adsorbent dose), X_1^2 and X_1X_2 are the significant model terms, as each of $Prob.>F$ was below 0.05. “Lack of fit” is required to compare the deviation of actual points from the fitted surface relative to pure error. A non-significant lack of fit is required to demonstrate the applicability of the model for predicting the response variables. The $Prob.>F$ of lack of fit for the quadratic model was 0.3215; this shows that the lack of fit was insignificant and sufficient to be used to predict RB5 removal efficiency. The quality of the model is

evaluated by the correlation coefficient value, R^2 . Here, the adjusted and predicted R^2 were both above 80% for the responses experiment, which shows that the experimental results fit well into the model. Additionally, the difference between predicted and adjusted R^2 should be less than 0.20 (20%) to confirm that they are in good agreement. The plot of predicted and actual RB5 removal efficiency (Figure 4.10) evaluates the accuracy and reliability of the predicted model (Equation 4.3). Furthermore, adequate precision (AP) of the model measures the signal to noise ratio. The AP value should be greater than 4 to indicate that the noise is insignificantly contributing to any error in the response surface. The AP for the model was 49.25 indicates an adequate signal. These statistical analyses showing that the model is reliable to navigate the effect of the parameters on RB5 removal efficiency.

Table 4.8: ANOVA results for the fitted model

Source	SS ^(a)	MS ^(b)	F-value	Prob>F ^(c)	R^2	Adj R^2	Pred R^2	AP ^(d)	SD ^(e)
Model	4945.34	1236.54	279.51	<0.0001	0.9947	0.9911	0.8777	49.25	2.10
LOF	21.66	5.47	2.34	0.3215					
X ₁	339.55	339.55	76.77	0.0001					
X ₂	3029.94	3029.94	685.00	<0.0001					
X ₂ ²	1546.40	1546.40	349.60	<0.0001					
X ₁ X ₂	29.44	29.44	6.66	0.0418					

- (a) SS: sum of squares
- (b) MS: mean of square
- (c) Prob>F: probability error of F-value
- (d) AP: adequate precision
- (e) SD: standard division
- (f) LOF: lack of fit

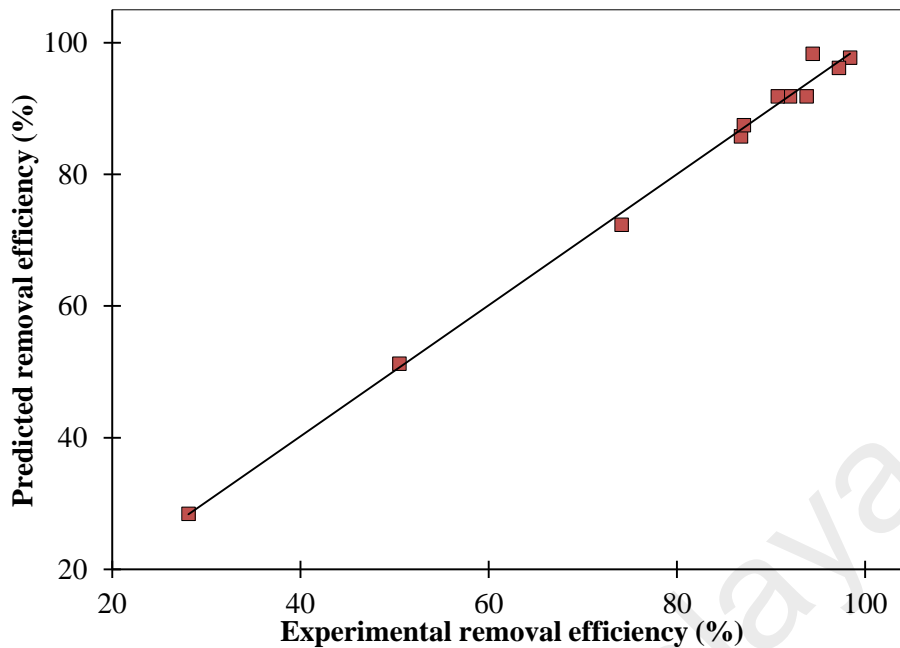


Figure 4.10: Predicted RB5 removal efficiency from the response surface model against experimental adsorption data

4.1.4.2 Interaction effect of parameters

The effect of pH and adsorbent dose on RB5 adsorption was developed as shown in Figure 4.11. It was found that decreasing the initial pH solution and increasing the adsorbent dose would improve the RB5 elimination due to the stronger electrostatic attraction between anionic RB5 and the adsorbent as well as the sufficient availability of binding sites on the adsorbent surface. At constant pH 2, RB5 was being almost completely adsorbed by 10.5 g/L adsorbent.

Although low pH is beneficial to adsorption, the removal was least affected when pH changed from 2.0 to 8.0. Thus, the influent pH should be maintained at the level of approximately 5.0 to 7.0 in order to avoid the extended addition of acid for pH adjustment. In addition, it was apparent that the adsorbent dose exerts the higher effect on RB5 removal as indicated by the steep slope. The relatively flat line for the pH parameter showed that RB5 removal was insensitive. In other words, the parameter of adsorbent dose plays a more significant role than pH when in the adsorption process.

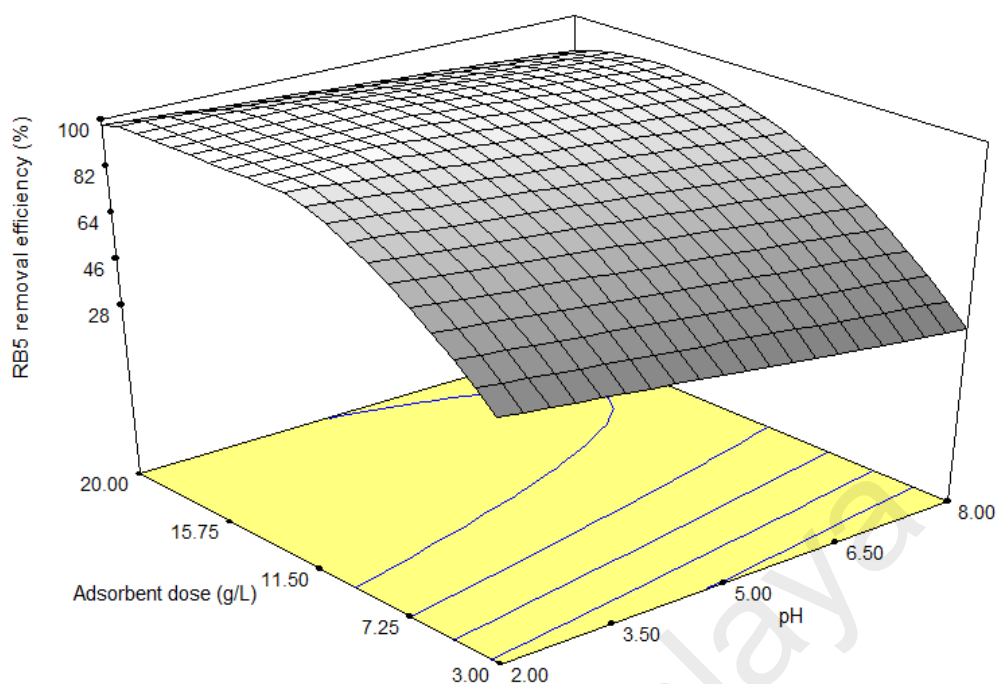


Figure 4.11: Interaction between initial pH solution and adsorbent dose on RB5 adsorption

4.1.4.3 Optimization operating conditions

Finally, to verify the proposed model, experiments were performed according to the optimum conditions suggested by RSM which were initial pH of 6.67 and adsorbent dose of 15.15 g/L. The RB5 removal under the optimum condition was 93.3%. The removal proposed by the model was 94% and the percentage error between experimental and predicted results was only between 1.0-3.0%. Hence, it can be concluded that the proposed model is sufficient to predict the adsorption of RB5 onto palm shell activated carbon under similar conditions. The optimum conditions will be used for subsequent combination studied in Section 4.3.

4.1.5 Column experiments

The column experiments were run at various initial RB5 concentrations to evaluate the dynamic performance of palm shell activated carbon. The breakthrough curves that express the normalised RB5 concentration (the ratio of effluent to influent RB5 concentrations) in terms of the treated volume of solution are shown in Figure 4.12. The

breakthrough curves were used to calculate the values of V_b , V_x , q_b , and q_s . In this study, the breakthrough point was defined as the maximum colour in the industrial effluent as set by the Environmental Quality Regulations Malaysia, which is 200 ADMI (3.15 mg/L of RB5). When the RB5 inlet concentration is increased at constant a flow rate and fixed bed height, the saturation of column occurs quicker and reduce the total treated volume because of limited adsorption sites (Table 4.9). This leads to the generation of a steeper breakthrough curve at higher initial concentration. However, the breakthrough capacity (q_b) and saturation capacity (q_s) are improved in higher influent concentration due to the larger concentration gradient between liquid and solid phases induce greater driving adsorption force. Thus, greater RB5 adsorption occurred when the column was fed with an RB5 concentration of 100 mg/L compared to 40 mg/L.

Table 4.9: Column parameters for RB5 adsorption onto palm shell-based activated carbon

C_0 (mg/L)	Q (ml/min)	V_b (L)	q_b (mg/g)	V_s (L)	q_s (mg/g)
40	6	2.52	7.98	11.88	0.32
100	6	1.08	9.94	6.84	0.52

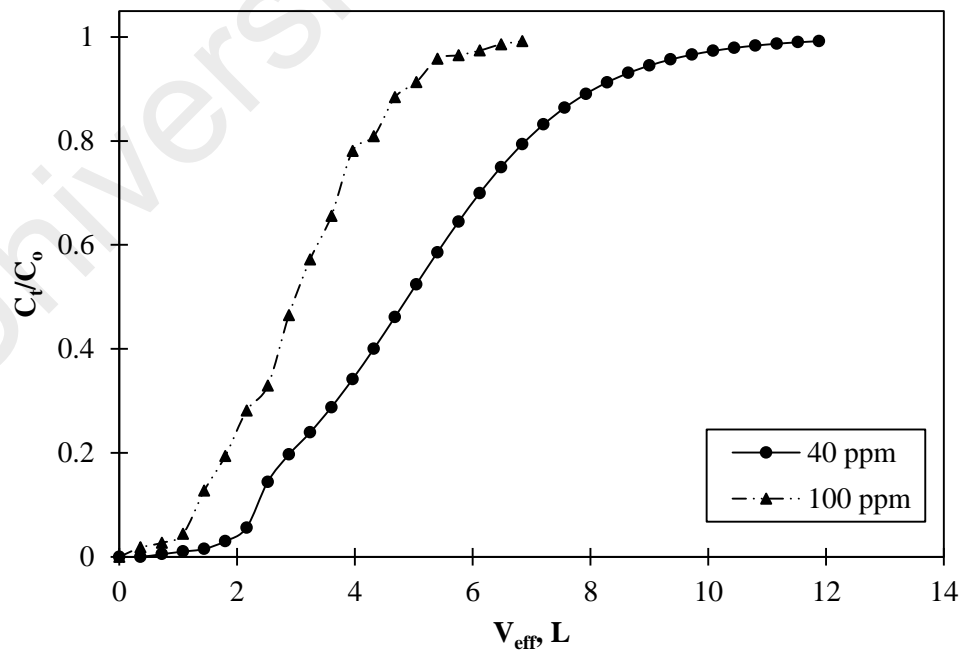


Figure 4.12: Breakthrough curve at different RB5 concentration

4.2 Electrocoagulation of RB5 by iron mesh

4.2.1 Anode configurations

Figure 4.13 shows the effect of the anode configuration on the effectiveness of RB5 removal. As can be seen, the electrocoagulation performance of the double layer iron mesh electrode was more efficient than for the single layer electrode. It was clearly observed that the trend of the RB5 removal rate on both electrodes was only comparable during first 10 min of process time. After 10 min, the removal rate of RB5 over the double layer increased compared to the single layer electrode which might be attributed to the faster passivation of the single layer electrode. Passivation leads to the formation of a passive film on the electrode surface that prevents continuous iron dissolution and reduces mass transfer Fe^{2+} to the electrolyte. This has the effect of decreasing the electrode efficiency for pollutant removal (Aber, Amani-Ghadim, & Mirzajani, 2009; Arroya, Perez-Herranz, Montanes, Garcia-Anton, & Guinon, 2009; Heidmann & Calmano, 2008). Hence, electrode passivity has a great influence in the electrocoagulation process (Yang et al., 2015). In addition, the COD removal efficiency for the single and double layer electrode was 59.6% and 97.7%, respectively. This confirmed that the double layer electrode demonstrated better performance in treating dye solution.

The electrocoagulation results of RB5 were subjected to kinetic analysis by the first-order model (Figure 4.14). A significant reduction in the RB5 concentration was observed at the double layer electrode as the treatment duration extends above 10 min. It was observed that a longer treatment time is required to achieve a complete depletion of single layer electrode. The calculated kinetic rate constant for the double layer and single layer electrodes was 0.0203 and 0.0385 min^{-1} , respectively, which confirms that RB5 removal by electrocoagulation occurs more readily on the iron mesh double layer electrode than on the single layer electrode.

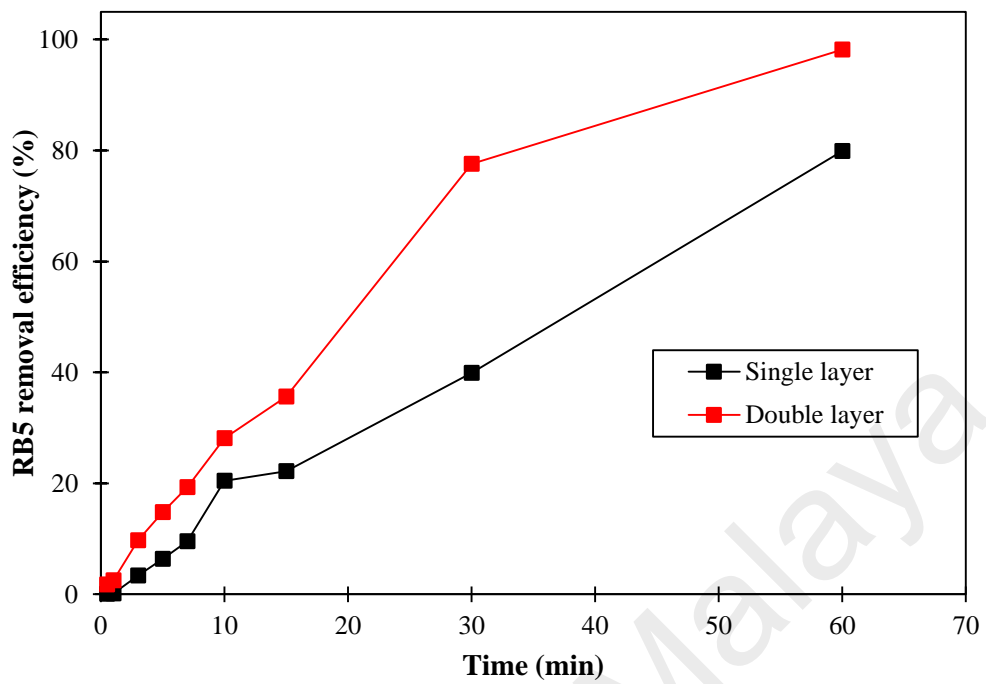


Figure 4.13: Comparison of anode configuration on RB5 removal

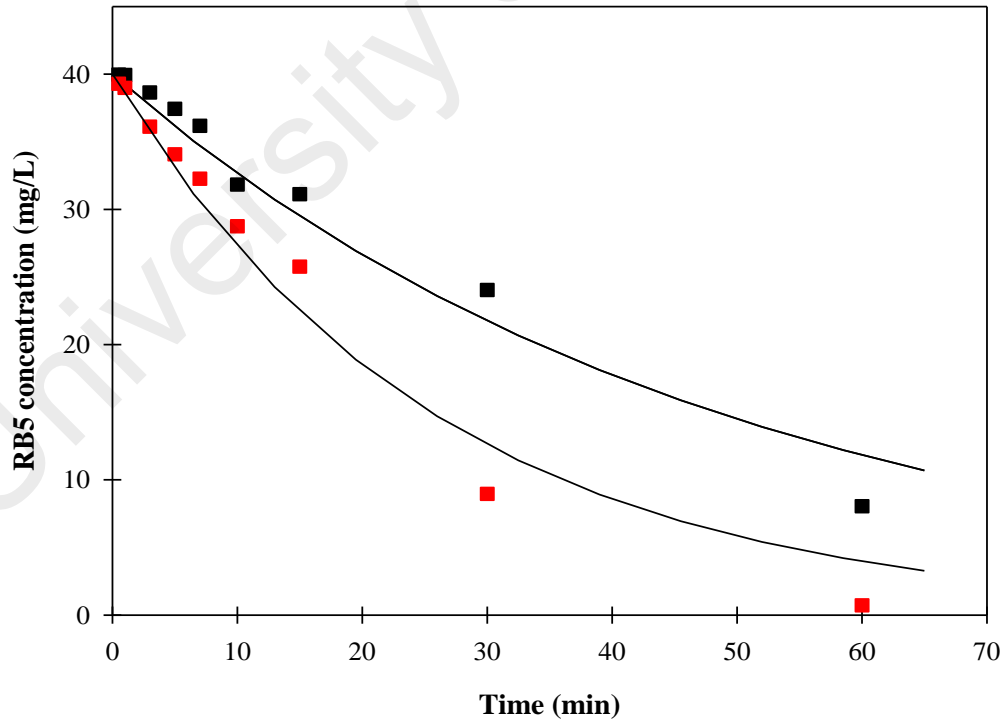


Figure 4.14: Kinetic analysis for single and double layer electrode

According to the mechanism of electrochemical reactions, the diffusion of ions from bulk solution to the electrode surface is a key step in the direct and indirect electro-degradation process (Chu, Wang, & Wang, 2010). In this study, the diffusion mechanism refers to the dye compound and hydroxide ions migrate to the anode surface film layer. The chronoamperometry technique and the Cottrell equation were used to estimate the diffusion coefficients of RB5 compound toward the single layer and double layer electrodes. The diffusion coefficients were 3.1×10^{-5} and 4.9×10^{-5} cm²/sec on the single layer and double-layer electrodes, respectively. A greater distance leads to a longer particle diffusion time which thereby lowers the rate of diffusion. Thus, it is apparent that the diffusivity of RB5 and hydroxide ions toward the double layer electrode would be higher as its diameter is two times smaller than the single layer electrode.

Figure 4.15 shows that the amount of current generated using double layer electrodes in blank and RB5 solutions were higher than for single layer electrodes. This confirms that the double layer electrode was more active than the single layer electrode. The values of current in both electrodes were higher in the RB5 solution than in blank solution due to the oxidation of RB5. Electrical energy consumption (EEC) in the double layer electrode was 20.53 kWh/kg_{dye removed}, which was 11.5% lower than the single layer. SVI is recognized as the best parameter to describe the sludge settling properties.

The SVI value below 150 mL/g indicates that the sludge has good settling properties, while the sludge with SVI above 150 mL/g is categorized as bulking sludge (Janczukowicz, Szewczyk, Krzemieniewski, & Pesta, 2001). The SVI for the single and double layer electrode was 126 and 132 mg/L, respectively. The sludge generated by both types of electrodes gave a good settling characteristic.

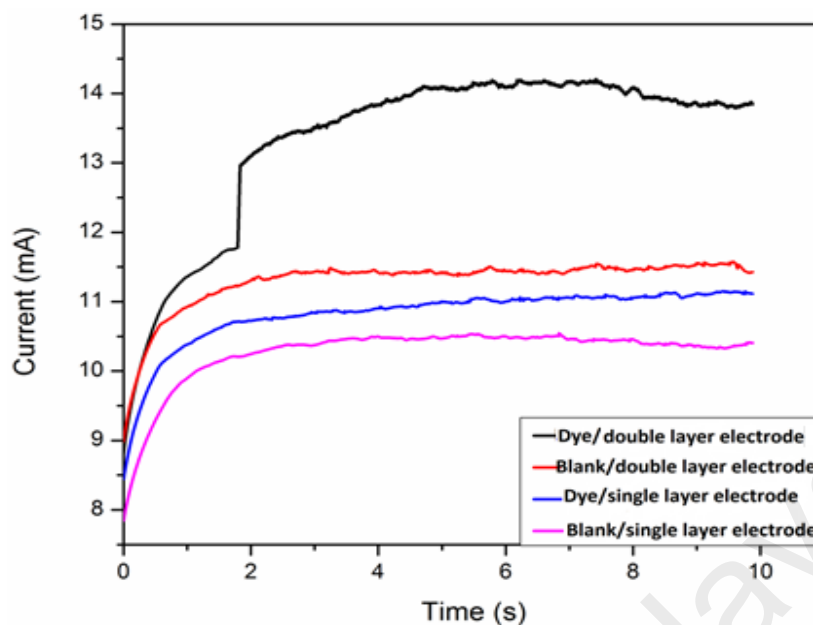


Figure 4.15: Chronoamperometry of iron mesh single and double layer electrodes in blank (0.2 g/L NaCl) and RB5 solution (0.2 g/l NaCl + 40 mg/L RB5 dye)

To investigate the applicability of double layer electrode to other dyes, an experiment was carried out with 40 mg/L of Levafix Blue CA reactive dye and 0.2 g/L of NaCl used as a model synthetic dye solution and operated at 5.02 mA/cm². The results found that the dye and COD removal was 98.2% and 89.5%, respectively. The obtained data are in a good agreement with the results presented by Körbahti et al. (2008), who reported the colour and COD removal of 99.6% and 61.6%, respectively at 25 g/L NaCl and 35.5 mA/cm² (B.K. Körbahti & Tanyolac, 2008).

Table 4.11 gives a comparison of RB5 removal efficiencies and EEC using iron as anode material. The achieved results in this study are comparable with other research. The double layer electrode produced a higher RB5 and COD removal efficiency than the single layer and it was therefore applied in subsequent experiments.

Sodium chloride (NaCl) and sodium sulphate (Na₂SO₄) are common supporting electrolytes that are utilised to increase the electrical conductivity. For a comparison purpose, NaCl was used as supporting electrolyte, which is similar to the experiment condition of other researchers. NaCl is more favourable than sodium sulphate (Na₂SO₄)

as it could generate strong oxidizing agents, i.e., hypochlorite ions (Yildiz, Koparal, İrdemez, & Keskinler, 2007). This could enhance the oxidization of Fe^{2+} to Fe^{3+} and then the easier formation of $\text{Fe}(\text{OH})_3$. However, when using the NaCl, there is a high possibility of forming hazardous by-products such as perchlorate, which has been recognized as carcinogenic (Bergmann & Rollin, 2007). Hence, in the subsequent study, Na_2SO_4 was selected as a supporting electrolyte.

Table 4.10: Performance summary for the single and double layer electrode

Parameter	Single layer electrode	Double layer electrode
RB5 removal (%)	79.9	98.2
COD removal (%)	59.6	97.7
Kinetic rate constant (min^{-1})	0.0203	0.0385
Diffusivity (cm^2s^{-1})	3.1×10^{-5}	4.9×10^{-5}
SVI (mL/g)	126.0	132.0
EEC (kWh/kg _{dye removed})	22.88	20.53
Operating cost (US\$/m ³)	0.676	0.664

Table 4.11: Comparison between different anode configurations for electrocoagulation of RB5

Electrode configuration	Experimental conditions	Results	Reference
A: Iron plate C: Iron plate	pH 5, 4.575 mA/cm ² , 3g/L NaCl	Dye removal: 98.8% EEC: 5.32 kWh/kg _{Fe}	Şengil & Özacar, 2009
A: Iron plate C: SS plate	pH 6.6, 7.5 mA/cm ² , 2 g/L NaCl	Dye removal: 90% EEC: 29 kWh/kg _{dye}	Patel et al., 2011
A: Iron mesh double layer C: Iron Plate	pH 6.3, 5.02 mA/cm ² , 0.2 g/L NaCl	Dye removal: 98.2%, EEC: 20.53 kWh/kg _{dye} ; 3.57 kWh/ kg _{Fe}	This work

4.2.2 Response Surface Methodology (RSM)

4.2.2.1 Development of regression equation and statistical analysis

CCD was employed to investigate the effect of four parameters (initial pH, current density, electrocoagulation time and supporting electrolyte dose) on RB5 removal. Table 4.12 shows the experimental and predicted values of RB5 removal corresponding to the design matrix of four parameters by CCD. The analysis suggested quadratic model fitting for the response function. The regression model was achieved (Equation 4.4), where Y_{act} represents RB5 removal efficiency and X_1 , X_2 , X_3 , and X_4 are the pH, current density, electrocoagulation time and supporting electrolyte dose, respectively, after excluding insignificant terms.

The quality and adequacy of the model are evaluated by the correlation coefficient value (R^2), adjusted and predicted R^2 , P-value, standard deviation and “lack of fit”. The adjusted R^2 measures the proportion of the variation about the mean as explained by the model, whereas predicted R^2 is a measurement of the model to predict the response value. The discrepancy between predicted and adjusted R^2 should be less than 0.20 in order to confirm that the data or model is reliable (Mook *et al.* 2016). Here, the adjusted and predicted R^2 are in good agreement, i.e. 0.9912 and 0.9808, respectively. The plot of predicted and actual RB5 removal efficiency (Figure 4.16) evaluates the accuracy and reliability of the predicted model. The actual values were close to the predicted values, showing that the model is reliable to describe the effect of the parameters on RB5 removal efficiency. The significance and adequacy of the model are determined by analysis of variance (ANOVA). Table 4.13 summarises the ANOVA results for RB5 removal. The Fisher variance ratio, F-value, is a valid statistical measurement used to describe the variation in the mean of data (Tak *et al.* 2015). The probability F-value ($Prob.>F$) below 0.05 is considered as a significant term; insignificant model terms are required to be eliminated in order to improve the quality of the regression model. Here, the suggested

quadratic regression model (Equation 4.4) is highly significant, which is proven by the low probability value ($Prob.>F = 0.0001$). Table 4.13 shows that X_1 (pH), X_2 (current), X_3 (electrocoagulation time), X_4 (electrolyte dose), X_1^2 , X_4^2 , X_1X_3 , X_1X_4 , X_2X_3 , X_2X_4 , X_3X_4 are the significant model terms, as each of $Prob.>F$ was below 0.05. Lack of fit” is required to compare the deviation of actual points from the fitted surface relative to pure error. A non-significant lack of fit is required to demonstrate the applicability of the model in order to predict the response variables (Mook *et al.* 2013). The $Prob.>F$ of lack of fit for the quadratic model was 0.2385; this shows that the lack of fit was insignificant and sufficient to be used to predict RB5 removal efficiency.

$$Y_{act} = -108.54872 + 34.90139X_1 - 4.36213X_2 + 0.17063X_3 + 744.48145X_4 - 2.59394X_1^2 - 5010.18351X_4^2 - 0.039205X_1X_3 + 10.54583X_1X_4 + 0.24051X_2X_3 + 57.06284X_2X_4 + 2.70864X_3X_4 \quad (4.4)$$

Table 4.12: Central composite design for experimental and predicted RB5 removal

Run	Independent variables				RB5 removal (%)	
	pH	Current (mA/cm ²)	Electrocoagulation time (min)	Electrolyte dose (g/L)	Experimental	Predicted
1	4	1.5	5	0.05	15.1	16.7
2	10	1.5	5	0.05	9.4	10.2
3	4	3.33	5	0.05	17.8	16.1
4	10	3.33	5	0.05	11.1	9.6
5	4	1.5	60	0.05	46.9	44.7
6	10	1.5	60	0.05	26.1	25.3
7	4	3.33	60	0.05	67.3	68.4
8	10	3.33	60	0.05	47.5	48.9
9	4	1.5	5	0.15	7.0	5.0
10	10	1.5	5	0.15	5.2	4.9
11	4	3.33	5	0.15	13.4	14.9
12	10	3.33	5	0.15	13.2	14.7

Table 4.12 continued

Run	Independent variables				RB5 removal (%)	
	pH	Current (mA/cm ²)	Electrocoagulation time (min)	Electrolyte dose (g/L)	Experimental	Predicted
13	4	1.5	60	0.15	46.4	47.9
14	10	1.5	60	0.15	33.1	34.9
15	4	3.33	60	0.15	82.8	82.1
16	10	3.33	60	0.15	70.5	68.9
17	5.5	2.43	32.5	0.1	63.2	64.6
18	8.5	2.43	32.5	0.1	62.8	59.7
19	7	1.97	32.5	0.1	61.4	63.8
20	7	2.87	32.5	0.1	69.3	72.1
21	7	2.43	18.75	0.1	56.9	57.7
22	7	2.43	46.25	0.1	79.0	78.2
23	7	2.43	32.5	0.08	61.3	63.8
24	7	2.43	32.5	0.13	70.1	65.9
25	7	2.43	32.5	0.1	69.54	67.9
26	7	2.43	32.5	0.1	67.04	67.9
27	7	2.43	32.5	0.1	69.18	67.9

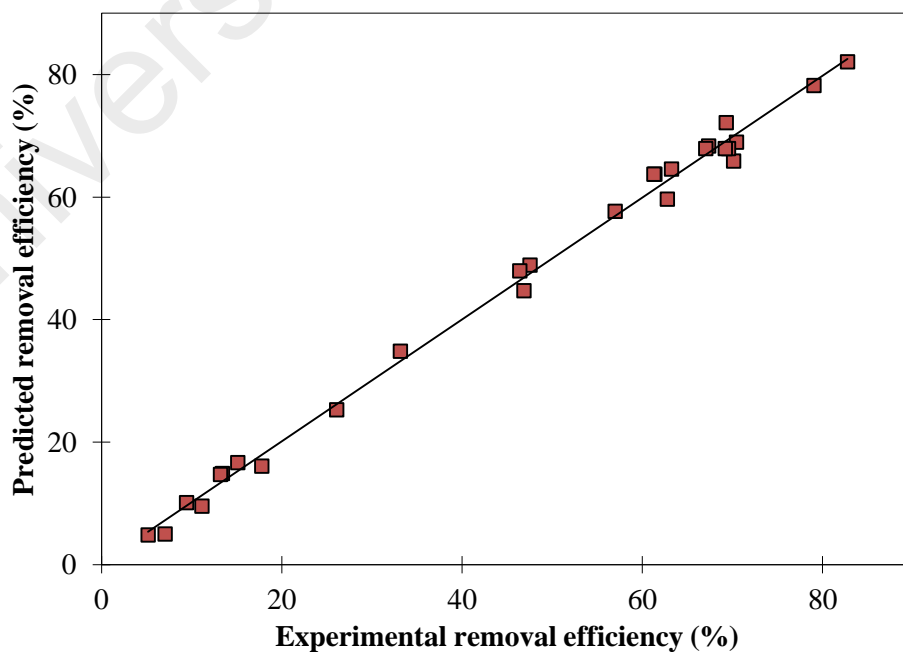


Figure 4.16: Predicted RB5 removal efficiency from the response surface model against experimental electrocoagulation data

Table 4.13: ANOVA results for the fitted model

Source	SS ^(a)	MS ^(b)	F-value	Prob>F ^(c)	R ²	Adj R ²	Pred R ²	AP ^(d)	SD ^(e)
Model	17433.53	1584.87	267.13	<0.0001	0.9949	0.9912	0.9808	47.544	2.44
LOF ^(f)	85.34	6.56	3.59	0.2385					
X ₁	396.16	396.16	66.77	<0.0001					
X ₂	1159.29	1159.29	195.4	<0.0001					
X ₃	6979.71	6979.71	1176.42	<0.0001					
X ₄	73.12	73.12	12.32	0.0032					
X ₁ ²	134.84	134.84	22.73	0.0002					
X ₄ ²	38.82	38.82	6.54	0.0219					
X ₁ X ₃	167.38	167.38	28.21	<0.0001					
X ₁ X ₄	40.04	40.04	6.75	0.0202					
X ₂ X ₃	586	586	98.77	<0.0001					
X ₂ X ₄	109.05	109.05	18.38	0.0006					
X ₃ X ₄	221.94	221.94	37.41	<0.0001					

(a) SS: sum of squares

(b) MS: mean of square

(c) Prob>F: probability error of F-value

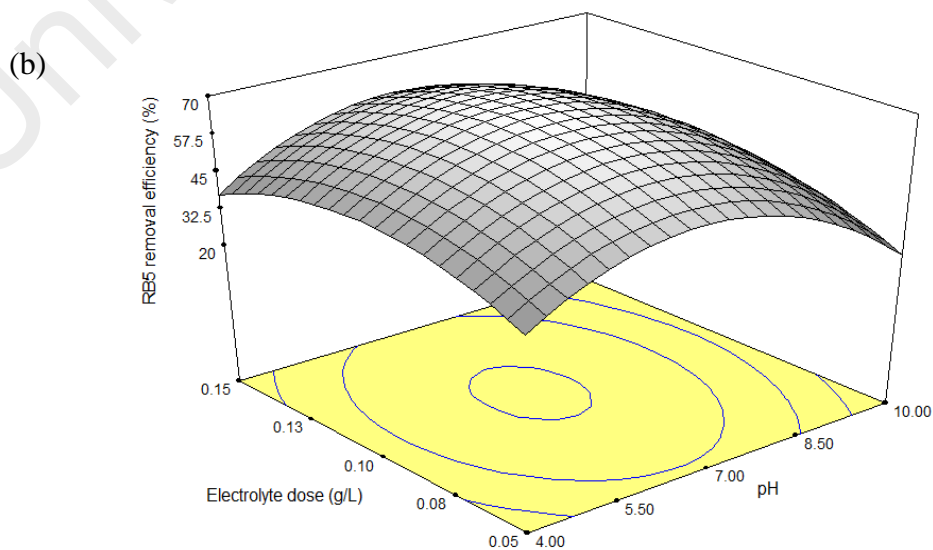
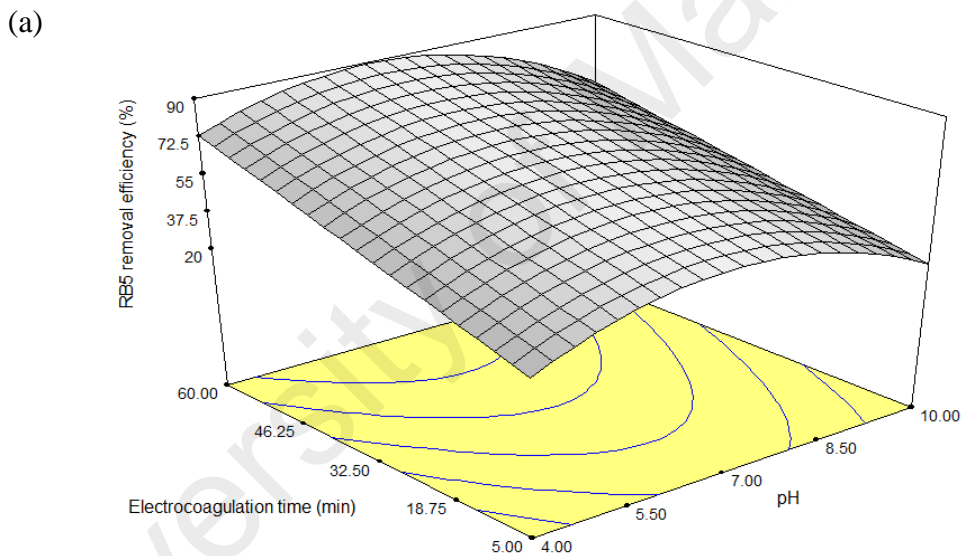
(d) AP: adequate precision

(e) SD: standard division

(f) LOF: lack of fit

4.2.2.2 Interaction effect of parameters

Figure 4.17 shows the effect of the four parameters on colour removal efficiency in a 3D plot according to Equation 4.4. Figure 4.17a shows the effect of pH and electrocoagulation time on RB5 removal at a constant current density of 2.42 mA/cm^2 and electrolyte dose of 0.1 g/L . The plot implies that the high removal of RB5 was achieved in weak acid to weak alkaline conditions (pH 5.8–8.22) and at longer process times (46–60 min). The RB5 removal decreased after pH 8.22 due to the formation of various iron hydroxides species that influenced by pH.



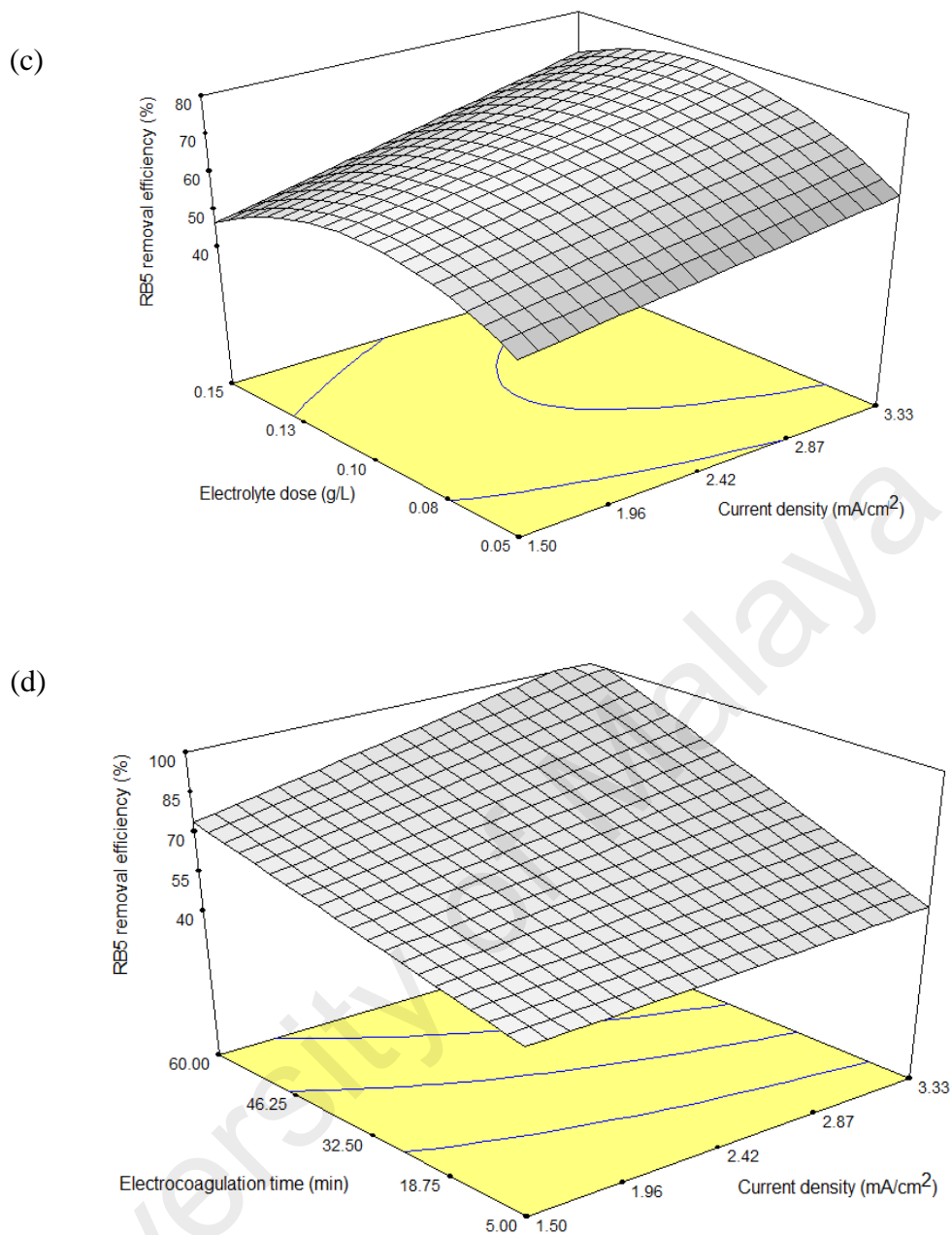


Figure 4.17: Response surface plot of RB5 removal efficiency (a) interaction between pH and electrocoagulation time, (b) interaction between pH and electrolyte dose, (c) interaction between electrolyte dose and current density, (d) interaction between current density and electrocoagulation time

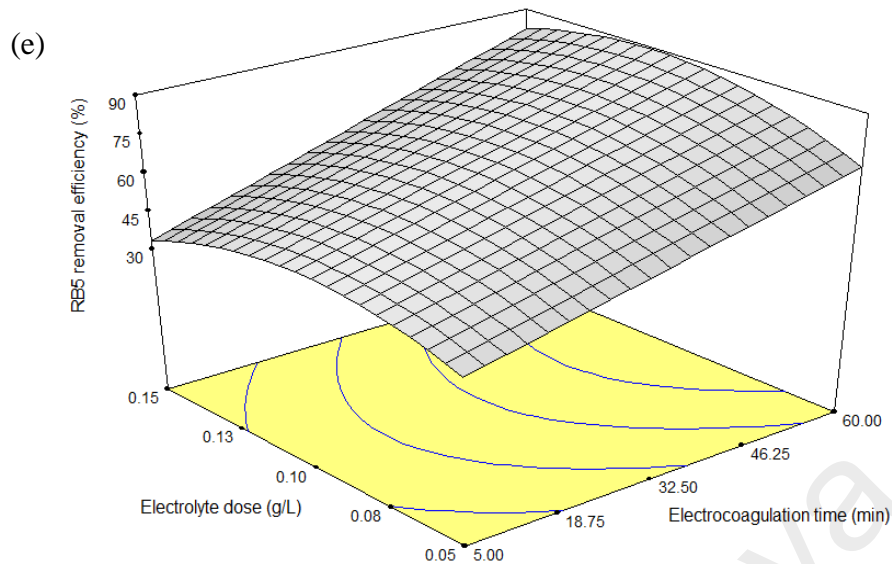
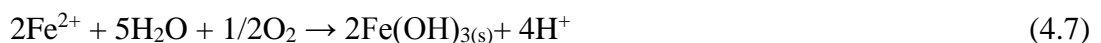
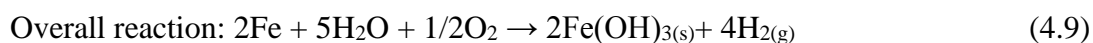


Figure 4.17 continued: (e) interaction between electrocoagulation time and electrolyte dose

There are three stages of electrocoagulation of RB5. Firstly, the iron ions (Fe^{2+}) are produced through anode dissolution. During water electrolysis, oxygen and hydroxide ions are produced at the anodic and cathodic region, respectively (Equations 4.5 and 4.9). The Fe^{2+} oxidized spontaneously to Fe^{3+} in the presence of oxygen species. Subsequently, the hydroxide ions further react with Fe^{3+} to form $\text{Fe}(\text{OH})_3$ as shown in Eq. 4.7 (Zaroual, Azzi, Saib, & Chainet, 2006). The $\text{Fe}(\text{OH})_n$ formed as a gelatinous suspension in the solution, which can remove pollutants by coagulation. The second stage is destabilization of contaminants, where the counter ions of $\text{Fe}(\text{OH})_n$ neutralize the charge of the RB5 present in the solution. The counter ions reduce the electrostatic interparticle repulsion to extend that the van der Waals attraction predominates; thus, stimulate coagulation process. The last stage is where the destabilized RB5 molecules begin to coalesce and absorbed into the floc formed (El-Taweel, Nassel, Elkheriany & Sayed, 2015).





At low pH, H^+ ions become more prevalent in the solution and are reduced to H_2 at the cathode (Eq. 4.10). The hydroxide ions are then difficult to be generated as the electrons are being used for H^+ reduction (Eq. 4.8). As shown in Fe(III) predominance-zone diagram (Şengil & Özacar, 2009) (Figure 4.18), the soluble $\text{Fe}(\text{OH})_2^+$ and $\text{Fe}(\text{OH})^{2+}$ were produced, which are not capable to remove pollutant compounds. These species are transformed into $\text{Fe}(\text{OH})_3$ in the pH aqueous solution of 6–9.5 (Şengil & Özacar, 2009). $\text{Fe}(\text{OH})_3$ is an insoluble metal hydroxide and it removes the dye molecule through precipitation and adsorption (Mook et al., 2016). When the initial pH of the solution is higher than 9.5, monomeric anions $\text{Fe}(\text{OH})_4^-$ are the dominant species formed via dissolution of $\text{Fe}(\text{OH})_3$ (Eq. 4.11) (Kobya et al., 2006; Babu, Bhadrinarayana, Begum & Anantharaman, 2007). The RB5 removal efficiency was found to be 89% at the initial pH of 6.3, which was the original pH of the dye solution. The obtained data are in a good agreement with the results presented by Daneshvar *et al.* (2006), who reported the maximum colour removal of Basic Red 46 and Basic Blue 3 are between pH 5.5–8.5.



During water electrolysis, hydrogen and hydroxide ions are produced as shown in Equations 4.5 and 4.8. The increasing of the final pH from acidic to alkaline is due to the presence of OH^- ions; whereas the final pH of alkaline conditions ($> \text{pH } 9$) decreases slightly due to the consumption of hydroxide ions to form $\text{Fe}(\text{OH})_4^-$ (Eq. 4.11) (Nandi & Patel, 2013).

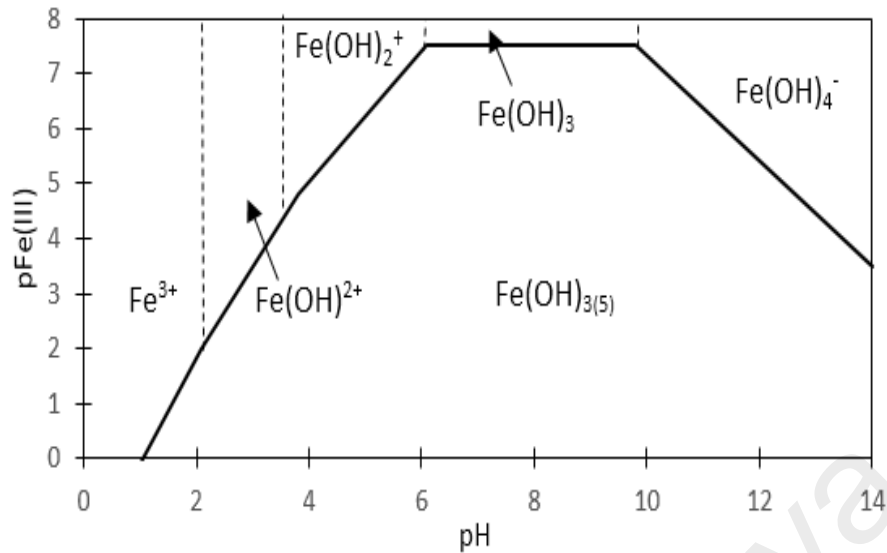
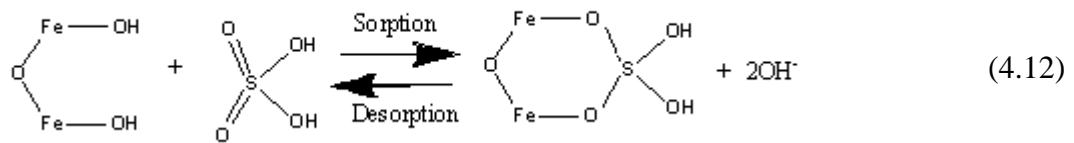


Figure 4.18: Predominance-zone diagrams for Fe(III) chemical species in aqueous solution (Şengil & Özacar, 2009)

Figure 4.17b shows the effect of pH and electrolyte dose on RB5 removal by maintaining current and electrocoagulation time in the middle range levels (2.42 mA/cm² and 32.5 min). It was observed that the trend of RB5 removal was initially increased, and then decelerated beyond the pH 7 at any Na₂SO₄ concentration. Increasing the concentration of Na₂SO₄ from 0.05 to 0.1 g/L slightly increased the RB5 removal efficiency. In other words, the increased conductivity of the solution had a minor effect on the efficiency of dye removal. Moreover, among the four parameters, initial pH, current density, electrocoagulation time and electrolyte dose, the *Prob.> F* of electrolyte dose was the highest, indicating that the electrolyte dose has only a minor effect on RB5 removal.

The RB5 removal efficiency decreases beyond 0.1 g/L of Na₂SO₄ concentration (Figure 4.17c). This might be attributed to the excess of SO₄²⁻ ions that interact with iron hydroxides via ligand exchange (Eq. 4.12). As a result, the required iron hydroxides for dye removal decreased (Kleinhenz, 1999). The removal trend is in a good agreement with

the results presented by Tezcan Ün et al (2009), who used electrocoagulation to treat wastewater from a cattle slaughterhouse.



The interactive effect of electrolyte dose and current density on dye removal at a constant pH of 7 and treatment time of 32.5 min is illustrated in Figure 4.17c. The higher removal of RB5 was obtained by the interaction between moderate electrolyte dosage and high current density. The increase in applied current had a positive effect on dye removal for any given electrolyte dose. According to Faraday's law (Equation 4.13), the amount of Fe^{2+} formed from the anode is directly proportional to the current (M.Y A. Mollah et al., 2004). The increment quantity of Fe^{2+} enhances the formation of $\text{Fe}(\text{OH})_3$, which is the essential component to eliminate dye compounds. Furthermore, the bubble generation rate comprises of oxygen (evaluated from the anode surface) and hydrogen gas (takes place in the cathode) and increases with current, which is beneficial for pollutants removed by flotation (Abdel-Gawad, Baraka, Omran, & Mokhtar, 2012).

However, increasing the current from 2.67 mA/cm^2 to 3.33 mA/cm^2 at a constant electrolyte dose of 0.1 g/L and pH 7 resulted in a slight improvement of RB5 removal, from 70.5% to 76.4%, respectively. The higher current density might cause excessive production of oxygen and hydrogen gas, which disperses current usage for the generation of Fe^{2+} and OH^- . Hence, the current density is one of the crucial parameters for electrocoagulation treatment of wastewater.

$$C = \frac{Mit}{ZFv} \quad (4.13)$$

where C is the iron concentration in the system, M is the molecular weight of anode (iron), I is the current, Z is the chemical equivalence (+2), F is the Faraday's constant and v is the volume of the solution.

The effect of current density and electrocoagulation time, while maintaining pH 7 and electrolyte dose of 0.1 g/L, is shown in Figure 4.17d. As the current density and duration of the electrocoagulation process increased, RB5 removal trend was growing. At a constant current density of 2.33 mA/cm², the RB5 removed as high as 86.6% after 60 min of treatment time. According to Equation 4.13, the production of Fe²⁺ increases with the time of the process. Then, the formation of Fe(OH)₃ was higher, and thus a sufficient amount of coagulants could react with dye compounds. Moreover, there was sufficient time for the coagulant to interact with RB5, and for the bubble generation that enhanced the flotation ability (Tezcan Ün, Koparal, & Bakir Öğütveren, 2013).

The interactive effect of electrocoagulation time and electrolyte dose on RB5 removal at a constant pH 7 and current of 2.42 mA/cm² is illustrated in Figure 4.17e. The higher RB5 removal was obtained by a simultaneous higher electrolysis time and an intermediate range of Na₂SO₄ from 0.08–0.12 g/L.

4.2.2.3 Optimization operating conditions

The RSM software proposes a specific point that maximizes desirability. The highest desirability value is 1.0, indicating that the response is close to the ideal value. The optimal operating conditions for the maximum RB5 removal were initial pH of 6.63, current density of 2.5 mA/cm², electrolyte dose of 0.11 g/L and electrocoagulation time of 50.3 min. Under the optimum conditions, the experimental removal efficiency of RB5 was 80.9%, close to the predicted value (83.3%). This proves that the proposed model (Equation 4.4) is reliable and sufficient to predict the RB5 removal efficiency.

The electrocoagulation of RB5 is a complicated mechanism. The colour of the solution was removed by adsorption or complexion with iron hydroxides to form ionic bonds. Figure 4.19 shows the adsorption spectra of RB5 along the electrocoagulation process using optimum experimental conditions. The spectra of RB5 before treatment are characterized by two main peaks: a visible region with an absorbance peak at 597 nm, and an ultraviolet region with an absorbance peak at 312 nm. The peak at 597 nm corresponds to chromophonic group $-N=N-$, and the peak at 312 nm is related to benzene rings. As seen in Figure 4.19, the peak at 597 nm decreased quickly within 20 min and the absorbance was reduced to 0.1825 after 50.3 min. This shows that the $-N=N-$ was a cleavage, and the colour disappeared rapidly. As the electrocoagulation process proceeds, the peak at 312 nm decreases concurrently with the reducing peak at 595 nm. During electrocoagulation degradation, cleavage of $-N=N-$ and aromatic rings occurred, resulting in a decrease of the absorbance band of the dye solution. The obtained data are in good agreement with the results presented by Daneshvar et al. (2006), who were using electrocoagulation process to treat C.I. Basic Blue 3. They found that the peaks in the visible and ultraviolet region were significantly reduced after treatment process (Daneshvar, Oladegaragoze & Djafarzadeh, 2006).

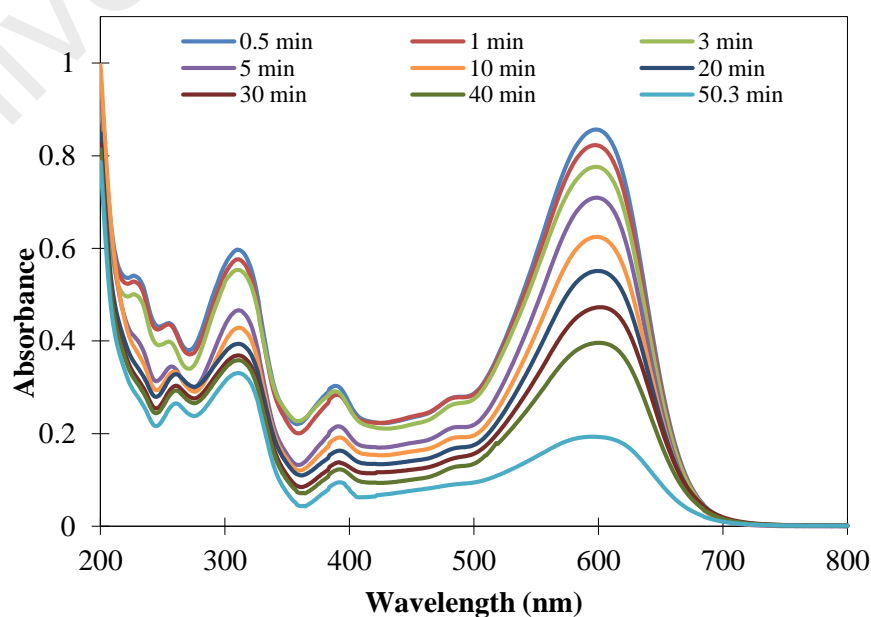


Figure 4.19: UV-Vis spectra of RB5 before and after treatment

4.2.2.4 Zeta potential

The colloid is recognized as a stable system, as similar charges will repel each other and can be difficult to aggregate. The charged colloidal particles attract opposite charged ions to their surface to maintain their electroneutrality. The attraction of counter-ions leads to an electric double layer that includes the Stern and diffuse layers. However, it is difficult to determine the charge at the colloid surface since the Stern layer is tightly bound to the colloid. Hence, the zeta potential is used as a measurement of the effective charge of the particle as it moves through the solution. In other words, zeta potential acts as an indicator of solution stability. The function of the coagulant generated through electrolysis is to destabilize the colloidal suspension, which enables the destabilized particles to aggregate (Holt, Barton, Wark, & Mitchell, 2002).

Figure 4.20 illustrates zeta potential measurements along with electrocoagulation time for optimum conditions. The zeta potential values changed with time, which indicates that there was a chemical interaction between the pollutants and iron hydroxide precipitates. The pollutants might be removed by hydrogen bonding and van der Waals interaction, but these types of attractions do not affect any change of zeta potential (Zaroual et al., 2006). During the first three minutes of the electrocoagulation process, there are no significant changes of zeta potential. This observation might be due to the low generation of ferrous ions, which limits the coagulation process. An increase in electrolysis time will increase the iron concentration, and as a consequence, the formation of coagulant will be greater. These cationic coagulants provide positive electric charges to reduce the negative charge (zeta potential) of the colloids, in order to aggregate the pollutant. As the quantity of the coagulant increases, the dye removal efficiency, and zeta potential increased (Emamjomeh, 2006).

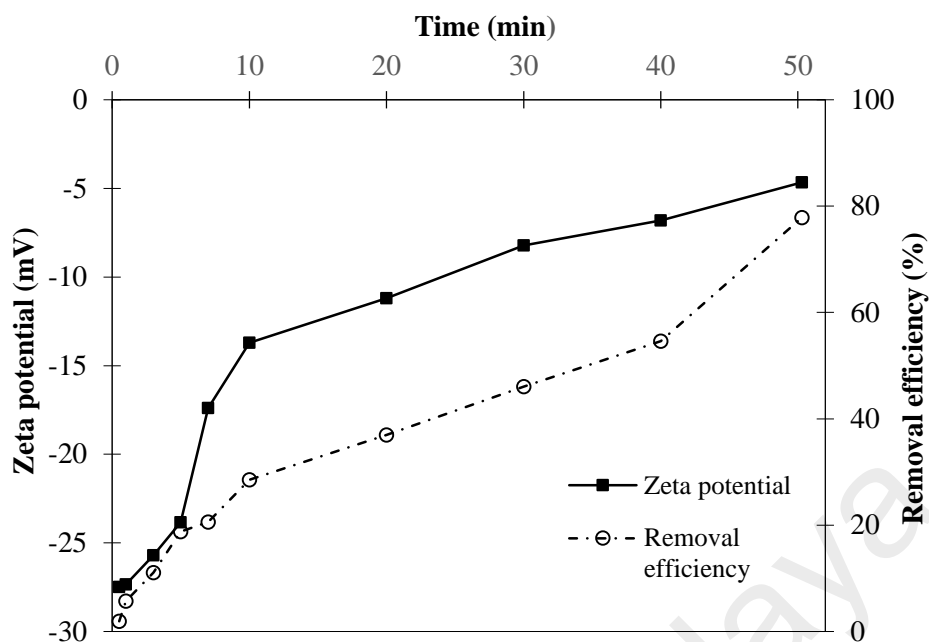


Figure 4.20: Changes in zeta potential with time at optimum conditions of the EC process

From the data gathered, the RB5 removal result can be improved by implementing the combination optimization conditions of adsorption and electrocoagulation processes. In practical applications, the combined process can be considered as the best option as it is simple, low cost, and projecting higher efficiency than the individual process. Due to these reasons, the hybrid of adsorption and electrocoagulation process is proposed for further experiment.

4.3 Combined adsorption and electrocoagulation process to treat RB5

4.3.1 Effect of process parameters

4.3.1.1 Effect of pH

To investigate the effects of pH on A-EC, four solutions of constant pH 4, pH 6, pH 8 and pH 10 were tested at a constant adsorbent dose of 16 g/L and a current density of 2.5 mA/cm². Figure 4.21 shows that the removal efficiency increased as the pH increased from 4 to 6. These results demonstrate that the highest RB5 removal was obtained at pH 6 after 60 min of treatment time. At lower pH values, adsorption may play a larger role

than electrocoagulation because $\text{Fe}(\text{OH})_3$ is only present in low levels in the solution. The activated carbon surface is positively charged because the point of zero charge (pH_{pzc}) for the adsorbent was at pH 8.1. Therefore, there was a strong electrostatic attraction between anionic RB5 and the adsorbent surface, which enhanced the adsorption process at lower pH values. However, the electrostatic attraction to RB5 became weaker as the pH of the solution was increased. When the pH changed from acidic to alkaline, the generation of iron hydroxide used to remove RB5 was promoted. Based on the predominance-zone diagram for Fe(III) in aqueous solution, $\text{Fe}(\text{OH})_3$ formation was predominant between pH 6 and 9.5 (Şengil and Özacar, 2009).

As shown by the individual adsorption data discussed in our previous work, in a pH range from 2 to 10, the adsorption capacity decreased from 12.07 to 10.03 mg/g (Mook et al., 2016a). However, when electrocoagulation was performed alone, the RB5 removal efficiency increased by approximately 25% as the pH increased from 4 to 7 (Mook et al., 2016b). Therefore, the pH has a more significant effect on electrocoagulation than adsorption in A-EC.

When the initial pH is higher than 7 (final pH to not less than 9.7), the $\text{Fe}(\text{OH})_3$ begins to dissolve to $\text{Fe}(\text{OH})_4^-$. The results imply that the iron hydroxide complex is incapable of removing RB5. Moreover, repulsion between the adsorbent and RB5 occurred when the pH of the solution was high; therefore, degradation of RB5 was negatively affected.

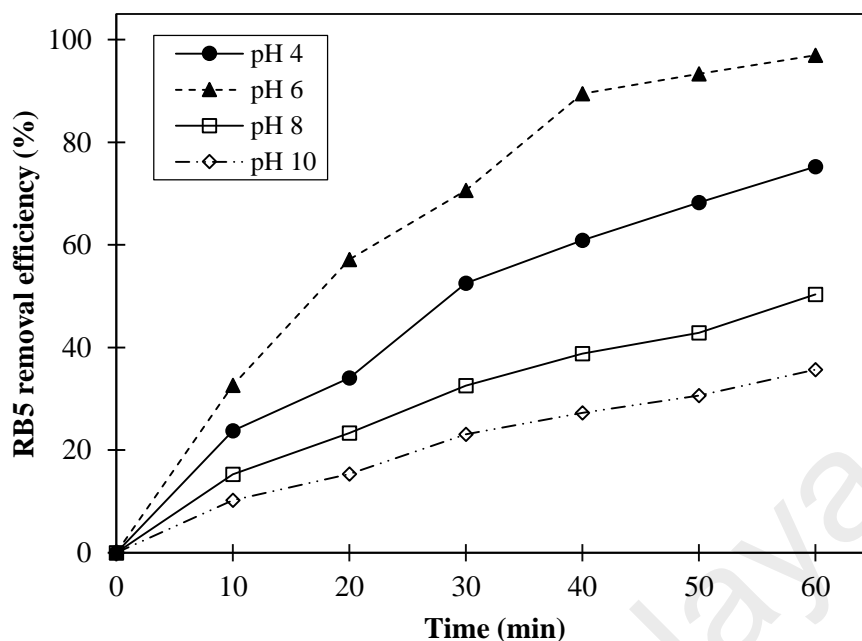


Figure 4.21: Effect of pH on RB5 removal by combined process ($C_0 = 40$ mg/L, current density = 2.33 mA/cm², adsorbent dose = 15 g/L, agitation = 160 rpm)

4.3.1.2 Effect of current density

Current density is an important parameter that influences the rate of coagulant production, bubble production and growth of flocs. Figure 4.22 shows that the RB5 removal efficiency was higher with higher current densities. For example, at a constant adsorbent dose of 12.5 g/L, removal efficiencies of 39.8% , 53.1% , 70.6% and 85.4% were obtained after 30 min of treatment at current densities of 1.67 , 2.33 and 3 mA/cm², respectively. According to Faraday's law (Equation 4.14), these higher current densities are sufficient to produce an adequate amount of iron hydroxides to remove RB5 (Mook et al., 2016). Additionally, the generation of hydrogen gas at the cathode is greater at higher current densities. These bubbles increase the degree of mixing of iron hydroxides and RB5, thus promoting the flotation process and leading to efficient RB5 removal (El-Taweel et al., 2015). The highest RB5 removal efficiency (99.9%) was obtained at the highest current density tested (3 mA/cm²) within 49.19 min of treatment.

$$m = \frac{Mit}{ZF} \quad (4.14)$$

where m is the mass of iron ions produced at the anode (g), M is the atomic weight of iron (56 g/mol), I is the current (A), t is the process time (s), z is the valence number of the iron ($z = 2$) and F is the Faraday constant (96485 C/mol).

However, it is advisable to limit the current density to avoid higher sludge production and eliminate other undesirable effects, such as heat generation (Mollah et al., 2004). The current density of 2.33 mA/cm² was selected for the subsequent experiments because of its high performance at much shorter treatment time and reasonable operating cost.

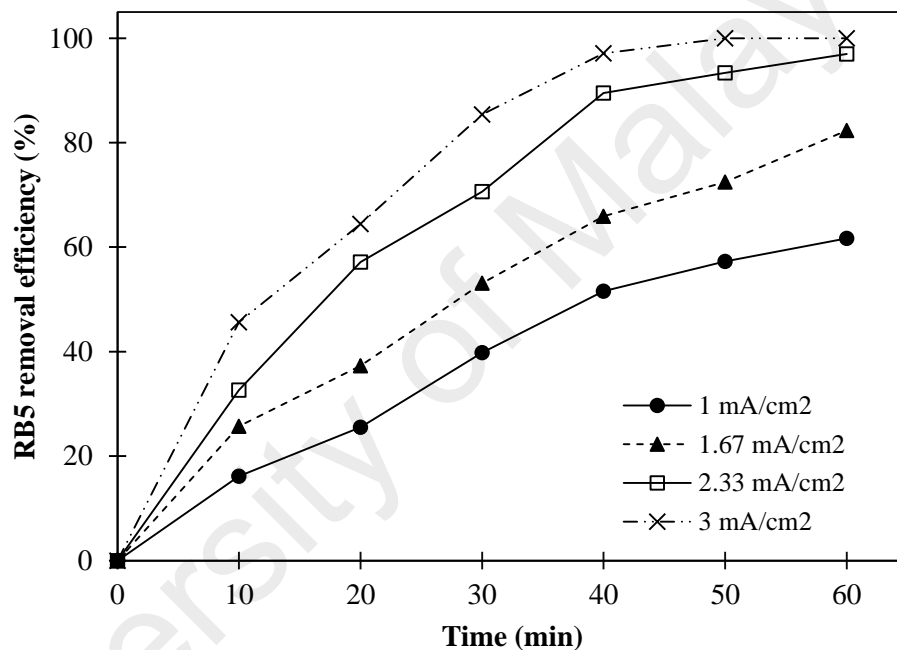


Figure 4.22: Effect of current density on RB5 removal by combined process ($C_0 = 40$ mg/L, pH = 6, adsorbent dose = 15 g/L, agitation = 160 rpm)

4.3.1.3 Effect of adsorbent dose

The effect of adsorbent dose and current density on RB5 removal efficiency at a constant initial pH of 6 is presented in Figure 4.23. As expected, increasing adsorbent dose resulted in more RB5 removal because a sufficient amount of binding sites on the adsorbent surface is required for RB5 adsorption.

It was clearly observed that the trend of the RB5 removal rate with tested adsorbent dose was comparable during first 10 min of process time. This might be attributed to

adsorption required time for the intra-particle diffusion, where the pollutants started to diffuse within the pores of activated carbon, binding the pores and capillary spaces (Samiey & Ashoori, 2012). After 40 min of A-EC treatment, the RB5 removal efficiency achieved at 5, 10, 15 and 20 g/L was 56.6%, 68.6%, 89.5% and 98.6%, respectively. This is attributed to that the more available adsorption sites on the adsorbent surface at a high adsorbent dose.

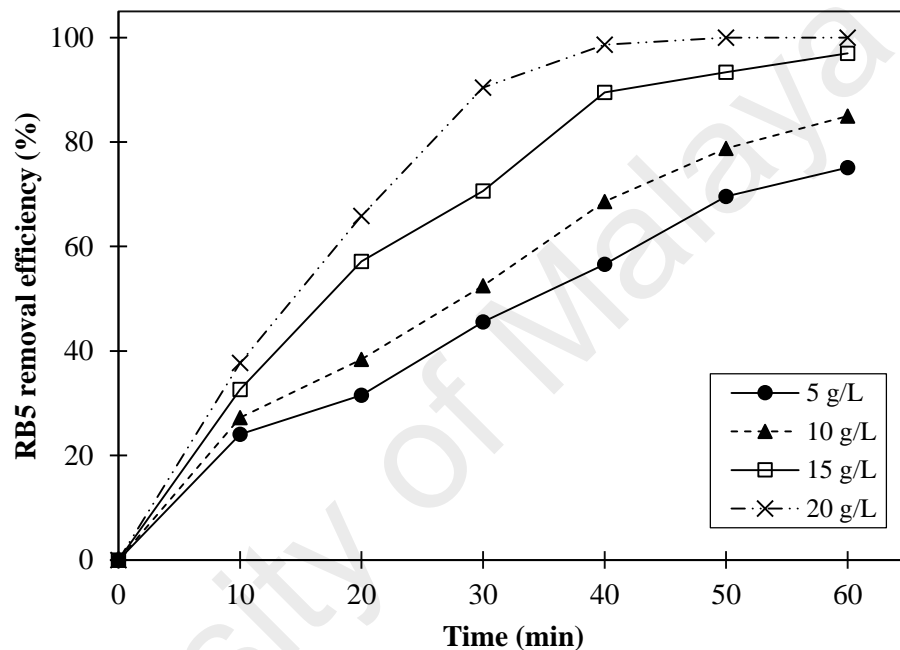


Figure 4.23: Effect of adsorbent dose on RB5 removal by combined process ($C_0 = 40$ mg/L, pH = 6, current density = 2.33 mA/cm², agitation = 160 rpm)

4.3.1.4 Effect of initial RB5 concentration

The effect of initial RB5 concentration was studied from 20 mg/L to 80 mg/L for 60 min, at the constant initial pH 6, current density of 2.33 mA and adsorbent dose of 15 g/L. As shown in Figure 4.24, the removal efficiency decreased from 99.9% to 70.8% as the initial RB5 concentration varied from 20 to 80 mg/L. There is inadequate amount of coagulant to remove excess RB5 at high concentration. As a result, with increasing the initial dye concentration, the RB5 removal efficiency was lower (Aoudj, Khelifa, Drouiche, Hecini, & Hamitouche, 2010). Moreover, increasing RB5 concentration

enhances passivation on the surface of anode and cathode, resulted in decreasing Fe dissolution rate at the anode and hydrogen gas evolution at the cathode. Hence, the longer treatment time is required to achieve complete elimination of high RB5 concentration.

Figure 4.25 shows the comparison RB5 removal efficiency of A-EC with individual adsorption and electrocoagulation at 40 and 60 mg/L of RB5 concentration. At a higher RB5 concentration of 60 mg/L, the removal efficiencies of 30.3%, 58.1%, and 85.7% were achieved after 60 min of treatment in the individual adsorption, electrocoagulation, and A-EC, respectively. This showed that A-EC has a better performance and great potential to treat higher dye concentration compared with the individual adsorption and electrocoagulation.

The parameters of pH, current density, adsorbent dose and operation time are affecting each other. Hence, it is essential to use RSM tool to investigate the effect of related parameters and optimize the operating conditions, which will be discussed in Section 4.3.3.

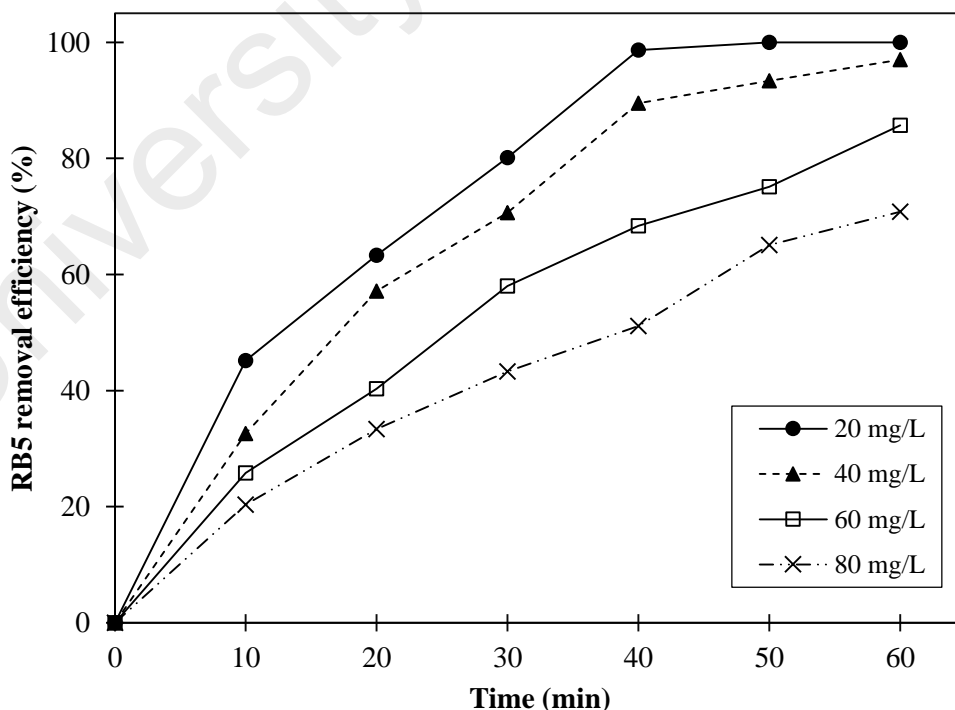


Figure 4.24: Effect of initial RB5 concentration on RB5 removal by combined process ($C_0 = 40$ mg/L, pH = 6, current density = 2.33 mA/cm², agitation = 160 rpm)

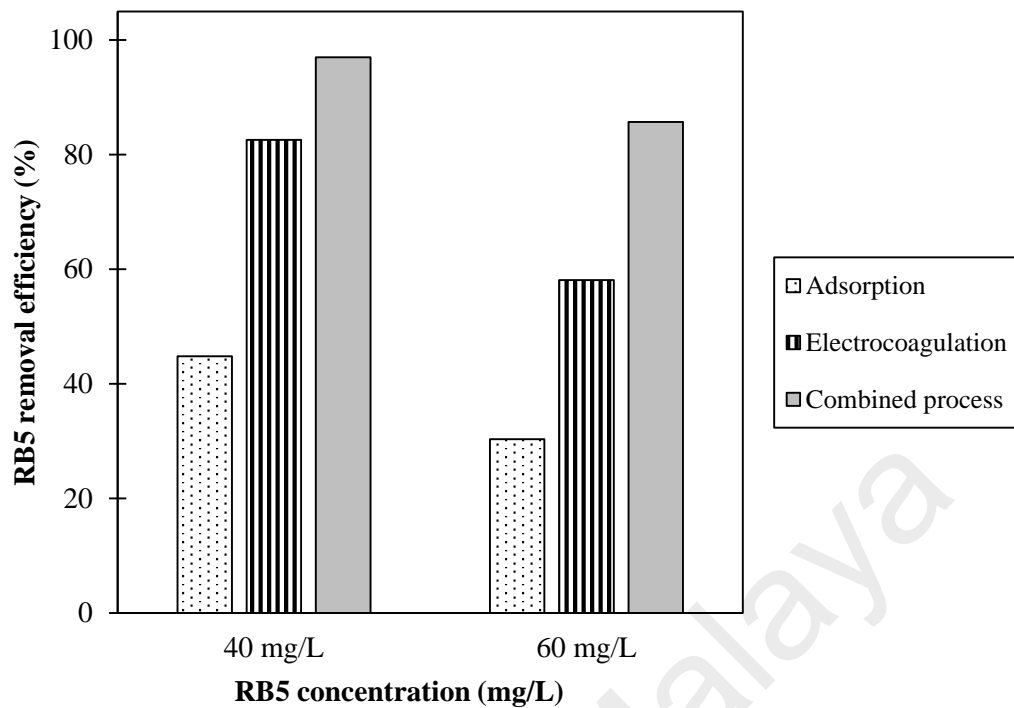


Figure 4.25: Comparison of combined process with individual adsorption and electrocoagulation (pH = 6, current density = 2.33 mA/cm², adsorbent dose = 15 g/L)

4.3.2 Response Surface Methodology (RSM)

4.3.2.1 Development of regression equation and statistical analysis

The interaction of initial pH, adsorbent dose, current density and process time on RB5 removal could be investigated using RSM. The total number of experiments designed by RSM amounted to 27 runs are shown in Table 4.14. The final regression model equation in terms of actual factors after eliminating the non-significant terms is expressed in Equation 4.15, where Y_{act} represents RB5 removal efficiency and X_1 , X_2 , X_3 , and X_4 are the pH, adsorbent dose, current density and process time, respectively, after excluding insignificant terms. ANOVA is used to check the significance and adequacy of the model and the terms. The results of the ANOVA are given in Table 4.15. The $Prob.>F$ below 0.05 is considered as a significant term; insignificant model terms are required to be eliminated to improve the quality of the regression model. The $Prob.>F$ of the model was significant and there is only a 0.01% change due to the noise. Additionally, the "Lack of

Fit F'' for the model was 0.1211, implying that the model was not relatively significant to the pure error since the $Prob.>F$ value was more than 0.05. Non-significant lack of fit was desirable and indicated that the model was in accordance with the range of the predicted response variables. In this study, the predicted R^2 and adjusted R^2 are in reasonable agreement, which both R^2 are within approximately 0.20 of each other. Moreover, the AP of the model equal to 34.273, which much higher than 4. This reveals that the adequate signal was obtained from the model. Based on the ANOVA and R^2 results, the suggested model by RSM could be used to navigate the design space.

$$Y_{act} = -166.59084 + 59.91274X_1 + 1.17509X_2 + 6.47402X_3 + 0.81229X_4 - 5.59493X_1^2 + 2.37157X_1X_3 - 0.48011X_2X_3 + 0.014509X_2X_4 \quad (4.15)$$

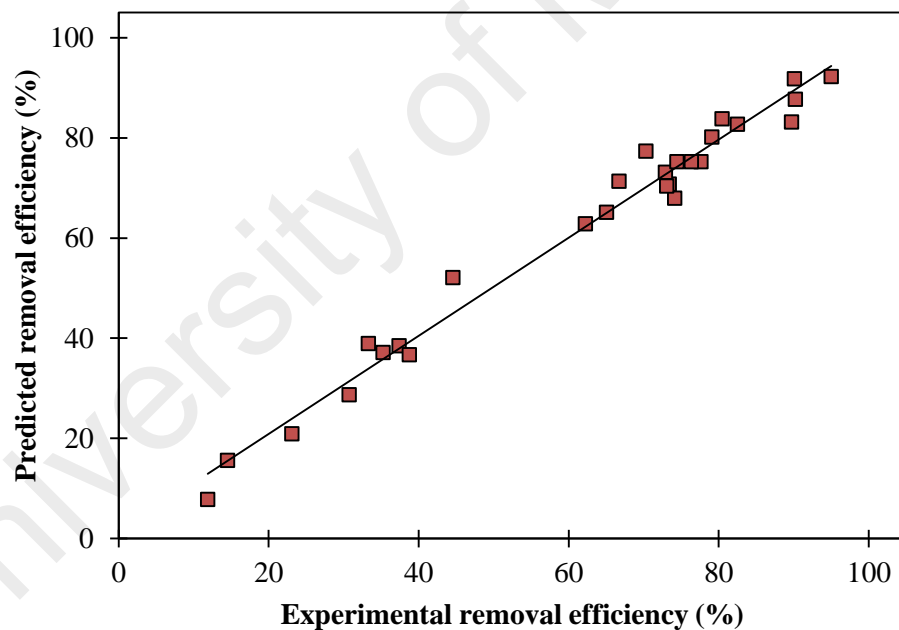


Figure 4.26: Predicted RB5 removal efficiency from the response surface model against experimental combined process data

Table 4.14: Central composite design for experimental and predicted RB5 removal

Run	Independent variables				RB5 removal (%)	
	pH	Adsorbent dose (g/L)	Current density (mA/cm ²)	Process time (min)	Experimental	Predicted
1	4	5	1.67	10	23.1	20.9
2	8	5	1.67	10	11.9	7.9
3	4	20	1.67	10	30.8	28.7
4	8	20	1.67	10	14.5	15.6
5	4	5	3	10	33.3	38.9
6	8	5	3	10	37.4	38.5
7	4	20	3	10	35.3	37.1
8	8	20	3	10	38.8	36.7
9	4	5	1.67	60	65.1	65.2
10	8	5	1.67	60	44.6	52.1
11	4	20	1.67	60	80.5	83.8
12	8	20	1.67	60	73.4	70.8
13	4	5	3	60	89.7	83.2
14	8	5	3	60	82.5	82.7
15	4	20	3	60	95.0	92.3
16	8	20	3	60	90.1	91.8
17	5	12.5	2.34	35	66.7	71.4
18	7	12.5	2.34	35	74.1	67.9
19	6	8.75	2.34	35	72.9	73.2
20	6	16.25	2.34	35	70.3	77.4
21	6	12.5	2	35	73.1	70.4
22	6	12.5	2.67	35	79.1	80.2
23	6	12.5	2.34	22.5	62.2	62.8
24	6	12.5	2.34	47.5	90.2	87.7
25	6	12.5	2.34	35	77.7	75.3
26	6	12.5	2.34	35	76.3	75.3
27	6	12.5	2.34	35	74.4	75.3

Table 4.15: ANOVA results for the fitted model

Source	SS ^(a)	MS ^(b)	F-value	Prob>F ^(c)	R ²	Adj R ²	Pred R ²	AP ^(d)	SD ^(e)
Model	15635.79	1954.47	107.38	< 0.0001	0.9795	0.9704	0.9242	34.273	4.27
LOF ^(f)	322.38	20.15	7.68	0.1211					
X ₁	188.25	188.25	10.34	0.0048					
X ₂	292.98	292.98	16.10	0.0008					
X ₃	1577.18	1577.18	86.65	< 0.0001					
X ₄	10182.07	10182.07	559.42	< 0.0001					
X ₁ ²	3025.98	3025.98	166.25	< 0.0001					
X ₁ X ₃	159.18	159.18	8.75	0.0084					
X ₂ X ₃	91.74	91.74	5.04	0.0376					
X ₂ X ₄	118.41	118.41	6.51	0.0201					

(a) SS: sum of squares

(b) MS: mean of square

(c) Prob>F: probability error of F-value

(d) AP: adequate precision

(e) SD: standard division

(f) LOF: lack of fit

4.3.2.2 Effect of the parameters on RB5 removal

To assess the effects of the parameters against the RB5 removal efficiency, three graphs were developed as shown in Figure 4.27. The response surface plot in Figure 4.27(a) implied that with increasing pH more RB5 were removed. The increase in pH promoted the generation of iron hydroxide used for RB5 removal. However, the removal of RB5 was observed to decrease at an initial pH beyond 6.26. This is probably because of higher pH enhances the dissolution of $\text{Fe}(\text{OH})_3$ to $\text{Fe}(\text{OH})_4$, which explains why the iron hydroxide complex is incapable to remove RB5. Moreover, repulsion between adsorbent and RB5 occurred when the influent pH was higher; hence, oxidation of RB5 was negatively affected. It was also found that the RB5 removal depends strongly on the current density. Iron hydroxides are the important element in the electrocoagulation process and it is controlled by the current density. When the current density increases, the RB5 removal improves rapidly. According to the Faraday's law, higher current density is sufficient to produce an adequate amount of iron hydroxides to then remove RB5. Figure 4.27 (a) also shows that the RB5 removal efficiency decreases was lower at low current density as well as at low and high pH.

The effect of adsorbent dose and current density on RB5 removal efficiency at a constant initial pH 6 and process time of 35 min was showed in Figure 4.27 (b). As expected, increasing adsorbent dose resulted in more RB5 removal because a sufficient amount of binding sites on the adsorbent surface is required for RB5 adsorption. A low adsorbent dose and current density did not remove significant amounts of RB5 due to insufficient binding sites and a lack of sufficient quantities of generated iron hydroxides. The RB5 removal efficiencies at higher adsorbent dose/lower current density (20 g/L and 1.67 mA/cm²) and lower adsorbent dose/higher current density (5 g/L and 3 mA/cm²) were 72.1% and 83.1%, respectively. This indicates that the current density was found to be a more significant parameter compared to the adsorbent dose. ANOVA further showed

that the *Prob.> F* of current density was lower than that the adsorbent dose, indicating that the current density had a major effect on RB5 removal.

Figure 4.27 (c) shows that a longer process time was required when lower adsorbent doses were applied. For the lowest adsorbent dose of 5 g/L, complete RB5 removal was attained only after more than 60 minutes. A longer process time is required for the RB5 molecules to diffuse across the boundary layer of the adsorbent and into surface pores, to finally be retained by the micropores of palm shell activated carbon. Therefore, a short contact time between the adsorbent and treated solution was also not beneficial for the adsorption process. A complete removal of RB5 could be achieved within 55.7 minutes with 16.89 g/L of palm shell activated carbon, an initial pH of 6 and a current density of 2.34 mA/cm² in the combined A-EC system.

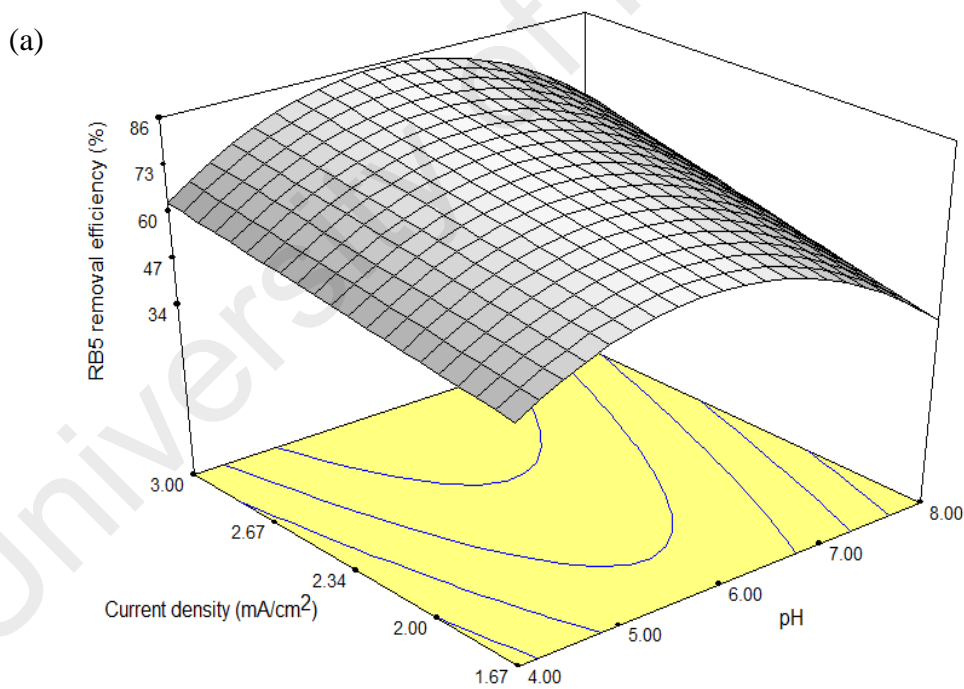


Figure 4.27: Response surface plot of combined process (a) interaction between pH and current density

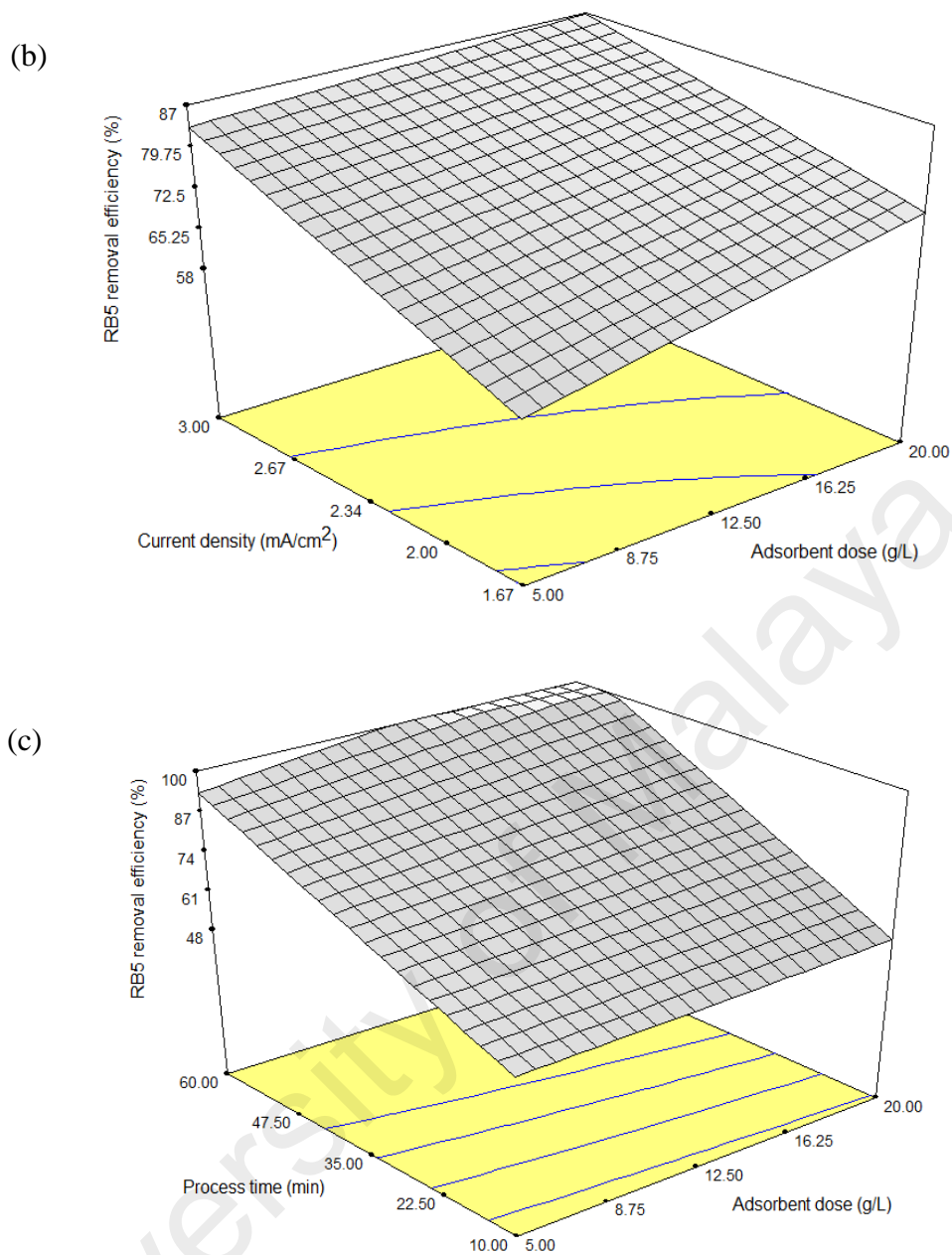


Figure 4.27: Continued. (b) interaction between current density and adsorbent dose
(c) the interaction between process time and adsorbent dose

4.3.2.3 Optimization operating conditions

RSM analysis proposes that the maximum RB5 removal efficiency at optimum operating conditions were pH of 6.17, adsorbent dose of 15.04 g/L, current density of 2.03 mA/cm² and process time of 57.18 min. Under these optimal conditions, the experimental removal efficiency of RB5 was 97.2%, which was close to the predicted value of 97.4%. This implies that the quadratic regression model (Equation 4.15)

reasonably optimizes the operating parameters and is a reliable way of predicting the effectiveness of RB5 removal.

A comparison of RB5 removal results obtained for combined A-EC process and individual adsorption and electrocoagulation under optimum operating conditions is illustrated in Figure 4.28. The individual adsorption of RB5 (pH 6.67 and 15.15 g/L of activated carbon) required a longer time to fulfil the discharge standard. The adsorption of RB5 was initially rapid and then decelerated before reaching a plateau. The highest depletion was reached following four hours of contact time, with a removal efficiency of 93.3%. A sharp slope of RB5 adsorption onto the adsorbent was observed during the first 20 min. The uptake of RB5 initially occurred on the surface of the adsorbent, then it diffused into the pores of the palm shell activated carbon for further adsorption (Al-Ghouti, Khraisheh, Ahmad, & Allen, 2009).

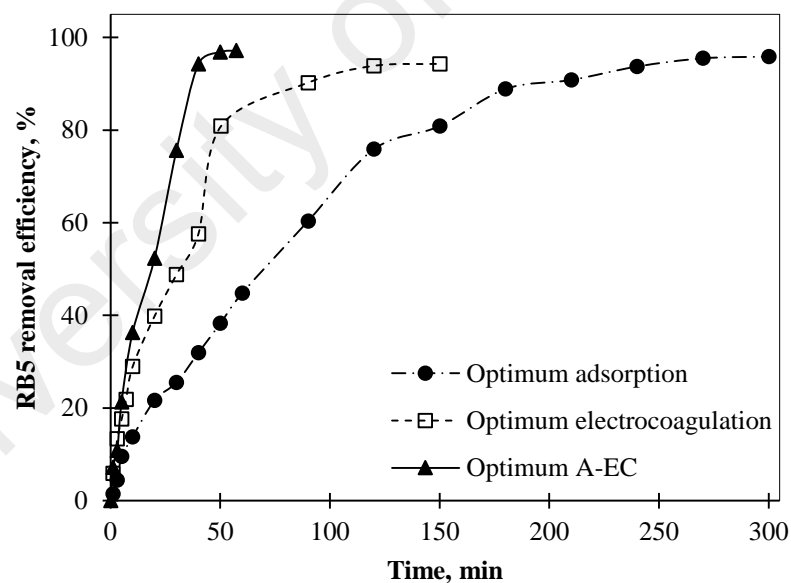


Figure 4.28: Comparison of RB5 removal efficiency of optimum combined and individual adsorption and electrocoagulation process

As seen in the individual electrocoagulation process, under optimum conditions (pH of 6.63 and current density of 2.5 mA/cm²), the removal efficiency of RB5 increased rapidly and attained 80.9% within 50 min (Figure 4.28). This was attributed to an

adequate amount of generated coagulant and a sufficient time for iron hydroxide to react with RB5. After 50 min, the removal rate of RB5 increased insignificantly due to the thickness of passive film that occurred on the electrode, causing a smaller effect of mass transfer of Fe^{2+} to the electrolyte required to generate the coagulant. Consequently, the removal rate of RB5 became slower.

The pattern of RB5 removal rate in the three examined systems was comparable during the first 7 min of the process. After this time, the removal rate of RB5 in the optimum combined A-EC increased rapidly compared to the individual adsorption and electrocoagulation processes. The time required for attaining an effluent with 3.155 mg/L of RB5 (less than 200 ADMI color index) was the shortest in the optimized A-EC. According to Malaysia Standards for Environmental Quality Regulations, the consent color discharge value found in the effluent is 200 ADMI color index. This demonstrated that A-EC showed better result in treating dye solutions than the adsorption or electrocoagulation processes performed individually.

Kinetic analysis of the first-order model fit the experimental data well. The kinetic rate constants (k) for optimal adsorption, electrocoagulation and A-EC were 0.0108, 0.0248, and 0.0476 min^{-1} , respectively. This revealed that RB5 removal performs more readily in the combined A-EC process than the individual processes (Table 4.16).

Electrical energy consumption (EEC, kWh/kg_{dye removed}) and operating cost (US\$/m³) are the most important economic parameters when considering the electrochemical treatment of coloured wastewater. Both parameters were calculated using Equation 4.16 and Equation 4.17, and results are listed in Table 4.16.

$$\text{EEC} = \frac{UIt \cdot 1000}{V(C_0 - C_t)} \quad (4.16)$$

$$\text{Operating cost} = (a \cdot C_{\text{energy}}) + (b_e \cdot C_{\text{electrode}}) \quad (4.17)$$

where C_0 and C_t denote the concentration of RB5 at time $t = 0$ and t , respectively, U represents the voltage (V), I is the current (A), t is the process time (h), V is the volume of dye solution (L), a is the electricity price in Malaysia for the year 2015 (US\$ 0.06/kWh), b_e is the retail iron mesh price in Malaysia for the year 2015 (2.73 US\$/kg iron mesh), C_{energy} is the electrical energy consumption (kWh/m³) and $C_{\text{electrode}}$ is the iron electrode consumption (kg/m³).

Electrical energy consumption (EEC) is an important economic parameter. The calculated EECs were 47.45 and 32.41 kWh/kg_{dye removed}, respectively, for electrocoagulation and A-EC. This difference is attributed to the fact that individual electrocoagulation employed a higher current density and required a longer process time than the combined process to treat the RB5 solution. Both parameters are directly proportional to the EEC calculation. The operating costs for the individual electrocoagulation and the combined process were 0.63 and 0.42 US\$/m³, respectively.

The RB5 and COD removal efficiency was slightly improved in A-EC, but the process time and operating cost gave better results compared with the individual adsorption and electrocoagulation. These factors are the critical parameters affecting the commercial applicability for the treatment of RB5 solutions. Hence, A-EC is a simple, inexpensive and efficient process for RB5 removal from aqueous solution.

Table 4.16: Performance summary for the single adsorption, electrocoagulation and combined process under optimum conditions

Parameter	Adsorption	Electrocoagulation	A/EC
Operating conditions	pH: 6.67 AD: 15.15 g/L Time: 240 min	pH: 6.63 CD: 2.5 mA/cm ² Time: 50.3 min	pH: 6.17 CD: 2.03 mA/cm ² AD: 15.04 g/L Time: 57.18 min
RB5 removal (%)	93.3	80.9	97.2
COD removal (%)	82.7	71.7	86.8
Kinetic rate constant (min ⁻¹)	0.0108	0.0248	0.0476
EEC (kWh/kg _{dye removed})	-	47.45	32.41
Operating cost (US\$/m ³)	-	0.63	0.42
Sludge volume (kg/m ³)	-	0.33	0.27

*AD: adsorbent dose; CD: current density

4.3.3 Sludge analysis

The surface of sludge produced during the combined process carried out under optimum conditions was analysed by FESEM, and the results are presented in Figure 4.29. The FESEM image shows the presence of an ultrafine particular structure at micrometers scale.

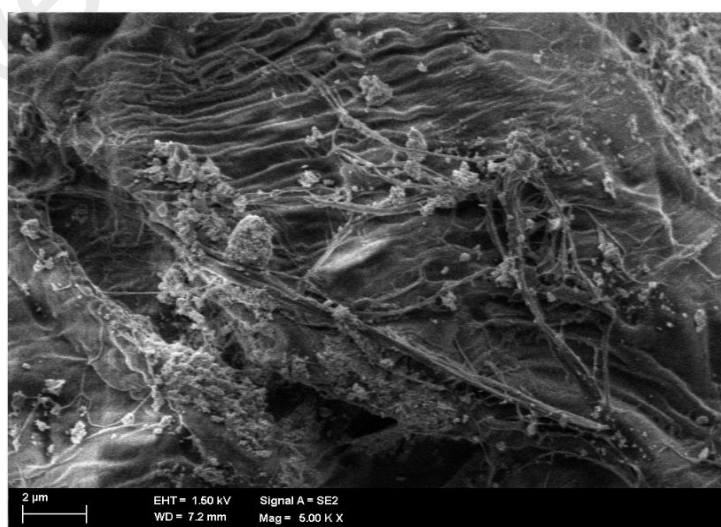


Figure 4.29: FESEM image of sludge in A-EC process

The XRD analysis was carried to identify the residue found in the sludge. Table 4.17 summarizes the chemical compounds observed from each peak in the XRD pattern. Iron complexes were present in the sludge. Kõrbahti proposed the possible mechanisms of formation iron complexes in the EC process. Iron complexes were obtained through the surface complexation pathway, whereby the pollutant (RB5) acted as a ligand to bind with an iron hydroxide molecule followed by bond-dissociation; the iron complexes were formed during the precipitation and adsorption route, as shown in Equations 4.18 – 4.21 (Kõrbahti *et al.* 2011).

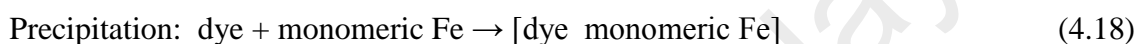


Table 4.17: XRD data of the sludge collected after the combined process

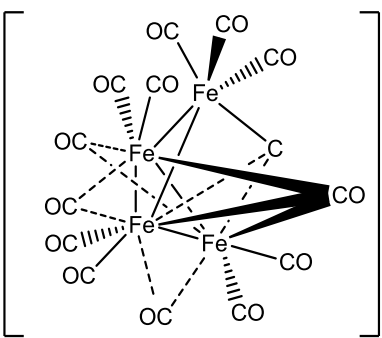
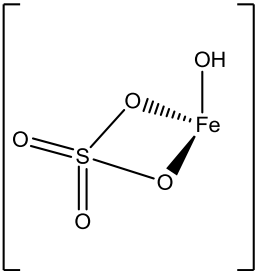
2θ ($^\circ$)	Structure name	Molecular formula	Molecular structure
8.22	-	$[\text{Fe}_4(\text{CO})_{13}\text{C}]^{3-}$	
11.82	Amarantite	$\text{Fe}^{3+}(\text{SO}_4)(\text{OH}) \cdot 3\text{H}_2\text{O}$	

Table 4.17: Continued

2θ ($^\circ$)	Structure name	Molecular formula	Molecular structure
21.32	Ferrotychite	$\text{Na}_6(\text{Fe})_2(\text{CO}_3)_4(\text{SO}_4)$	
23.66, 26.85, 28.19	-	$[\text{Fe}_4(\text{CO})_{13}\text{C}]^{3-}$	
31.06, 33.18	-	$(\text{Fe}(\text{CO})_3)_5\text{C}$	
34.85, 59.67	-	$\text{Fe}_3(\text{CO})_{12}$	

4.3.4 Effluent analysis

To identify the residues that remained after the A-EC process, GC-MS analysis was performed. The GC-MS chromatogram (Figure 4.30) shows that only a single compound, caprolactam, was detected in the final treated solution, at a retention time of 13.5 min. The GC-MS fragmentation pattern of caprolactam is shown in Figure 4.31. Caprolactam is a crystalline cyclic amide that is highly soluble in water. It is primarily used in the manufacture of Nylon 6 fibres, resins, plastics, brush bristles, synthetic leather and lysine (US EPA 1988). It is worth noting that no aromatic compounds were detected in the treated solution. The RB5 compound was completely decomposed and transformed into a heterocyclic compound with a smaller molecular size. Caprolactam is classified in the Group 4 hazardous category under the International Agency for Research on Cancer and is defined as “probably not carcinogenic to humans” (Caprolactam 2018).

Consistent with the study by Pirkarami and Olya (2017), a reaction pathway for the degradation of RB5 can be proposed (Figure 4.32). The metal hydroxide is most likely to first attack the carbon atom bearing the dye linkage, leading to the cleavage of the azo bond and further generation of sodium 2-((4-aminophenyl)sulphonyl)ethyl sulphate and sodium 3,4,6-triamino-5-hydroxynaphthalene-2,7-disulphonate. As the process continues, these compounds may further decompose to CO_2 , H_2O , NO_2 and NO_3 (Pirkarami and Olya, 2017). Sodium 2-((4-aminophenyl)sulphonyl)ethyl sulphate can also further react to form of cyclohexanone, which is subsequently converted into oxime. In the presence of acid, oxime undergoes Beckmann rearrangement to give caprolactam (William, Li & Sankholkar, 2001).

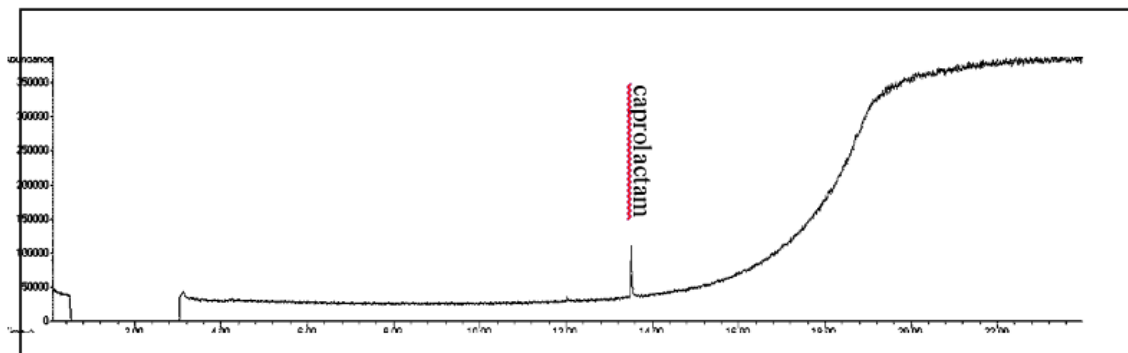


Figure 4.30: Total ion chromatogram of the final treated solution from GC-MS analysis

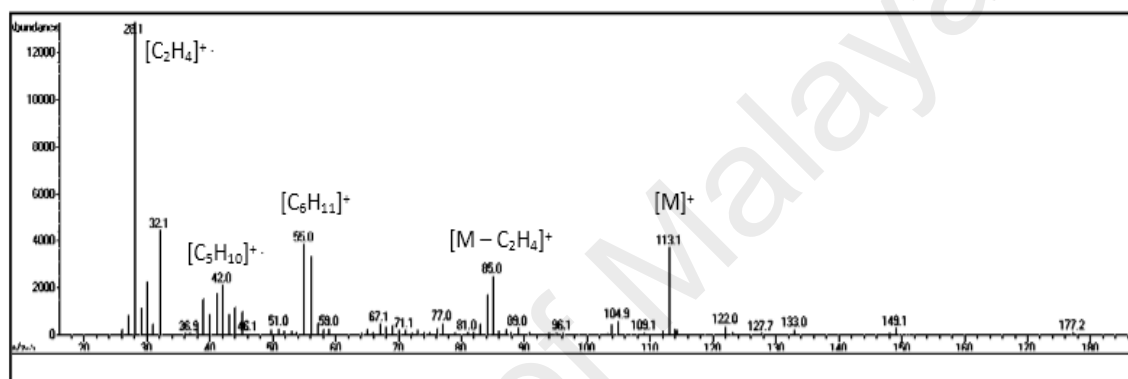


Figure 4.31: GC-MS spectrum of Caprolactam (at retention time = 13.5 min)

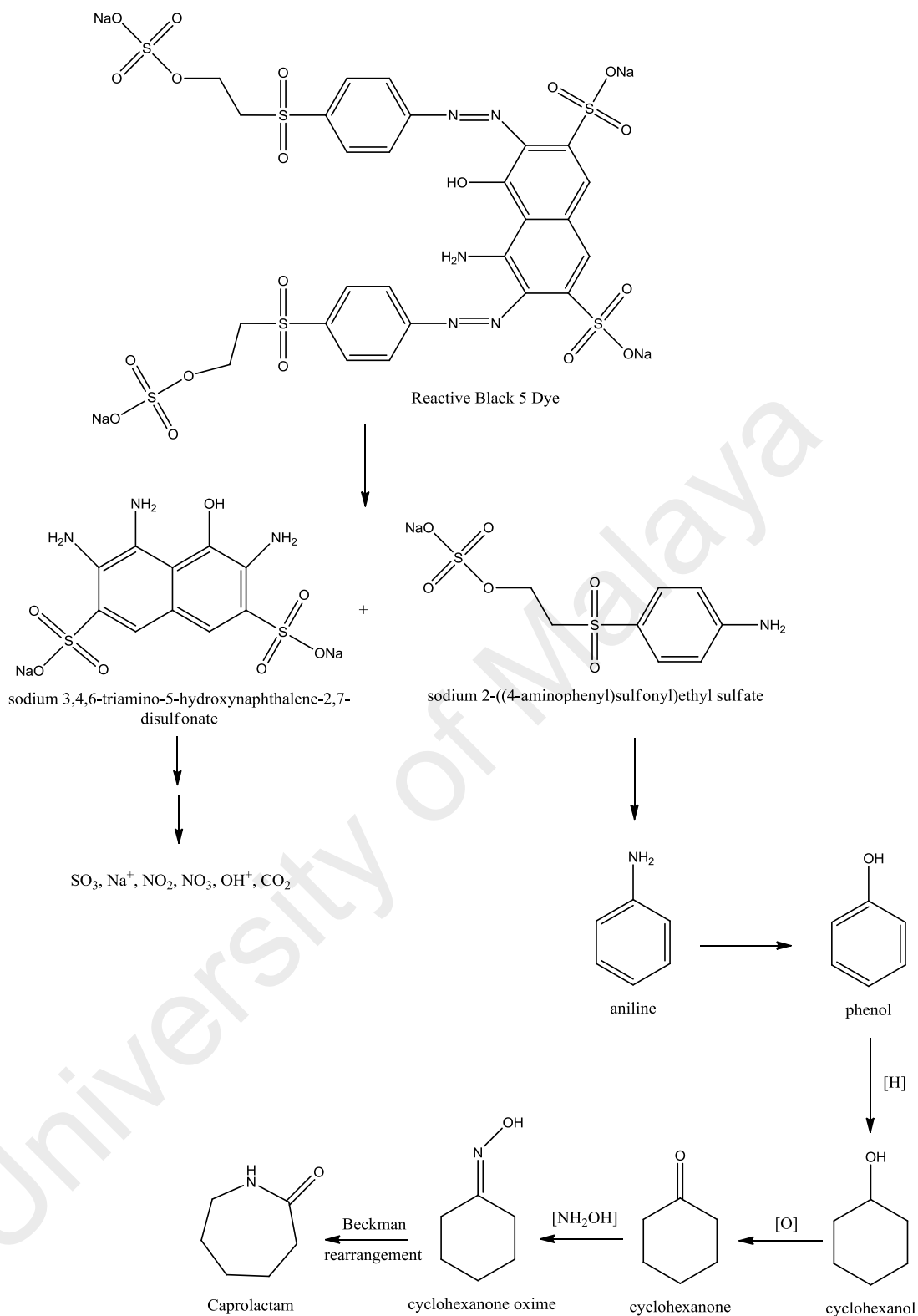


Figure 4.32: Proposed reaction pathway for the degradation of RB5 dye

4.3.5 Comparison studies

It also has to be noted that the achieved RB5 removal values in a combined process in a single setup is comparable to the one in the sequential setup as shown in Table 4.18. An ozonation followed by electrocoagulation process (Ozone/EC) was developed by Song et al. (2007) to treat RB5 solution. The reactor was equipped with ozone supply system and iron plate as anode and cathode in electrocoagulation system. They found that ozone-assisted electrocoagulation process gave 94% of RB5 and 60% of COD removal efficiency by 10 mA/cm² and ozone flow rate of 20 ml/min. However, ozone treatment might form toxic and carcinogenic by-products, which would require further purification step.

Chang et al. (2010) designed a sequential process with electrocoagulation and adsorption (EC/AC) where iron as electrodes and commercial coconut-based activated carbon was used as an adsorbent. The highest RB5 and COD removal efficiency reached almost 100% when the influent pH, current density, supporting electrolyte, adsorbent dose and adsorption contact time were pH 7, 27.7 mA/cm², 1 g/L, 20 g/L and 4 hours, respectively. The sequential process EC/AC is considered to be a good method to treat RB5 solution, but the longer adsorption contact time might not be practical in the industry.

Table 4.18: Comparison between different combined approaches for the removal of RB5 dye solution

Mode	Process	Experimental Conditions	Results	References
Sequential	Ozone/EC	Ozone: 20 ml/min pH: 5.5 CD: 10 mAcm ⁻² 5 g/L K ₂ SO ₄ Time: 20 min	RB5 removal: 94% COD removal: 60%	Song et al., 2007

Table 4.18: Continued

Mode	Process	Experimental Conditions	Results	References
Sequential	EC/AC	pH: 7 CD: 27.7 mAcm ⁻² 1 g/L NaCl AC: 20 g/L Time _{EC} : 8 min Time _{AC} : 4h	RB5 removal: ~100% COD removal: ~100%	Chang et al., 2010
Combined	A-EC	pH: 6.17 CD: 2.03 mAcm ⁻² 0.11 g/L Na ₂ SO ₄ AC: 15.04 g/L Time: 57.18 min	RB5 removal: 97.18% COD removal: 86.83%	This study

CHAPTER 5: CONCLUSIONS AND RECOMMENDATIONS

5.1 Conclusions

The current research aimed at developing a low-cost, easy to operate and highly effective method to remove Reactive Black 5 dye from aqueous solution. The study investigated the possibility of applying combined adsorption and electrocoagulation process to remove the pollutants. The research started with adsorption process using commercialized palm shell activated carbon as an adsorbent. The equilibrium data were best represented by the Langmuir isotherm model, where the accessible surfaces of palm shell activated carbon was occupied by a monolayer of RB5 molecules in the equivalent sites. The pseudo-first-order model showed the best fit to the kinetic data as the highest correlation values for each tested initial dye concentration where the calculated (q_e) and experimental equilibrium adsorption capacities (q_{exp}) were in a good agreement. The variables of contact time, pH, temperature, adsorbent dose and coexisting anion were noticeably affecting the RB5 adsorption. The removal of RB5 increases with the increase of contact time, temperature and adsorbent dose. RB5 adsorption was found to be endothermic in nature, with a low activation energy of 12.619 kJ/mol. Based on these results, it seems fair to suggest that the palm shell-based activated carbon is a very promising material to remove RB5 and it is comparable to other adsorbents derived from agricultural waste, as reported in the literature studies.

Next, an iron mesh single and double layer electrode were employed in the electrocoagulation process. The electrocoagulation performance of the iron mesh double layer electrode was more efficient than the single layer electrode. The RB5 removal efficiencies, 79.9%, and 98.2% were obtained for the single and double layer, respectively after 60 min of electrocoagulation process. It was found that the single layer electrode was more influenced by the passivation phenomenon than double layer during RB5

electrocoagulation process. Furthermore, the smaller diameter of the double layer increases the diffusion coefficient, the kinetic rate constant, lower electrical energy consumption and operating costs. The results seem to suggest that the iron mesh double layer electrode could become a novel alternative electrode for electrocoagulation in wastewater treatment.

The results of the combined process of adsorption and electrocoagulation (A-EC) on RB5 removal has shown a better performance than each of the process performed individually. It was found that the A-EC shows the best RB5 removal efficiency which was higher than 49.1% and 12.3% than that the single adsorption and electrocoagulation. The effects of initial pH, current density, adsorbent dose and initial RB5 concentration in the combined process were fully investigated. The RB5 removal efficiency decreased with increasing initial RB5 concentration and increased with increasing current density and adsorbent dose. It was found that RB5 removal increased with increasing initial pH from 4 to 6. Beyond pH 6, the RB5 removal efficiency decreases. The A-EC has a better performance and greater potential to treat higher dye concentration compared with the individual adsorption and electrocoagulation.

The main parameters affecting the adsorption of commercialized palm shell activated carbon, electrocoagulation of the iron mesh double layer and A-EC on RB5 removal were optimized using Response Surface Methodology (RSM). The results showed that the adsorption of RB5 favoured low pH solution and high adsorbent dose. Under optimum conditions suggested by RSM, i.e. initial pH of 6.67 and adsorbent dose of 15.15 g/L, about 93.3% of RB5 was removed within 4 hours. In contrast, the electrocoagulation process preferred weak acid to weak alkaline conditions (pH 5.8–8.22). The increase of current density and electrocoagulation time had a positive effect on the RB5 removal. The supporting electrolyte had a minor effect on the parameters of electrocoagulation RB5. The optimum operating conditions for the maximum electrocoagulation RB5

suggested by RSM were initial pH of 6.63, the current density of 2.5 mA/cm², electrolyte dose of 0.11 g/L and electrocoagulation time of 50.3 min. Under the optimum conditions, the experimental removal efficiency of RB5 was 80.9%, close to the predicted value (83.3%). On the other hand, the RB5 removal efficiency for A-EC was 97.2% when in the optimum conditions of pH of 6.17, adsorbent dose of 15.04 g/L, the current density of 2.03 mA/cm² and a process time of 57.18 min. Hence, the A-EC shows the best performance than the individual adsorption and electrocoagulation in term of highest RB5 and COD removal and kinetic rate constant. In addition, the electrical energy consumption and operating costs in A-EC were found to be lower than the others.

The compounds contained in the final effluent in A-EC treatment were identified by the GC-MS analysis. In this study, it is worth to notice that no aromatic compounds were detected in the discharged solution. The RB5 compound was completely decomposed and transformed into a heterocyclic compound with smaller molecular size. The peak in the XRD pattern indicated that the chemical compounds found in the sludge were iron complexes.

5.2 Recommendations

In this study, the developed A-EC was used to treat RB5 solution, a recalcitrant and highly organic compound. Based on the promising results obtained in this work, it is suggested to use A-EC for future research in order to treat colour and high COD solution such as wastewater from petroleum refinery and palm oil mill.

The current density has a significant effect in electrical energy consumption and operating costs. Hence, it is recommended to study the alternatives to direct electricity supply for example photovoltaic solar energy supply.

It is recommended to study the desorption and regeneration process, to assure the life span of the adsorbent.

The presence of sludge after treatment is the main challenge in this work. Therefore, studies on the usage and application of the sludge could be a new scope for future research. In addition, more depth study on mechanism of RB5 degradation is recommended.

University of Malaya

REFERENCES

- Abdel-Gawad, S.A., Baraka, A.M., Omran, K.A., & Mokhtar, M.M. (2012). Removal of some pesticides from the simulated waste water by electrocoagulation method using iron electrodes. *International Journal of Electrochemical Science* 7, 6654-6665.
- Aber, S., Amani-Ghadim, A.R., & Mirzajani, V. (2009). Removal of Cr(VI) from polluted solutions by electrocoagulation: Modeling of experimental results using artificial neural network. *Journal of Hazardous Materials*, 171(1-3), 484-490.
- Aguedach, Abdelkahhar, Brosillon, Stephan, Morvan, Jean, & Lhadi, El Kbir. (2005). Photocatalytic degradation of azo-dyes reactive black 5 and reactive yellow 145 in water over a newly deposited titanium dioxide. *Applied Catalysis B: Environmental*, 57(1), 55-62.
- Ahmad, A. A., & Hameed, B. H. (2010). Fixed-bed adsorption of reactive azo dye onto granular activated carbon prepared from waste. *Journal of Hazardous Materials*, 175(1-3), 298-303.
- Al-Degs, Yahya S., El-Barghouthi, Musa I., El-Sheikh, Amjad H., & Walker, Gavin M. (2008). Effect of solution pH, ionic strength, and temperature on adsorption behavior of reactive dyes on activated carbon. *Dyes and Pigments*, 77(1), 16-23.
- Al-Ghouti, Mohammad A., Khraisheh, Majeda A. M., Ahmad, Mohammad N. M., & Allen, Stephen. (2009). Adsorption behaviour of methylene blue onto Jordanian diatomite: A kinetic study. *Journal of Hazardous Materials*, 165(1-3), 589-598.
- Alchin, D. (2008). *Ion exchange resins*. New Zealand: Institute of Chemistry.
- Alexandrica, M.C., Sillion, M., Hritcu, D., & Popa, M.I. (2015). Layered double hydroxides as adsorbents for anionic dye removal from aqueous solutions. *Environmental Engineering and Management Journal*, 14(2), 381-388.
- Aljeboree, Aseel M., Alshirifi, Abbas N., & Alkaim, Ayad F. (2014). Kinetics and equilibrium study for the adsorption of textile dyes on coconut shell activated carbon. *Arabian Journal of Chemistry* (Corrected Proof).
- Amani-Ghadim, A.R., Olad, A, S. Aber, s, & Ashassi-Sorkhabi, H. (2012). Comparison of organic dyes removal mechanism in electrocoagulation process using iron and aluminum anodes. *Environmental Progress & Sustainable Energy*, 32 (3), 547-556.
- Amaral, A.L., & Ferreira, E.C. (2005). Activated sludge monitoring of a wastewater treatment plant using image analysis and partial least squares regression. *Analytica Chimica Acta*, 544, 246-253.
- Ambler, Jack R., & Logan, Bruce E. (2011). Evaluation of stainless steel cathodes and a bicarbonate buffer for hydrogen production in microbial electrolysis cells using a new method for measuring gas production. *International Journal of Hydrogen Energy*, 36(1), 160-166.

- Ani, Y.B.C. (2004). Adsorption studies of dyes using clay-based and activated carbon adsorbents. (Master dissertation), University Sains Malaysia.
- Aoudj, S., Khelifa, A., Drouiche, N., Hecini, M., & Hamitouche, H. (2010). Electrocoagulation process applied to wastewater containing dyes from textile industry. *Chemical Engineering and Processing: Process Intensification*, 49(11), 1176-1182.
- Appel, C., Ma, L. Q., Rhue, R. D., & Kennelley, E. (2003). Point of zero charge determination in soils and minerals via traditional methods and detection of electroacoustic mobility. *Geoderma*, 113(1-2), 77-93.
- Arroya, M.G., Perez-Herranz, V., Montanes, M.T., Garcia-Anton, J., & J.L, Guinon. (2009). Effect of pH and chloride concentration on the removal of hexavalent chromium in a batch electrocoagulation reactor. *Journal of Hazardous Materials*, 169(1-3), 1127-1133.
- Ashtekar, V.S., Bhandari, V.M., Shirsath, S.R., Sai Chandra, P.L.V.N., Jolhe, P.D., & Ghodke, S.A. (2014). Dye wastewater treatment: Removal of reactive dyes using inorganic and organic coagulants. *Journal of Industrial Pollution Control*, 30(1), 33-42.
- Babu, R.R., Bhadrinarayana, N.S., Begum, K.M.M.S., & Anantharaman, N. (2007). Treatment of tannery wastewater by electrocoagulation. *Journal of University of Chemical Technology and Metallurgy*, 42(2), 201-206.
- Baker, F.S. (1998). *Kirk-Othmer Encyclopedia of Chemical Technology: Activated Carbon* (4th Edition ed.): John Wiley and Sons.
- Banerjee, Sushmita, & Chattopadhyaya, M. C. Adsorption characteristics for the removal of a toxic dye, tartrazine from aqueous solutions by a low cost agricultural by-product. *Arabian Journal of Chemistry*, 10, 1629-1638.
- Bard, A.J., & Faulkner, L.R. . (1980). *Electrochemical methods: fundamentals and applications*. Vol. 2.
- Barka, N., Qourzal, S., Assabbane, A., Nounah, A., & Ait-Ichou, Y. (2010). Photocatalytic degradation of an azo reactive dye, Reactive Yellow 84, in water using an industrial titanium dioxide coated media. *Arabian Journal of Chemistry*, 3(4), 279-283.
- Bellebia S., Kacha S., Bouberka Z., Bouyakoub A.Z., & Derriche Z. (2009). Color removal from acid and reactive dye solutions by electrocoagulation and electrocoagulation/adsorption processes. *Water Environment Research*, 81(14), 382-393.
- Bergmann, M. E. Henry, & Rollin, Johanna. (2007). Product and by-product formation in laboratory studies on disinfection electrolysis of water using boron-doped diamond anodes. *Catalysis Today*, 124(3-4), 198-203.

- Bhatnagar, A., Sillanpaa, M., & Witek-Krowiak. (2015). Agricultural waste peels as versatile biomass for water purification - a review. *Chemical Engineering Journal*, 270, 244-271.
- Bulut, Yasemin, & Aydın, Haluk. (2006). A kinetics and thermodynamics study of methylene blue adsorption on wheat shells. *Desalination*, 194(1), 259-267.
- Caprolactam. (2016). Agents Classified by the IARC Monographs, Volume 71, page 395. <https://monographs.iarc.fr/ENG/Monographs/vol71/mono71-16.pdf>. Retrieved 6 April 2016.
- Cestari, Antonio R., Vieira, Eunice F. S., Pinto, Alane A., & Lopes, Elaine C. N. (2005). Multistep adsorption of anionic dyes on silica/chitosan hybrid: 1. Comparative kinetic data from liquid- and solid-phase models. *Journal of Colloid and Interface Science*, 292(2), 363-372.
- Chang, Shih-Hsien, Wang, Kai-Sung, Liang, Hsiu-Hao, Chen, Hsueh-Yu, Li, Heng-Ching, Peng, Tzu-Huan, . . . Chang, Chih-Yuan. (2010). Treatment of Reactive Black 5 by combined electrocoagulation–granular activated carbon adsorption–microwave regeneration process. *Journal of Hazardous Materials*, 175(1–3), 850-857.
- Chong, Meng Nan, Jin, Bo, Chow, Christopher W. K., & Saint, Chris. (2010). Recent developments in photocatalytic water treatment technology: A review. *Water Research*, 44(10), 2997-3027.
- Chu, Yan-yang, Wang, Wei-jing, & Wang, Meng. (2010). Anodic oxidation process for the degradation of 2, 4-dichlorophenol in aqueous solution and the enhancement of biodegradability. *Journal of Hazardous Materials*, 180(1–3), 247-252.
- Colindres, P., Yee-Madeira, H., & Reguera, E. (2010). Removal of Reactive Black 5 from aqueous solution by ozone for water reuse in textile dyeing processes. *Desalination*, 258(1–3), 154-158.
- Daneshvar, N., Khataee, A. R., & Djafarzadeh, N. (2006). The use of artificial neural networks (ANN) for modeling of decolorization of textile dye solution containing C. I. Basic Yellow 28 by electrocoagulation process. *Journal of Hazardous Materials*, 137(3), 1788-1795.
- Daneshvar, N., Oladegaragoze, A., & Djafarzadeh, N. (2006). Decolorization of basic dye solutions by electrocoagulation: An investigation of the effect of operational parameters. *Journal of Hazardous Materials*, 129(1-3), 116-122.
- Del Río, A. I.; Benimeli, M. J.; Molina, J.; Bonastre, J.; & Cases, F. (2012). Electrochemical Treatment of C.I. Reactive Black 5 Solutions on Stabilized Doped Ti/SnO₂ Electrodes. *International Journal of Electrochemical Science*, 7(12), 13074-13092.
- Desta, Mulu Berhe. (2013). Batch Sorption Experiments: Langmuir and Freundlich Isotherm Studies for the Adsorption of Textile Metal Ions onto Teff Straw (Eragrostis tef) Agricultural Waste. *Journal of Thermodynamics*, 2013, 6.

- DOE. (2012). Malaysia environmental quality report. Department of Environment, Strategic Communication Division, Putrajaya, Malaysia.
- El-Ashtoukhy, E-S.Z., Amin, N.K., & Abdel-Aziz, M.H. (2012). Decolorization of Acid Brown and Reactive Blue dyes by anodic oxidation in a batch recycle electrochemical reactor. *International Journal of Electrochemical Science*, 7, 11137-11148.
- El-Taweel, Y.A., Nassel, E.M., Elkheriany, I & Sayed, D. (2015). Removal of Cr(VI) ions from waste water by electrocoagulation using iron electrode. *Egyptian Journal of Petroleum*, 24 (2), 183-192.
- El-Zawahry, Manal M., Abdelghaffar, Fatma, Abdelghaffar, Rehab A., & Hassabo, Ahmed G. (2016). Equilibrium and kinetic models on the adsorption of Reactive Black 5 from aqueous solution using Eichhornia crassipes/chitosan composite. *Carbohydrate Polymers*, 136, 507-515.
- Elwakeel, K.Z., El-Kousy, S., El-Shorbagy, H.G., & El-Ghaffar, M.A.A. (2016). Comparison between the removal of Reactive Black 5 from aqueous solutions by 3-amino-1,2,4 triazole,5-thiol and melamine grafted chitosan prepared through four different routes. *Journal of Environmental Chemical Engineering*, 4(1), 733-745.
- Emamjomeh, M.M. (2006). Electrocoagulation technology as a process for defluoridation in water treatment. University of Wollongong.
- Figueroa, G., Valenzuela, J.L., Parga, J.R., Vazquez, V., & Valenzuela, A. (2015). Recovery of gold and silver and removal of copper, zinc and lead ions in pregnant and barren cyanide solutions. *Materials Sciences and Applications*, 6, 171-182.
- Forrest, S.C. (2012). Physical Adsorption of Gases onto Mesoporous Silica Material SBA-15 University of Tennessee, Knoxville.
- Garg, Krishan Kishor, & Prasad, Basheshwer. (2016). Development of Box Behnken design for treatment of terephthalic acid wastewater by electrocoagulation process: Optimization of process and analysis of sludge. *Journal of Environmental Chemical Engineering*, 4(1), 178-190.
- Ghaly, A.E., Ananthashankar, R., Alhattab, M., & Ramakrishnan, V.V. (2014). Production, characterization and treatment of textile effluents: a critical review. *Journal Chemical Engineering and Process Technology*, 5, 1-18.
- Ghernaout, D., Al-Ghonamy, A.I., Boucherit, A., Ghernaout, B., Naceur, M.W., Messaoudene, N.A., . . . Elboughdiri, N.A. (2015). Brownian motion and coagulation process. *American Journal of Environmental Protection*, 4, 1-15.
- Gomes, Jewel A. G., Daida, Praveen, Kesmez, Mehmet, Weir, Michael, Moreno, Hector, Parga, Jose R., . . . Cocke, David L. (2007). Arsenic removal by electrocoagulation using combined Al-Fe electrode system and characterization of products. *Journal of Hazardous Materials*, 139(2), 220-231.

- Gowri, R.S., Vijayaraghavan, R., & Meenambigai, P. (2014). Microbial degradation of reactive dyes- A Review. *International Journal of Current Microbiology and Applied Sciences*, 3(3), 421-436.
- Grassi, M., Kaykioglu, G., Belgiorno, V., & Lofrano, G. (2012). Removal of emerging contaminants from water and wastewater by adsorption process *Emerging compounds removal from wastewater* (pp. 15-37). Springer Netherlands.
- Güzel, Fuat, Saygılı, Hasan, Akkaya Saygılı, Gülbahar, & Koyuncu, Filiz. (2015). New low-cost nanoporous carbonaceous adsorbent developed from carob (*Ceratonia siliqua*) processing industry waste for the adsorption of anionic textile dye: Characterization, equilibrium and kinetic modeling. *Journal of Molecular Liquids*, 206, 244-255.
- Han, Runping, Wang, Yu, Zhao, Xin, Wang, Yuanfeng, Xie, Fuling, Cheng, Junmei, & Tang, Mingsheng. (2009). Engineering with Membranes 2008 Adsorption of methylene blue by phoenix tree leaf powder in a fixed-bed column: experiments and prediction of breakthrough curves. *Desalination*, 245(1), 284-297.
- Hassan, Saad S. M., Awwad, Nasser S., & Aboterika, Awaad H. A. (2009). Removal of synthetic reactive dyes from textile wastewater by Sorel's cement. *Journal of Hazardous Materials*, 162(2-3), 994-999.
- Heibati, Behzad, Rodriguez-Couto, Susana, Amrane, Abdeltif, Rafatullah, Mohd, Hawari, Alaa, & Al-Ghouti, Mohammad A. (2014). Uptake of Reactive Black 5 by pumice and walnut activated carbon: Chemistry and adsorption mechanisms. *Journal of Industrial and Engineering Chemistry*, 20(5), 2939-2947.
- Heidmann, I., & W., Calmano. (2008). Removal of Cr(VI) from model wastewaters by electrocoagulation with Fe electrodes. *Separation and Purification Technology*, 61(1), 15-21.
- Holkar, Chandrakant R., Jadhav, Ananda J., Pinjari, Dipak V., Mahamuni, Naresh M., & Pandit, Aniruddha B. (2016). A critical review on textile wastewater treatments: Possible approaches. *Journal of Environmental Management*, 182, 351-366.
- Holt, Peter K., Barton, Geoffrey W., Wark, Mary, & Mitchell, Cynthia A. (2002). A quantitative comparison between chemical dosing and electrocoagulation. *Colloids and Surfaces A: Physicochemical and Engineering Aspects*, 211(2-3), 233-248.
- Hoseinzadeh Hesas, Roozbeh, Arami-Niya, Arash, Wan Daud, Wan Mohd Ashri, & Sahu, J. N. (2013). Preparation of granular activated carbon from oil palm shell by microwave-induced chemical activation: Optimisation using surface response methodology. *Chemical Engineering Research and Design*, 91(12), 2447-2456.
- Hsu, Y.C, Yen, C.H, & Huang, H.C. (1998). Multistage treatment of high strength dye wastewater by coagulation and ozonation. *Journal of Chemical Technology and Biotechnology*, 71, 71-76.

- Hsueh, Chan-Li, Lu, Yu-Wen, Hung, Chil-Chang, Huang, Yao-Hui, & Chen, Chuh-Yung. (2007). Adsorption kinetic, thermodynamic and desorption studies of C.I. Reactive Black 5 on a novel photoassisted Fenton catalyst. *Dyes and Pigments*, 75(1), 130-135.
- Huff, M.D., Lee, J.W. (2016). Biochar-surface oxygenation with hydrogen peroxide. *Journal of Environmental Management*, 165, 17–21.
- Ismail, A.A., Aroua, M.K, & Yusoff, R. (2013). Palm shell activated carbon impregnated with task-specific ionic-liquids as a novel adsorbent for the removal of mercury from contaminated water. *Chemical Engineering Journal*, 225, 306-314.
- Issabayeva, Gulnaziya, Aroua, Mohamed Kheireddine, & Sulaiman, Nik Meriam Nik. (2006). Removal of lead from aqueous solutions on palm shell activated carbon. *Bioresource Technology*, 97(18), 2350-2355.
- Jaafar, S.N.B.S. (2006). Adsorption study- Dye removal using clay. (Bachelor), University College of Engineering & Technology Malaysia.
- Janczukowicz. W., Szewczyk. M., Krzemieniewski. M., & Pesta. J. (2001). Settling properties of activated sludge from a sequencing batch reactor (SBR). *Polish Journal of Environmental Studies*, 10(1), 15-20.
- Jiwalak, Naparat, Rattanaphani, Saowanee, Bremner, John B., & Rattanaphani, Vichitr. (2010). Equilibrium and kinetic modeling of the adsorption of indigo carmine onto silk. *Fibers and Polymers*, 11(4), 572-579.
- Karcher, Silke, Kornmüller, Anja, & Jekel, Martin. (2002). Anion exchange resins for removal of reactive dyes from textile wastewaters. *Water Research*, 36(19), 4717-4724.
- Keane, J., & De Velde, D.W. (2008). The role of textile and clothing industries in growth and development strategies. Mimeo, London: Overseas Development Institute Investment and Growth Programme.
- Khan, T., Chaudhuri, M., Isa, M.H., & Hamid, A.Z.B.A. (2013). Use of incinerated rice husk for adsorption of reactive dye from aqueous solution. *Journal of Energy Technologies and Policy*, 3(11), 234-239.
- Khatri, A., Peerzada, M.H., Mohsin, M., & White, M. (2015). A review on developments in dyeing cotton fabrics with reactive dyes for reducing effluent pollution. *Journal of Cleaner Production*, 87, 50-57.
- Kleinhenz, V. (1999). Sulfur and chloride in the soil-plant system. In K. S. Group (Ed.), (pp. 99). Kassel.
- Koby, M., Demirbas, E., Can, O. T., & Bayramoglu, M. (2006). Treatment of levafix orange textile dye solution by electrocoagulation. *Journal of Hazardous Materials*, 132(2–3), 183-188.

- Koby, Mehmet, Can, Orhan Taner, & Bayramoglu, Mahmut. (2003). Treatment of textile wastewaters by electrocoagulation using iron and aluminum electrodes. *Journal of Hazardous Materials*, 100(1–3), 163-178.
- Körbahti, B.K., & Tanyolac, A. (2008). Electrochemical treatment of simulated textile wastewater with industrial components and Levafix Blue CA reactive dye: Optimazation through response surface methodology. *Journal of Hazardous Materials*, 151, 422-431.
- Körbahti, Bahadır K., Artut, Kahraman, Geçgel, Cihan, & Özer, Ayla. (2011). Electrochemical decolorization of textile dyes and removal of metal ions from textile dye and metal ion binary mixtures. *Chemical Engineering Journal*, 173(3), 677-688.
- Kuokkanen, V. (2016). *Utilization of electrocoagulation for water and wastewater treatment and nutrient recover* (Doctoral dissertation). Retrieved from <http://jultika.oulu.fi/files/isbn9789526211084.pdf>
- Kuroda, Yosuke, Kawada, Yoshihiro, Takahashi, Takeo, Ehara, Yoshiyasu, Ito, Tairo, Zukeran, Akinori, . . . Yasumoto, Kouji. (2003). Effect of electrode shape on discharge current and performance with barrier discharge type electrostatic precipitator. *Journal of Electrostatics*, 57(3–4), 407-415.
- Lee, C.-K., Liu, S.-S., Juang, L.-C., Wang, C.-C., Lin, K.-S., Lyu, M.-D. (2007). Application of MCM-41 for dyes removal from wastewater. *Journal of Hazardous Materials*, 147 (3), 997–1005.
- Lee, Jae-Wook, Choi, Seung-Phil, Thiruvenkatachari, Ramesh, Shim, Wang-Geun, & Moon, Hee. (2006). Evaluation of the performance of adsorption and coagulation processes for the maximum removal of reactive dyes. *Dyes and Pigments*, 69(3), 196-203.
- Liu, Xuanmo, Qiu, Muqing, & Huang, Chengcai. (2011). Degradation of the Reactive Black 5 by Fenton and Fenton-like system. *Procedia Engineering*, 15, 4835-4840.
- Lucas, Marco S., & Peres, José A. (2006). Decolorization of the azo dye Reactive Black 5 by Fenton and photo-Fenton oxidation. *Dyes and Pigments*, 71(3), 236-244.
- Majouli, A., Tahiri, S., Younssi, S.A., Loukili, H., Albizane, A. (2012). Elaboration of new tubular ceramic membrane from local Moroccan Perlite for microfiltration process. Application to treatment of industrial wastewaters. *Ceramic International*, 38, 4295-4303.
- Méndez-Martínez, Ana J., Dávila-Jiménez, Martín M., Ornelas-Dávila, Omar, Elizalde-González, María P., Arroyo-Abad, Uriel, Sirés, Ignasi, & Brillas, Enric. (2012). Electrochemical reduction and oxidation pathways for Reactive Black 5 dye using nickel electrodes in divided and undivided cells. *Electrochimica Acta*, 59, 140-149.

- Merzouk, B., Gourich, B., Madani, K., Vial, Ch, & Sekki, A. (2011). Removal of a disperse red dye from synthetic wastewater by chemical coagulation and continuous electrocoagulation. A comparative study. *Desalination*, 272(1–3), 246-253.
- MIDA. (2017). Textiles and textile products. <http://www.mida.gov.my/home/textiles-and-textile-products/posts/> . Retrieved 10 October 2016
- Mimi Sakinah, A. M., Ismail, A. F., Illias, Rosli Md, & Hassan, O. (2007). Fouling characteristics and autopsy of a PES ultrafiltration membrane in cyclodextrins separation. *Desalination*, 207(1), 227-242.
- Modirshahla, N., Behnajady, M. A., & Ghanbary, F. (2007). Decolorization and mineralization of C.I. Acid Yellow 23 by Fenton and photo-Fenton processes. *Dyes and Pigments*, 73(3), 305-310.
- Mohan, N., Balasubramanian, N., & Basha, C. Ahmed. (2007). Electrochemical oxidation of textile wastewater and its reuse. *Journal of Hazardous Materials*, 147(1–2), 644-651.
- Mollah, M. Yousuf A., Schennach, Robert, Parga, Jose R., & Cocke, David L. (2001). Electrocoagulation (EC) — science and applications. *Journal of Hazardous Materials*, 84(1), 29-41.
- Mollah, M.Y A., Pathak, Saurabh R., Patil, Prashanth K., Vayuvegula, Madhavi., Agrawal, Tejas S., Gomes, Jewel A. G., . . . Cocke, David L. (2004). Treatment of orange II azo-dye by electrocoagulation (EC) technique in a continuous flow cell using sacrificial iron electrodes. *Journal of Hazardous Materials*, 109(1–3), 165-171.
- Mook, W. T., Aroua, M. K., & Issabayeva, G. (2014). Prospective applications of renewable energy based electrochemical systems in wastewater treatment: A review. *Renewable and Sustainable Energy Reviews*, 38, 36-46.
- Mook, W.T., Ajeel, M.A., Aroua, M.K., & Szlachta, M. (2016). The application of iron mesh double layer as anode for the electrochemical treatment of Reactive Black 5 dye. *Journal of Environmental Sciences*, 54, 184-195.
- Moreira, R.F.P.M., Soares, J.L., José, H.J., & Rodrigues, A.E. (2001). The removal of reactive dyes using high-ash char. *Brazilian Journal of Chemical Engineering*, 18(3), 327-336.
- Myoung-Jun, Kim †, & Gyu-Hoon, Chea. (2012). Study on the PV Driven Dehumidifying System with Oyster Shell and Thermoelectric Device. *Journal of the Korean Society of Marine Environment and Safety*, 18(3), 287-293.
- Nandi, Barun Kumar, & Patel, Sunil. (2013). Effects of operational parameters on the removal of brilliant green dye from aqueous solutions by electrocoagulation. *Arabian Journal of Chemistry*.

- Nekouei, Farzin, Nekouei, Shahram, Tyagi, Inderjeet, & Gupta, Vinod Kumar. (2015). Kinetic, thermodynamic and isotherm studies for acid blue 129 removal from liquids using copper oxide nanoparticle-modified activated carbon as a novel adsorbent. *Journal of Molecular Liquids*, 201, 124-133.
- Newcombe, G., & Drikas, M. (1997). Adsorption of NOM onto activated carbon: Electrostatic and non-electrostatic effects. *Carbon*, 35(9), 1239-1250.
- Nourouzi, M.M., Chuah, T.G., & Choong, T.S.Y. (2009). Equilibrium and kinetic study on reactive dyes adsorption by palm kernel shell-based activated carbon: In single and binary systems. *Journal of Environmental Engineering*, 135, 1393-1398.
- Oram, B. (2014). Ozonation in water treatment. <http://www.water-research.net/index.php/ozonation>. Retrieved 2/1/2017.
- Osma, Johann F., Saravia, Verónica, Toca-Herrera, José L., & Couto, Susana Rodríguez. (2007). Sunflower seed shells: A novel and effective low-cost adsorbent for the removal of the diazo dye Reactive Black 5 from aqueous solutions. *Journal of Hazardous Materials*, 147(3), 900-905.
- Ozyonar, F., & Karagozoglu, B. (2011). Operating cost analysis and treatment of domestic wastewater by electrocoagulation using aluminium electrodes. *Polish Journal of Environmental Studies*, 20(1), 173-179.
- Pajootan, Elmira, Arami, Mokhtar, & Mahmoodi, Niyaz Mohammad. (2012). Binary system dye removal by electrocoagulation from synthetic and real colored wastewaters. *Journal of the Taiwan Institute of Chemical Engineers*, 43(2), 282-290.
- Palm oil (2014). Palm oil facts & figures. http://www.simedarby.com/upload/Palm_Oil_Facts_and_Figures.pdf. Retrieved 25-4-2015
- Papić, Sanja, Koprivanac, Natalija, Lončarić Božić, Ana, & Meteš, Azra. (2004). Removal of some reactive dyes from synthetic wastewater by combined Al(III) coagulation/carbon adsorption process. *Dyes and Pigments*, 62(3), 291-298.
- Patel, Upendra D., Ruparelia, J. P., & Patel, Margi U. (2011). Electrocoagulation treatment of simulated floor-wash containing Reactive Black 5 using iron sacrificial anode. *Journal of Hazardous Materials*, 197, 128-136.
- Pawar, V., & Gawande, S. (2015). An overview of the Fenton process for industrial wastewater. *Journal of Mechanical and Civil Engineering*, IOSR-JMCE, 127-136.
- Philips, D. (1996). Environmentally friendly, productive and reliable: Priorities for cotton dyes and dyeing processes. *Journal of Society of Dyers and Colourists*, 112, 183-186.
- Pirkarami, A., & Olya, M.E. (2017). Removal of dye from industrial wastewater with an emphasis on improving economic efficiency and degradation mechanism. *Journal of Saudi Chemistry Society* 21, Supplement 1, 179-186.

- Popli, S., & Patel, U.D. (2015). Destruction of azo dyes by anaerobic-aerobic sequential biological treatment: a review. *International Journal of Environmental Science and Technology* 12(405-420).
- Qiu, M., Shou, J., Ren, P., & Jiang, K. (2014). A comparative study of the azo dye reactive black 5 degradation by UV/TiO₂ and photo-fenton processes. *Journal of Chemical and Pharmaceutical Research*, 6(7), 2046-2051.
- Raghu, S., & Ahmed Basha, C. (2007). Chemical or electrochemical techniques, followed by ion exchange, for recycle of textile dye wastewater. *Journal of Hazardous Materials*, 149(2), 324-330.
- Rashed, Mohamed Nageeb. (2013). Adsorption Technique for the Removal of Organic Pollutants from Water and Wastewater *Organic Pollutants - Monitoring, Risk and Treatment: InTech, Croatia*
- Reddy, S.S., Kotaiah, B., & Reddy N.S.P. (2008). Color pollution control in textile dyeing industry effluents using tannery sludge derived activated carbon. *Bulletin of the Chemical Society of Ethiopia*, 22(3), 369-378.
- Rivera, Maria, Pazos, Marta, & Sanromán, Maria Ángeles. (2011). Development of an electrochemical cell for the removal of Reactive Black 5. *Desalination*, 274(1-3), 39-43.
- Saffaj, N., Persin, M., Younsi, S.A., Albizane, A., Cretin, M., Larbot, A. (2006). Elaboration and characterization of microfiltration and ultrafiltration membranes deposited on raw support prepared from natural Moroccan clay: application to filtration of solution containing dyes and salts. *Applied Clay Science*, 31, 110-119.
- Samiey, B., & Ashoori, F. (2012). Adsorption removal of methylene blue by agar: effects of NaCl and ethanol. *Chemistry Central Journal*, 6(14), 1-13.
- Sandic, Z.P., Zunic, M.J., Maksin, D.D., Milutinovic-Nikolic, A.D., Popovic, A.R., Jovanovic, D.M., & Nastasovic, A.B. (2014). Glycidyl methacrylate macroporous copolymer grafted with diethylene triamine as sorbent for Reactive Black 5. *Hemijaska Industrija*, 68(6), 685-699.
- Sarasa, J., Roche, M.P., Ormad, M.P., Gimeno, E., Puig, A., & Ovelleiro, J.L. (1998). Treatment of a wastewater resulting from dyes manufacturing with ozone and chemical coagulation. *Water Research*, 32(9), 2721-2727.
- Sasson, Moshe Ben, Calmano, Wolfgang, & Adin, Avner. (2009). Iron-oxidation processes in an electroflocculation (electrocoagulation) cell. *Journal of Hazardous Materials*, 171(1-3), 704-709.
- Schumacher, C. (2012). More Challenges in the Greenpeace Detox Campaign. <https://blog.stepchange-innovations.com/2012/11/more-challenges-in-the-greenpeace-detox-campaign/>. Retrieved 26-1-2016
- Şengil, İ Ayhan, & Özacar, Mahmut. (2009). The decolorization of C.I. Reactive Black 5 in aqueous solution by electrocoagulation using sacrificial iron electrodes. *Journal of Hazardous Materials*, 161(2-3), 1369-1376.

- Soni, Bhavna D., & Ruparelia, Jayesh P. (2013). Decolourization and Mineralization of Reactive Black-5 with Transition Metal Oxide Coated Electrodes by Electrochemical Oxidation. *Procedia Engineering*, 51, 335-341.
- Sun, D., Zhang, Z., Wang, M., & Wu, Y. (2013). Adsorption of reactive dyes on activated carbon developed from *Enteromorpha prolifera*. *American Journal of Analytical Chemistry*, 4, 17-26.
- Szlachta, Małgorzata, & Chubar, Natalia. (2013). The application of Fe–Mn hydrous oxides based adsorbent for removing selenium species from water. *Chemical Engineering Journal*, 217, 159-168.
- Textile. (2016). https://en.wikipedia.org/wiki/Textile_industry. Retrieved 19/12/2016
- Tezcan Ün, Ümran, Koparal, A. Savaş, & Bakir Ögütveren, Ülker. (2009). Hybrid processes for the treatment of cattle-slaughterhouse wastewater using aluminum and iron electrodes. *Journal of Hazardous Materials*, 164(2–3), 580-586.
- Tezcan Ün, Ümran, Koparal, A. Savaş, & Bakir Ögütveren, Ülker. (2013). Fluoride removal from water and wastewater with a batch cylindrical electrode using electrocoagulation. *Chemical Engineering Journal* 223, 110-115.
- Thirugnanasambandham, K., Sivakumar, V., & Maran, J. Prakash. (2015). Response surface modelling and optimization of treatment of meat industry wastewater using electrochemical treatment method. *Journal of the Taiwan Institute of Chemical Engineers*, 46, 160-167.
- Thomas, B.N., & George, S.C. (2015). Production of activated carbon from natural sources. *Trends in Green Chemistry*, 1(1).
- Tran, H.N., Wang, Y-F., You, S-J., & Chao, H-P. (2017). Insights into the mechanism of cationic dye adsorption on activated charcoal: The importance of π - π interactions. *Process Safety and Environmental Protection*, 107, 168-180.
- U.S. Environmental Protection Agency. Health and environmental effects profile for caprolactam. ECAO-CIN-G018. Environmental criteria and assesment office, Office of health and environment assesment, Office of research and development, Cincinnati, OH. 1988.
- Vepsäläinen, M. (2012). *Electrocoagulation in the treatment of industrial waters and wastewaters* (Doctoral thesis, VTT Technical Research Centre of Finland, Espoo, Finland). Retrieved from <https://www.vtt.fi/inf/pdf/science/2012/S19.pdf>
- Vijayaraghavan, J., Basha, S.J.S., & Jegan, J., ` . (2013). A review on efficacious methods to decolorize reactive azo dye. *Journal of Urban and Environmental Engineering*, 7, 30-47.
- Wallace, T.H. (2001). Biological treatment of a synthetic dye water and an industrial textile wastewater containing azo dye compounds. (Master dissertation), Virginia, United States.

- Water treatment. (2017). *Coagulation and flocculation Water Treatment*. Retrieved from <https://ocw.tudelft.nl/wp-content/uploads/Coagulation-and-flocculation-1.pdf>
- Wawrzekiewicz, M, & Hubicki, Z. (2015). *Anion Exchange Resins as Effective Sorbents for Removal of Acid, Reactive, and Direct Dyes from Textile Wastewaters*. A.Kilislioglu (ED), In: Ion exchange- Studies and Applications, InTechOpen.
- Williams, M.C., Li, N.H., & Sankholkar, Y. (2001). Process for the production of a polymerized material and the product produced thereby. US6291598 B1
- Xu, Z., Cai, J.G., & Pan, B.C. (2013). Mathematically modeling fixed-bed adsorption in aqueous system. *Journal of Zhejiang University-Science A*, 14(3), 155-176.
- Yacob, A.R., Majid, Z.A., Dasril, R.S., & Inderan, V. (2008). Comparison of various sources of high surface area carbon prepared by different types of activation. *The Malaysian Journal of Analytical Sciences*, 12(1), 264-271.
- Yang, Zhao-hui, Xu, Hai-yin, Zeng, Guang-ming, Luo, Yuan-ling, Yang, Xia, Huang, Jing, . . . Song, Pei-pei. (2015). The behavior of dissolution/passivation and the transformation of passive films during electrocoagulation: Influences of initial pH, Cr(VI) concentration, and alternating pulsed current. *Electrochimica Acta*, 153, 149-158.
- Yeganeh, M.M., Kaghazchi, T., & Soleimani, M. (2006). Effect of Raw Materials on Properties of Activated Carbons. *Chemical Engineering and Technology*, 29, 1-5.
- Yildiz, Yalçın Şevki, Koparal, Ali Savaş, İrdemez, Şahset, & Keskinler, Bülent. (2007). Electrocoagulation of synthetically prepared waters containing high concentration of NOM using iron cast electrodes. *Journal of Hazardous Materials*, 139(2), 373-380.
- Zaroual, Z., Azzi, M., Saib, N., & Chainet, E. (2006). Contribution to the study of electrocoagulation mechanism in basic textile effluent. *Journal of Hazardous Materials*, 131(1-3), 73-78.
- Zhang, Yimin, Merrill, Matthew D., & Logan, Bruce E. (2010). The use and optimization of stainless steel mesh cathodes in microbial electrolysis cells. *International Journal of Hydrogen Energy*, 35(21), 12020-12028.
- Zheng Q., Dai Y., & Han X. (2016). Decolorization of azo dye C.I. Reactive Black 5 by ozonation in aqueous solution: influencing factors, degradation products, reaction pathway and toxicity assessment. *Water Science and Technology*, 73(7), 1500-1510.

LIST OF PUBLICATIONS AND PAPERS PRESENTED

No.	Manuscript Title	Status
1	Mook, W.T. , Aroua, M.K., Issabayeva, G. (2014). Prospective applications of renewable energy based electrochemical systems in wastewater treatment: A review. <i>Renewable and Sustainable Energy Reviews</i> 38, 36-46. (ISI-Cited Publication)	Published
2	Mook, W.T. , Aroua, M.K., Szlachta, M. (2016). Palm Shell-based Activated Carbon for Removing Reactive Black 5 Dye: Equilibrium and Kinetics Studies. <i>BioResources</i> 11(1), 1432-1447. (ISI-Cited Publication)	Published
3	Mook, W.T. , Ajeel, M.A., Aroua, M.K., Szlachta, M. (2016). The application of iron mesh double layer as anode for the electrochemical treatment of Reactive Black 5 dye. <i>Journal of Environmental Sciences</i> , Article in Press. (ISI-Cited Publication)	Published
4	Mook, W.T. , Aroua, M.K., Szlachta, M., Lee, C.S. (2016). Optimisation of Reactive Black 5 Dye Removal by Electrocoagulation Process Using Response Surface Methodology. <i>Water Science and Technology</i> . (ISI-Cited Publication)	Published

Conference or Proceeding Paper

1. **Mook, W.T.**, Aroua, M.K. (2014). Decolourization of Reactive Black 5 Dye by Electrochemical Oxidation Using Different Anode Materials. IWA Regional Conference on Water Reuse and Energy, 21-24 October 2014, Daegu, Korea. (International). (Oral Presentation).
2. **Mook, W.T.**, Aroua, M.K., Szlachta, M., Lee, C.S. (2016). Optimization of Reactive Black 5 Dye Removal by Electrocoagulation Process Using Response Surface Methodology. IWA 8th Eastern European Young Water Professionals Conference, 12-14 May 2016, Gdańsk University of Technology, Poland. (International). (Poster Presentation).
3. **Mook, W.T.**, Aroua, M.K., Szlachta, M. (2016). Optimization of Reactive Black 5 Dye Removal by Electrocoagulation Process and Energy Consumption. The 8th International Conference on Environmental Science and Technology, 6-10 June 2016, American Academy of Sciences, Houston, USA. (International) (Poster Presentation).

4. **Mook, W.T.**, Aroua, M.K., Szlachta, M., Lee, C.S. (2017). Combined Adsorption and Electrocoagulation Process for Removal of Reactive Black 5 Dye from Aqueous Solution. IWA 9th Eastern European Young Water Professionals Conference, 24-27 May 2017, Budapest University of Technology and Economics, Hungary. (International). (Poster Presentation).

University of Malaya